I. THERMAL CONDUCTIVITY OF NITROGEN DIOXIDE IN THE LIQUID PHASE

II. THERMAL CONDUCTIVITY OF NITRIC OXIDE

III. VISCOSITY OF NITROGEN DIOXIDE AND NITROGEN DIOXIDE-NITRIC OXIDE MIXTURES

Thesis by

George Neal Richter

In Partial Fulfillment of the Requirements

For the Degree of

Doctor of Philosophy

California Institute of Technology

Pasadena, California

1957

ACKNOWLEDGMENT

I wish to express my appreciation to Professor Bruce H. Sage for the assistance I have received throughout my graduate studies. His work and guidance in the design, construction, and operation of the equipment used in this research project have made it possible to carry this program to a conclusion. Willard M. DeWitt constructed part of the cell and his assistance in the assembly of the equipment, including many overtime hours, is gratefully acknowledged. George Griffith made many of the parts of the cell and assisted in its installation. H. Hollis Reamer helped materially in the operation of the laboratory equipment and Lee T. Carmichael was also of assistance in this part of the work. Virginia Berry did part of the calculations and made some of the figures. The suggestions of Professor William N. Lacey, who reviewed this thesis, were very helpful. During my studies I have been the recipient of fellowships from the Dow Chemical Company and the Union Carbide and Carbon Corporation and Institute scholarships. I wish to express my appreciation for these gifts. Finally I wish to thank my parents for all of the help they have given me while I have been in school.

ABSTRACT

I. An apparatus has been constructed for the determination of the thermal conductivity of fluids. In this equipment the thermal flux between concentric spheres is measured. The apparatus has been used to measure the thermal conductivity of nitrogen dioxide in the liquid state at 40°, 100°, and 160°F., and at pressures up to 5000 pounds per square inch.

II. The thermal conductivity of nitric oxide was measured at atmospheric pressure from 40° to 400°F., and the variation of its thermal conductivity with pressure was observed at 40°, 220°, and 340°F. to a maximum pressure of 1400 pounds per square inch. At higher pressures the nitric oxide was found to undergo catalytic decomposition.

III. A rolling ball viscometer was utilized to measure the viscosity of nitrogen dioxide and mixtures of nitrogen dioxide and nitric oxide. A temperature range of 40° to 280°F. was used at pressures from bubble point to 5000 pounds per square inch. Mixtures containing up to 20 weight per cent nitric oxide were studied.

TABLE OF CONTENTS

INTRODUCTION

The oxides of nitrogen are compounds of increasing industrial and scientific importance. Nitrogen dioxide, alone or in combination with nitric oxide, is of value as an oxidant in special fuel systems. In order to make the best use of these compounds, and to design equipment to handle them, a knowledge of their physical properties is needed. Investigators at the Chemical Engineering Laboratory of the California Institute of Technology have studied the volumetric behavior of nitrogen dioxide, nitric oxide, and some of their mixtures. In operations involving heat transfer or fluid flow a knowledge of their transport properties is necessary. The present work is concerned with the evaluation of their thermal conductivity and viscosity. The viscosity measurements were done under an Office of Naval Research contract and the thermal conductivity measurements were sponsored by Project SQUID which is jointly supported by the Office of Naval Research, the Office of Scientific Research (Air Force), and the Office of Ordnance Research (Army).

PART I

THERMAL CONDUCTIVITY OF NITROGEN DIOXIDE IN THE LIQUID PHASE

INTRODUCTION

The measurement of the thermal conductivity of fluids as a function of temperature and pressure has been one of the more difficult research problems to solve. A knowledge of this molecular transport property is of importance because of its theoretical interest as well as its engineering applications. Yet only a limited amount of experimental data is available, and most of it is in the realm of low pressure gases. Many different types of apparatus have been employed, but none has been free from limitations or inaccuracies. The object of the present work has been to construct an apparatus for measuring the thermal conductivity of fluids over a wide range of temperature and pressure and then to study nitrogen dioxide.

Experimental Results

The literature concerning experimental studies of thermal conductivity is extensive. Some of the most important work has been summarized in several reviews which give critical evaluations of the experimental results and many references to the original sources. The thermal conductivities of a number of the most common gases at atmospheric pressure may be found in the reviews of Keyes (1), Hilsenrath and Touloukian (2), and in a very comprehensive set

of tables published by the National Bureau of Standards (3). Sakiadis and Coates present a very good summary of available data on liquids (4) and in a later work give their results for 53 organic liquids (5). Mason (6) reports the thermal conductivity of twenty industrial fluids at temperatures from 0° to 100°C. The effect of pressure has been considered by Comings and co-workers (7,8,9) and Stolyarov (10). Keyes has reported some values of thermal conductivity at higher pressures (11).

There has been very little experimental work on nitrogen dioxide, and the small amount done is for the gas phase. Magnanini and Zunino (12) studied the rates of cooling of bulbs of nitrogen dioxide. From these data Nernst (13) calculated the thermal conductivity. These data are for the gas phase near atmospheric pressure, and cover the temperature range of 20° to 70°C. The errors in these values are probably large. The thermal conductivity of nitric oxide and nitrogen dioxide at atmospheric pressure was measured by Todd (14). The design of the experiment and the difficulties reported vitiate his results.

In the design and operation of a thermal conductivity cell other physical properties, chiefly volumetric behavior and viscosity, are needed. Much information on the oxides of nitrogen is presented by Yost and Russell (15). The properties of nitrogen dioxide are summarized by a comprehensive literature survey by Gray and Yoffe (16). In-

vestigators at the Chemical Engineering Laboratory of the California Institute of Technology have determined a number of the needed properties of nitrogen dioxide (17,18,19).

Theoretical Studies

The greatest amount of theoretical study of molecular transport properties has been concentrated on the behavior of gases at low pressure. Maxwell derived the first equation for thermal conductivity that had any success in agreeing with experiments. His relation is*

$$k = FC_v\eta \qquad (1)$$

His derivation gave a value of 2.5 for the constant F. The basis of the relation is rigorous kinetic theory and the assumption of molecules repelling each other according to an inverse fifth power of distance. It has been found that this value of F holds only for monatomic gases, which have no internal degrees of freedom. This result for monatomic gases has been generalized to include any inverse power repulsion law or any case of spherical symmetry by Chapman (20,21). The value of F remains between 2.522 and 2.5 for monatomic gases for any type of intermolecular force

*Symbols appearing in the text are defined in the nomenclature on page 55 .

that has been considered. The experimental values are within one per cent of 2.5, except in the case of helium for which the experimental results are about 3 per cent lower.

From a consideration of the energy of internal motions, Eucken (22) developed a correction for the case of polyatomic molecules,

$$k = \frac{1}{4}(9\gamma - 5) C_v \eta \qquad (2)$$

Using the Chapman-Enskog kinetic theory of gases, Hirschfelder has developed the form

$$k = \frac{15R}{4M}\left(\frac{4C_v}{15R} + \frac{3}{5}\right) C_v \eta \qquad (3)$$

This form gives somewhat improved results for monatomic gases, especially helium. For most diatomic gases the agreement of theory to experiment is within two or three per cent, but for triatomic or larger molecules the agreement is not good.

Another valuable result of theoretical studies is Sutherland's formula for the termperature dependence of the viscosity of gases. The formula is

$$\eta = \eta_\infty \left(\frac{T}{T_\infty}\right)^{3/2} \left(\frac{C + T_\infty}{C + T}\right) \qquad (4)$$

This formula may be combined with the known temperature variation of heat capacity and equation 3 to give an approximation for the temperature variation of thermal conductivity.

These relations depend upon knowledge of molecular behavior, particularly intermolecular forces and collisions. For simple gases at low pressures, values of the thermal conductivity can be calculated that agree well with experimental work. For more complicated systems a better theoretical knowledge is needed. The equations are derived and the theory presented by Jeans (23), Kennard (24), and Hirschfelder, Curtis, and Bird (25). The last authors in particular give a complete treatment of molecular theory and the transport properties as understood today.

For gases at high densities or for liquids the theoretical results are not satisfactory. No adequate theory has been developed to describe either of these states. The approximate theory of Enskog for dense gases and Eyring's theory of absolute reaction rates for liquids are the best descriptions available. Until a more rigorous theory may be completed, the transport properties in these regions cannot be derived satisfactorily from theory.

Several attempts have been made to develop simple equations for liquids that could be used in correlating

data. One such equation was developed first by Bridgman (26) and later modified by Kardos (27). Bridgman's equation is

$$k = L U_s \rho C_p \tag{5}$$

Errors involved in the use of this equation average over twenty per cent. One example of its use is by Sakiadis and Coates (28). A more recent work by Uhlir (29) considers a liquid as a dense gas of hard spheres in a uniform potential well. Applied to liquid argon and nitrogen, theory and experiment agreed to within five per cent. Most of the work on generalized liquid thermal conductivity has been done with a purely empirical equation such as that of Smith (30) or by modification of the theorem of corresponding states as was carried out by Sakiadis and Coates (5). Such methods may be used for classes of similar compounds, but are not successful for all liquids.

The only methods that have been presented for calculation of thermal conductivities of gases at high pressure have not been based on rigorous theory. The most reasonable correlations seem to be those of Comings and Nathan (7), which is based on the theorem of corresponding states, and the empirical equation of Stolyarov (10).

In the case of a chemically reacting system, there can

be anomalous values of the thermal conductivity. For a simplified example, consider thermal transfer across a fluid in which a reaction is occurring of the type

$$A + A \rightleftharpoons B \qquad (6)$$

that is, an association-dissociation reaction. A concentration gradient of both the monomer and the dimer will be set up because a temperature gradient is imposed upon the fluid. This assumes that the equilibrium is shifted by temperature change and that the rate of reaction is large compared to the rates of transport of molecules within the fluid by diffusion. Under the influence of this concentration gradient, the dimers will be transported to the region of high temperature and the monomers to that of low temperature. At the higher temperature the dimer will dissociate with the absorption of the energy of dissociation and in the low temperature region the monomers will associate and liberate the energy of dissociation. So the net result is the diffusion of the dissociation energy across the fluid, which gives a high thermal conductivity for the reacting system. Actual cases can be more complicated owing to complex reaction mechanisms and higher polymers, but the basic phenomenon is the same. This effect is especially large in the case of the gas phase equilibrium involving nitrogen dioxide and dinitrogen tetroxide in the region from 0° to 150°C. where the equilibrium between

the species shifts from dinitrogen tetroxide to nitrogen dioxide as the primary constituent of the gas. The effective thermal conductivity of this system is several times as large as would be predicted from kinetic theory. Similar increases are also found in fluids near the critical state and in very high temperature systems in which the common gases, such as nitrogen, dissociate. The additional conduction due to the transport of the energy developed in the chemical reaction must be added to the thermal transfer due to the transport of the kinetic and internal energy of the molecules. The subject of reacting systems was first considered by Nernst (13) and has been presented more recently by Prigogine et al. (31) and Hirschfelder (32).

Design of Equipment

General Criteria

The rational choice of a design for a thermal conductivity cell involves a consideration of many factors. The geometrical configuration involved must be amenable to mathematical analysis and it must be possible to make all of the needed measurements. Difficulty of construction may be a deterrent to the use of some systems. It must be possible to calibrate the cell with precision. This involves determination of sizes and distances and calibration of electrical energy measurement circuits and temperature measurement devices. The cell must be designed so that these determinations are stable. The possible limits of accuracy in measuring the quantities needed to calculate the thermal conductivity depend upon the design. But perhaps the most useful criterion in making a decision is the ability to eliminate methods of energy transport other than conduction through the fluid of interest.

Transport by radiation cannot be eliminated, but its effect can be minimized and corrected for. The surfaces of the containing walls of the cell should be made to have as low an emissivity as is possible. This can be done by constructing the cell from material that has a low emissivity, or by putting a special coating on the surface, such as gold

or silver plating. Special efforts must be made to insure that the surface condition does not change with time. Radiation is considered in some detail by McAdams (33).

Natural convection can be eliminated by proper design. This may be accomplished in two ways. First, when a fluid is confined between two walls a stabilization occurs that tends to prevent convection. The tendency for circulation to occur depends upon the state of the fluid, increases with increased temperature gradient, and decreases as the spacing between the walls decreases. The most common design method of eliminating energy transport by convection, is to use a thin film of fluid, however the use of thin films, of the order of a few hundredths of an inch, creates additional problems in gaining precision in measurements of the spacing and the temperature drop across the film. Kraussold (34) has accumulated a considerable amount of data and made an analysis of the problem. From this work he determined that, for cases in which the product of the Grashof and Prandtl numbers is less than 1000, convection would be negligible. That is, convection is unimportant when

$$\left(\frac{\ell^3 \rho^2 \beta \Delta T}{\eta^2}\right)\left(\frac{C_p \eta}{k}\right) \leq 1000 \qquad (7)$$

Kraussold's work and some later work is summarized by Lenoir and Comings (8).

The second method for eliminating convection is to arrange the heated surfaces so that the least dense fluid occurs at the highest point in the system. Thus the tendency for circulation is eliminated. In general this means placing the higher temperature surface highest because the isobaric change of volume with temperature is usually positive.

There is another class of errors that affect the results obtained in any cell. No actual cell corresponds exactly to the mathematical model used to describe it. There are always some end effects, where the geometry disagrees with the ideal used as the model, and almost always there are mechanical supports or measuring instruments whose presence is not considered in the analysis. These factors can be minimized and corrected for, but they do place a limit on the inherent accuracy of interpretation of the results from any design.

An additional difficulty arises in some types of equipment when they are used at low pressures. When a temperature gradient is imposed upon a confined fluid there is a discontinuity in the temperature at the boundaries. This discontinuity, or so called temperature jump, occurs because of incomplete interchange of energy when the molecules hit the wall. It is usually treated by means of the accommodation coefficient, which is the fractional extent to which the molecules colliding with the wall adjust their

energy to that corresponding to equilibrium with the wall. The phenomenon becomes important when the mean free path of the molecules becomes significant with respect to the dimensions of the container, and depends on the temperature gradient, the fluid, and the type of surface. It is treated from the standpoint of kinetic theory by Jeans (35) or Kennard (36), and Dickens (37) gives an analysis of the problem as it occurs within a thermal conductivity cell.

Types of Designs Used

There are two major classes of designs in use, steady and unsteady state. Those operating at steady state may be subdivided according to geometry into parallel plate, cylindrical, or spherical systems. The analysis of all the steady state systems leads to relatively simple equations, but they differ greatly with respect to other factors.

A cell involving heat transfer between parallel plates is the simplest system to consider. In general it consists of two parallel circular plates, one a heat source and the other a heat sink. The plates are placed in a horizontal position, generally the one with the higher temperature uppermost. This orientation eliminates convection by having the most dense fluid at the lowest point. The basic parts are very simple and the geometrical constants,

spacing and areas, are very easily determined. The spacings used vary from a thin film to a layer of perhaps an inch. The major difficulty lies in eliminating heat losses from the edges of the plates and in eliminating deviations in the pattern of heat flux from that found in the model of infinite parallel plates. Many schemes have been proposed for eliminating these effects of the ends of the plates, but none is completely satisfactory. The method of parallel plates has not been used extensively recently. Bates (38) utilized this design with a thick layer of fluid and also discusses other types of equipment. Martin and Lang (39) utilized parallel plates with a thin layer of fluid.

There are two main types of cylindrical cells. The hot wire types have a thin wire mounted along the axis of a cylinder. The wire serves both as a heat source and as a resistance thermometer. The other method uses concentric cylinders, or what may be called a thick wire system.

In the hot wire methods, care must be taken to eliminate convection and the effect of a non-unity value of the accommodation coefficient, as well as to eliminate the end effects. Experimental and computational techniques make it possible to eliminate convection and correct for the temperature jump. Two schemes have been used to eliminate thermal losses from the ends and to insure that only radial heat flow is obtained. The first is due to Schleirmacher (40)

and is often called the potential lead type cell. By attaching potential leads to the ends of a central section of the hot wire, the temperature and heat loss of this portion of the wire may be determined. This section is assumed to be free of all end effects, and the calculations are based on this section. The Schleirmacher principle has been utilized by Weber (41) and Taylor and Johnston (42). Another type of approach, originated by Goldschmidt (43), utilizes two hot wire cells, identical except for length. It assumes that the end effects are the same in each cell and that they can be eliminated from the results by working with the differences between the two cells. The Goldschmidt, or compensating type of cell, has been used by Weber (44) and by Dickens (37), who also analyzed the equipment. The greatest part of the thermal conductivity data for gases has come from hot wire cells. Their behavior has been extensively studied and is well understood. At high pressures and for use with liquids they have some disadvantages due to increased tendency for circulation and to mechanical problems. So their application lies in the area of gases at pressures from the vicinity of atmospheric to that of a millimeter of mercury or less.

In the thick wire, or concentric cylinder method, end effects are eliminated by a combination of guard heaters to block heat losses and corrections applied to the data by analysis of the actual situation. A thin film of fluid is

used to minimize convection, and the temperature jump phenomenon is not important. This design is suited to high pressure work and either liquids or gases may be studied. The method was used and analyzed by Kannuluik and Martin (45,46) and has been used by Keyes and Samdell (47), Keyes (48), and Kannuluik and Carman (49).

The use of concentric spheres to contain the fluid offers the advantage of reducing end effects to a minimum. The major deviation from the ideal case of spheres, which have no boundaries at which end effects can occur, is a small shaft needed to carry the electrical leads to the heater in the center sphere. By the use of a guard heater the energy losses through this shaft may be essentially eliminated. The deviations from radial flow of heat caused by the shaft should be negligible. It is a design suitable for high pressures, and it is adaptable to both liquids and gases. The greatest drawback to this design is the extreme difficulty of construction of the cell. The only reported use of a spherical cell is by Riedel (50,51).

Unsteady state methods may be employed to measure thermal conductivity. In general, the rate of change of temperature is obtained for some point in a container of the fluid being studied, when the container is subjected to some predetermined change in temperature. An example of this is the cooling thermometer method which has been used by Curie and Lepape (52). In this method the rate of temperature

change at the center of a spherical flask of the fluid is obtained when the exterior of the flask is changed from one steady temperature to another. Cells of this type are very susceptible to errors caused by convection.

Any unsteady state method will have less accuracy than a steady state method for several reasons. An analysis of such a system shows that it is the thermometric conductivity which is obtained. Hence, to get the thermal conductivity, a knowledge of the fluid's density and heat capacity is needed. Also, owing to their nature as unsteady values, the measurements are more difficult to obtain precisely than steady values. And in the particular case of the cooling thermometer method only comparative measurements can be made. This is not desirable, since the accuracy of the results must depend upon the accuracy of values of thermal conductivity determined by other investigators.

Choice of Design

For the present work it was decided to use the method of heat transfer between concentric spheres. This method has been utilized previously in only one instance because of problems of construction, but these can be overcome. It was believed that the difficulties of overcoming the mechanical problems of construction would be more than compensated for by the minimization of end effects in the completed cell. In addition to minimizing end effects, this type of cell is

more easily adapted than most others to the immediate objectives of the work, a study of a corrosive fluid at high pressures and over a wide temperature range. All of the cell that is exposed to sample can be made of metals that are resistant to chemical attack and the cell can be made to withstand the effects of high pressure and temperature. Figure 1 shows a schematic view of the cell. By using four concentric spheres the effects of pressure on the cell can be made negligible. The fluid is contained between the inside and outside spheres. Thus the intermediate spheres are pressure compensated since they are immersed in the high pressure fluid, and the measurements can be based on them. Thermocouples are used to measure the temperature difference between the spheres. Use of a small spacing between the spheres makes it possible to minimize convection. The effect of mechanical supports is small. Special preparation of the surfaces keeps radiation transfer small, and the temperature jump phenomenon is negligible. Calibration of all the geometric factors and measuring instrument characteristics is possible, and the analysis of the operation of the cell leads to a calculation method that is straightforward. It is possible to make accurate measurements of the quantities needed to calculate the thermal conductivity.

Equations of Thermal Transport by Conduction between Concentric Spheres

The basic hypothesis for the mathematical theory of conduction of heat is that the heat flux at a point across an isothermal surface is

$$\dot{q} = -k \frac{\partial T}{\partial n} \tag{8}$$

This hypothesis is generally known as Fourier's Law. The only assumption made in this equation is that all of the transport is by the mechanism of conduction. For the case of an isotropic, quiescent medium the heat flux at a point may be generalized to

$$\dot{q} = -k \, \text{grad} \, T \tag{9}$$

A complete treatment of the mathematical theory of conduction may be found in Carslaw and Jaeger (53) or in the work of Fourier (54).

In the case of transfer between spheres, if the spheres are concentric and each is isothermal, the temperature and heat flux will depend only upon the radial position and the time. Under these conditions, and expressing the equations in spherical polar coordinates, the heat flux becomes

$$\dot{q} = -k \frac{dT}{dr} \tag{10}$$

At steady state the heat transferred through any spherical surface is constant and given by

$$\dot{Q}_c = -4\pi r^2 k \frac{dT}{dr} \tag{11}$$

This equation may be integrated over the distance between the spheres to give

$$\dot{Q}_c = \frac{4\pi k (T_i - T_o) r_i r_o}{(r_o - r_i)} \tag{12}$$

This may be rearranged to give the thermal conductivity

$$k = \frac{\dot{Q}_c (r_o - r_i)}{4\pi r_i r_o (T_i - T_o)} \tag{13}$$

In the actual thermal conductivity cell two of the assumptions used in the derivation are not strictly correct. There is transfer of heat by other mechanisms than conduction through the fluid, and the shaft to the center sphere alters the geometry from complete spheres. The amount of heat transferred by conduction may be calculated by subtracting from the measured total heat transfer the amounts transferred by radiation and by conduction through the supporting mechanism. These quantities may be obtained by calibration and calculation. The heat transfer

through the supporting pieces is considered in two parts, that through the shaft leading to the center sphere and that through the pins used to space the spheres. In addition to conducting heat away from the center sphere the shaft changes the area of the fluid film by intersecting part of the surface of the spheres. If it is assumed that the only effect of the shaft is to prevent heat from being carried across the intercepted, spherical area, the ratio of heat transferred across a complete sphere to that actually transferred is the same as the ratio of the area of the complete sphere to that of the sphere minus the area intercepted by the shaft. Using this to correct the amount of heat transferred, the complete equation for the calculation of the thermal conductivity becomes

$$k = \frac{(\mathring{Q}_m - \mathring{Q}_p - \mathring{Q}_r - \mathring{Q}_s)(r_o - r_i)\phi_A}{4\pi r_o r_i (T_i - T_o)} \qquad (14)$$

Construction of Equipment

Description of the Apparatus

A schematic view of the thermal conductivity cell is shown in Figure 2. The heavy walled pressure vessel A is mounted within a constant temperature bath B. The central sphere C contains an electrical heater D which maintains the temperature of sphere C above that of the rest of the equipment. The amount of energy dissipated in D is determined electrically. Two carefully machined spherical shells E and F are mounted in the space between the central sphere C and the pressure vessel A. These shells are supported relative to C and to each other by means of small pins shown at G. Thermocouples are mounted in the interior of E and F so that the junctions are near the surfaces of the shells that are adjacent to each other. The leads enter from the inner surface of F and the outer surface of E so that the space between the shells is free of wires. The dimensions of shells E and F can be determined precisely and the variation of their dimensions with temperature and pressure can be calculated. Since they are pressure compensated they will not deform under high pressures. The pins G are made very small to minimize energy transport through them. A shaft H supports the inner members of the cell in relation to the outer vessel A. In addition the

electrical leads to the heater D and other electrical equipment from the junction box J on top of the cell pass through H. In order to make energy losses through the shaft negligible a compensating or guard heater is mounted at K. A differential thermocouple mounted below K measures the temperature gradient in the shaft. The guard heater is regulated to keep the gradient zero thus eliminating thermal transport. The pressure within the cell is measured with a diaphragm type pressure gauge at L. Samples are introduced into the cell by conventional vacuum techniques through a line entering the cell through the valve M. Figure 3 is a photograph of the completed apparatus.

Details of Construction

A sectional view of the thermal conductivity cell is shown in Figure 4. All of the components were machined from stainless steel 310, which contains twenty five weight per cent chromium and twenty weight per cent nickel. This alloy is resistant to chemical attack.

Unsupported-area-type seals with lead gaskets were used in the vessel A to make pressure seals around the shaft H, the pressure gauge L, and in the bottom half of the spherical section. Details of the unsupported-area seal between the spherical sections of A are given in inset P of Figure 4. Initially, pure, annealed gold gaskets were used in these seals. This was not a satisfactory type of

gasket, however, because of work hardening of the gold before the seal was completely made. This problem of making a pressure seal was made more difficult to solve because the particular steel alloy used is comparatively soft and was deformed by the gold. Teflon packing was used around the stem of the sample admission valve and lead gaskets were used in the tubing connections to the cell. The interior of the vessel A was plated with pure chromium.

The shells E and F were carefully machined to a spherical surface within a maximum deviation of 0.0005 inch. The average deviation from sphericity is less than 0.0002 inch. Figure 5 is a photograph of the outer shell E before assembly. The effective difference in radii of the inner surface of E and the outer surface of F is approximately 0.0200 inch, as measured with a micrometer. Sphere F was supported from the center sphere C by six steel pins. Three pins were mounted in the lower half of C and three in the upper half. The diameter of the pins was 0.020 inch and at the point of contact they were tapered to 0.010 inch. Sphere E was supported from sphere F in a similar fashion. The spacing between the outer vessel A and E and between F and the center sphere C was 0.055 inch.

Four-junction platinum, 90 platinum-10 iridium thermocouples were used to measure the temperature difference between E and F. A schematic diagram of the arrangement of one of the thermocouples is shown in Figure 6. One such

thermocouple was mounted in the upper half of the spheres and one in the lower half. They were constructed from 0.003 inch diameter wire with two layers of fiber glass insulation. The insulation was impregnated with teflon for further mechanical protection. The junctions were welded together and then imbedded in teflon and enclosed in a sealed glass tube with walls 0.002 inch in thickness before mounting in the shells. This type of close fitting mounting not only gives good electrical insulation, but, by giving good thermal contact with the shell, minimizes uncertainties in the measured temperature because of thermal conduction through the leads. The mounting of the thermocouples is shown in insert Q of Figure 4. The junctions are within 0.015 inch of the inner surface of E and the outer surface of F. The arrangement of the pins G and the thermocouple junction wells R in the upper half spheres can be seen in Figure 7. In each half sphere the pins are spaced at 120 degree intervals and the wells are 180 degrees apart. In order to minimize the effect of the pins and wells on the results they were so arranged that no two wells or pins in the upper half occur at the same azimuthal angle. The bottom half is identical with the upper half with the exception that all the pins and wells were rotated 90 degrees.

Two split rings S, of Figure 7, machined to the same spherical surface as the shells E and F, closed the gap

between the shells and the shaft H. The rings were machined to a knife edge where they come in contact with the shaft.

The electrical leads from the thermocouples were brought up the side of the shaft H through steel tubes T for protection. In the upper section of the apparatus they pass out of the high pressure sample region through soapstone seals. The location and design of the seals are shown in Figure 8. At this point the platinum wires were joined to 0.010 inch, glass-insulated, copper wire contained inside of copper tubes. The copper wires were connected to terminals in the junction box J of Figure 2, on top of the apparatus. All of the internal wiring of the equipment terminates in this box, which is sealed against the oil of the thermostat bath.

A considerable amount of trouble was encountered before a satisfactory pressure seal for electrical leads could be found. In the final seal a larger diameter platinum wire was used to go through the soapstone. During the process of designing a satisfactory seal several conclusions were reached: the hole through the soapstone must fit closely to the wire; a good grade of homogeneous, natural soapstone is needed; a flat, hardened ferrule, as shown at U in Figure 8, was found to be superior to beveled and softer types sometimes used; and considerable force must be brought to bear upon the soapstone in making the seal since the soapstone must be crushed and reformed.

Details of construction of the center sphere C are given in Figure 9. An unsupported area seal of a different type than that used in sphere A was used to close the sphere and is shown in detail in the inset to Figure 9. A gold gasket was used successfully in this case since the process of making a seal is simpler in this design and is thus less susceptible to adverse effects from work hardening. The heater D was wound in a spiral groove cut in the inner surface of C. The groove is 0.020 inch square and has a 0.044 inch spacing between turns. Figure 10 is a photograph of the sphere showing the groove while it was being cut. The total length of the heater is 86 inches in each half of the sphere. The heater was constructed from 0.005 inch diameter, advance wire which was covered with a double layer of glass insulation. After the heater was in place, the inside of the sphere was coated with alundum cement to hold the wire in place. A separate but identical heater was wound in each half sphere and provisions were made to use the two in parallel or in series.

The electrical energy was measured and controlled by conventional calorimetric techniques. Figure 11 is a diagram of the circuit used. The power for the heater was supplied by a group of six-volt storage batteries. The current resistors and the voltage divider were made from manganin wire to make variations of resistance with temperature negligible. The two current resistors, two voltage divider

ratios, and two methods of heater hookup provide flexibility in the operation of the cell by making it possible to run with a wide range of rates of energy addition.

The ends of the heater were supported on two mica disks V in the center of sphere C as shown in Figure 7. At V, 0.010 inch diameter, glass-covered, copper wire was attached to the heater and led up the shaft H. Above the guard heater K the diameter of the copper wire was increased to 0.020 inch. This was done at this point in the shaft in order to minimize the cross sectional area of metal available for heat transfer in the part of the shaft that passes through spheres E and F. In order to determine the electrical energy dissipated within the cell, the potential drop across the heater and the portion of the leads within the cell was needed. To find this, 0.003 inch diameter, glass-covered, copper leads were attached to the 0.010 inch copper power leads at a point within the guard heater. These junctions were enclosed within 0.030 inch diameter glass tubes. A photograph of one of these junctions made by wrapping the 0.003 inch diameter wire around the power lead and silver soldering it in place is shown in Figure 12. Figure 13 is a schematic diagram of the wiring of the heater.

Four copper-constantan thermocouples, made from 0.003 inch diameter, glass-covered wire, were installed to measure the temperature difference between sphere C and the outer pressure vessel A. They were mounted in positions as indi-

cated in Figure 7 as R' and R'' and were insulated by the use of glass tubes as shown in the insert to Figure 9. The junctions in the outer vessel were enclosed in hypodermic tubing to keep them free of the thermostat oil. The tubes were sealed to the junction box J on one end and silver soldered shut at the end inside of sphere A. Two of the junctions in the center sphere were placed in the upper half and two in the lower half, but all four of the junctions in the outer sphere were put in the upper half. The junctions were made by silver soldering the wires together and were enclosed in glass tubes. The wires to the thermocouples in the center sphere were also supported by the mica disks at V. Figure 14 is a photograph of the interior of the center sphere with the heater and thermocouples in place.

The details of the guard heater K may be seen in Figure 7. The heater was wound in a 0.015 inch, square, double-lead thread cut on the outside of the upper part of the heater. Alternating current, controlled by two variable autotransformers and an isolation transformer in series, supplies the power for the heater. It was constructed of eight inches of 0.005 inch diameter, double-glass-covered, advance wire. The heater was wound non-inductively in the double thread.

Heat losses are guarded against by reducing the temperature gradient in the shaft to zero. To determine the

gradient, a differential thermocouple was mounted in the lower part of the guard heater where the shaft goes through the shells E and F. The location is shown at W in Figure 7. The thermocouple was made of 0.003 inch diameter, glass-covered, copper and constantan wire silver soldered at the junctions. The junctions were installed inside of glass tubes 0.020 inch in diameter with a wall thickness of 0.002 inch. The ends of the tubes were sealed and ground to fit the bottom of the wells. Figure 15 is a photograph of the completed guard heater prior to its installation in the apparatus, and Figure 16 is a schematic diagram of the wiring of the guard heater and thermocouple and a typical sphere-A-to-sphere-C thermocouple. Figure 17 is a photograph of the assembled center sphere.

The pressure within the apparatus was measured with a rotating-cylinder fluid pressure balance that has been previously described (55). The balance was connected to the cell through a diaphragm of the aneroid type similar to that used in previous work (17). Pressures within the cell were known to 0.3 pound per square inch or 0.15 per cent, whichever was the larger measure of uncertainty.

The assembled conductivity cell A was placed within a thermostated oil bath of conventional design as shown in Figure 18. Agitation was provided by the impeller X which was driven by a shaft brought through a packing gland located at the bottom of the bath. A radiation

shield Y was provided in order to keep the amount of power that must be supplied by the heater in the bath small. Both heaters and cooling coils were installed in the radiation shield and in the bath for control purposes and large heaters were put around the bath for use in making large changes in temperature. The energy added to the bath heater to control the temperature was supplied by a modulating circuit (56). A silicone oil was used in the bath so that the temperature could be varied from 40° to 460°F. The exterior electrical connections to the terminals in the junction box on top of the apparatus were made through steel tubes that were brought through the side of the tank. In order to exclude oil from the electrical system and to prevent leaks from the tank, the tubes were sealed to both the tank and the box with lead gaskets. Temperatures of the bath were measured with a strain-free platinum resistance thermometer of the filament type obtained from the Leeds and Northrup Company. It was calibrated by comparison to a similar instrument that had been calibrated by the National Bureau of Standards. It is believed that the temperature of the bath was known within 0.01°F. relative to the international platinum scale at any time. Fluctuations of the bath temperature were kept within 0.02°F. and the average deviation from the desired temperature was less than 0.01°F.

The thermocouple voltages were measured with a White-

type double potentiometer. An uncertainty of 0.1 microvolts was involved in the use of the instrument. A K-type potentiometer was used to determine voltages in the measurements of the energy supplied to the heater in the center sphere. The errors involved in its use were less than 0.02 per cent. The resistance of the thermometer was measured on a Mueller bridge which had an uncertainty of 0.0001 ohm, which corresponds to less than 0.002°F. All of the electrical measuring devices were obtained from the Leeds and Northrup Company.

Calibration of Equipment

The average spacing between shells E and F was determined by finding the weight of mercury needed to fill the gap between them. Special disks, with the proper spherical surfaces, were made to close the holes where the shaft H goes through the shells. The disks were held in place and the shells were sealed with wax. Then the space between the shells was evacuated and filled with mercury while they were thermostated. The weight before and after filling was determined with an analytical balance. The outer radius of sphere F was taken to be 1.665 inches as measured by a micrometer. Based on this value, the weight of mercury, and the density of mercury, the spacing was found to be 0.019972 inch at 74.32°F. The variation of the spacing and the value of the term $\frac{r_o - r_i}{4\pi r_o r_i}$ were calculated as a function of temperature from the known properties of the steel. The change of dimensions of the steel with pressure was found to be negligible. The results of the calculations of the geometrical constants of the cell are given in Table I. The value of the factor ϕ_A, the ratio of area of the complete spherical surface to that of the surface minus the area intercepted by the shaft, was based on the average of the radii of the two shells. The error in the values of the geometrical constants is less than 0.01%.

The resistors in the energy addition circuit were calibrated by comparison to standard resistors obtained from the Leeds and Northrup Company. The known resistors were placed in series with the addition circuit and the voltage drop across both the known and unknown resistors was measured. From these measurements the values of the unknown resistors were calculated. The values of all but the smallest current resistor are known to within 0.02% and the error in the case of the smallest one is 0.06%.

The thermocouples mounted in spheres E and F were calibrated by comparison to a platinum resistance thermometer. The hotter junctions were installed in the thermostat bath and the colder junctions in an ice bath. Equations of the following form were fitted to the voltages of the thermocouples by least squares techniques

$$\mathcal{E} = a\tau + b\tau + c\tau \qquad (15)$$

From these the thermoelectric power was obtained by differentiation

$$\mathcal{P} = \frac{d\mathcal{E}}{d\tau} = a + 2b\tau + 3c\tau^2 \qquad (16)$$

Methods of Operation and Calculation

The thermal conductivity apparatus has a nearly constant total volume. Pressure variation at any particular temperature was secured by varying the amount of sample within the cell. High liquid pressures were easily attained by introducing the nitrogen dioxide at a lower temperature and then heating to the desired temperature.

In determining the thermal conductivity of a fluid at a given state, as fixed by a bath temperature and an amount of sample, measurements were made for several different rates of thermal transport. By the use of equation 14 the apparent thermal conductivity for each thermal flux was calculated from the measured energy addition rate and temperature difference. The rate of heat loss due to conduction through the supports and to radiation was taken into account. From these calculated apparent thermal conductivities the value at zero flux was determined by extrapolation. The results should be free from errors due to convection because circulation disappears as the temperature difference goes to zero. The extrapolated values of the thermal conductivity correspond to a state of the fluid determined by the temperature of the bath and the pressure corresponding to that in the cell when it was at bath temperature. The extrapolation procedure also minimized the chance that random errors could affect the results because

the different energy rates served as mutual checks.

In securing the measurements required to caclulate the thermal conductivity at a desired state, the pressure was first determined with no energy flux. Then the heater in the center sphere was turned on and held at a constant rate of energy addition until the temperature differences between the various spheres became constant, at which time the measurements were made. While steady state was being attained the guard heater in the shaft was adjusted to keep the temperature gradient in the shaft zero to minimize heat losses. It required two to three hours to reach steady state and the thermocouple voltages were recorded over a minimum period of thirty minutes after this to insure no further changes were occurring. This procedure was repeated for three levels of energy addition in most cases and was followed by a check on the cell pressure with no energy added. Small corrections were made to the observed thermocouple voltages for parasitic electromotive forces arising in the thermocouples and lines to the measuring instruments. These values were determined by measuring the voltages with no energy added to the cell and with the thermocouples short circuited. These corrections were found to have little variation with time and never exceeded 0.25 microvolts.

In calculating the temperature difference between spheres E and F from the observed thermocouple voltages, the temperature of the thermocouple junctions had to be

known to make use of the calibration equation. Since the final result of the calculations was the value of the thermal conductivity of the fluid when its temperature was extrapolated to that of bath, it was possible to use the bath temperature to calculate the thermoelectric power and have no error introduced as a result. The temperature difference was computed by dividing the corrected value of the thermocouple voltage by its thermoelectric power evaluated at the bath temperature.

The energy addition rate was calculated from the voltage drops across the current resistor and one segment of the voltage divider coil. From these measured quantities, and the known values of the resistances, the energy addition rate was computed from

$$\dot{Q}_m = \left(\frac{\mathcal{E}_c}{R_c} - \frac{\mathcal{E}_d}{R_d}\right)\frac{\mathcal{E}_d R_t}{R_d} \qquad (17)$$

Heat Losses

Conduction through Shaft

By proper regulation of the guard heater in the shaft the thermal losses were kept negligibly small. Based on the observed temperature gradient and the known dimensions and properties of the shaft the actual leakage was calculated. The thermal flux in the shaft as a function of time for two typical runs is shown in Figure 19. In all cases the instantaneous rate was less than 0.0001 of the energy added to the heater in the center sphere and the time average was less than this amount. The magnitude of the calculated thermal flux was checked by observing the changes in temperature of the spheres while the temperature gradient in the stem was varied, with the energy input to the heater in the center sphere maintained constant.

Conduction through Pins

Thermal flux in the supporting pins was minimized by making them small and tapering the ends that contacted the adjacent sphere. Based on some simplifying assumptions concerning the geometry of the pins, an approximate equation for the thermal leakage was derived. Expressed in terms of the diameter of the pins the equation is

$$\dot{Q}_p = \frac{24\pi k_{st} r_p^2 (T_i - T_o)}{5(r_o - r_i)} \qquad (18)$$

The thermal flux was calculated to be between 0.0043 and 0.0060 of the energy dissipated in the central heater. Because of the small size of this, as well as the other corrections, even relatively large errors in estimating the leakage fluxes would have only a small effect on the calculated thermal conductivity.

Radiation

Because of the high absorbance of nitrogen dioxide in the liquid phase, the transfer by radiation had a negligible effect on the calculated thermal conductivity. For work with transparent fluids the correction for radiation transport in the cell was determined by making measurements with the pressure inside the cell reduced to less than 10^{-6} inches of mercury. At such a low pressure, where the mean free path becomes of the same order of magnitude as the space between the spheres, the amount of heat transferred by conduction is very small compared to the radiant transfer. Uncertainties caused by energy transfer by radiation are small in the limiting cases of a completely absorbing fluid, where there is no radiation transport, or a transparent fluid, where the radiation transport is taken into account by subtracting the radiation transfer from the

total energy transfer, as in equation 14. The effect for a partially absorbing fluid is more complicated and no rational method of correction for it appears to have been developed or discussed. Since a part of the radiant energy is absorbed, the actual temperature gradient does not correspond to that gradient determined by measuring the overall temperature difference.

Preparation of Materials

The nitrogen dioxide was obtained from the Matheson Company, Inc. The purity was stated as 0.98 weight fraction nitrogen dioxide, so further purification was needed prior to its use. The complete removal of water was particularly important to prevent corrosion. The impurities were primarily other oxides of nitrogen and a small amount of water. The nitrogen dioxide was fractionated at atmospheric pressure in a glass column containing thirty bubble plates. The column was operated with a reflux ratio of approximately five, and the initial and final fifteen per cent of the overhead were discarded. The central portion was dried over phosphorus pentoxide at atmospheric pressure and collected at low pressure at liquid nitrogen temperature. The purified material was stored in a stainless steel cylinder until used. This purification system was used in previous work and found to give a product of at least 0.998 weight fraction nitrogen dioxide as determined by measurements of the vapor pressure.

Results

Measurements were successfully made with liquid nitrogen dioxide in the cell at 40°, 100°, and 160°F. and at pressures up to 5000 pounds per square inch. It had been the plan to continue the study to higher temperatures and into the gas phase, but, as shown below, the needed measurements could not be made.

At temperatures in excess of 160°F. the thermocouples did not function properly. The observed voltages were internally inconsistent, large, very erratic, and often of the wrong polarity. This behavior can be attributed to the ionization of the nitrogen dioxide which was found by Clusius and Vecchi (57) to occur in the following manner

$$N_2O_4 \rightleftharpoons NO^+ + NO_3^- \qquad (19)$$

In addition it appears that the cell was attacked by the nitrogen dioxide at the higher temperatures. At the conclusion of the work the lower closure in the outer pressure vessel was opened and some pitting and discoloration was observed on the surfaces. Checks on the thermocouples in the shells at the conclusion of the work showed that their characteristics were changed. The two no longer agreed and the thermoelectric power of both appeared to have been in-

creased.

In the low temperature, liquid phase studies the results were reproducible, but after the higher temperatures had been tried the initial results could not be duplicated. From these observations on the behavior of the thermocouples it was concluded that only data for liquid nitrogen dioxide at 160°F. and lower temperatures was valid and that the initial thermocouple calibrations were no longer correct.

The cause of the attack on the cell, which was believed to be resistant to pure nitrogen dioxide, might be attributed in part to electrolytic action. However it seems probable that some foreign substance, such as water, must have been present. A trace of water would lead to the formation of nitric acid which would attack the cell. Since none of the effects of the corrosion were noticed initially, it would seem that the sample was pure and the foreign materials were contained somewhere within the cell and were brought into solution by the action of the high temperature and pressure. One such possible source of water could have been the materials used in the soapstone seals, even though they were baked to remove water.

Details of the experimental results are given in Table II. The temperature differences and energy addition rates were calculated from the observed voltages by the methods given. The apparent thermal conductivity was cal-

culated from equation 14. The thermal conductivity at each state was computed from these apparent values by extrapolation to zero temperature gradient. This process is illustrated for one run at 40°F. and one at 100°F. in Figure 20. It can be seen that the change in apparent conductivity with temperature gradient is significant, and that the results based on the upper and lower hemispheres are different. Yet the uncertainties in the extrapolated value caused by these deviations are slight. The discrepancies between the two thermocouples, which increase with the temperature gradient, may be attributed to convection in parts of the cell. Local circulation could very well exist in the upper hemisphere since the direction of the temperature and density gradients with respect to the gravitational field is reversed in the two halves of the cell. The relatively large free volume between spheres E and A of Figure 2 at the base of the shaft H would further increase the possibility of local convection at that point. If such local behavior occurred, the effect on the measurements would be in the direction found. The temperature distribution within the central sphere C was measured with thermocouples during the runs and was uniform. So the discrepancies cannot be attributed to uneven thermal flux because of improper operation of the heater or to the effect of the shaft or the closure in sphere C on the geometry.

The experimental values of the thermal conductivity

of nitrogen dioxide are presented in Table III as a function of pressure at each temperature. Figure 21 illustrates the effect of pressure upon the thermal conductivity of liquid nitrogen dioxide at the three temperatures 40°, 100°, and 160°F. The variation with pressure is in agreement with results reported for other fluids and is similar to the change of the analogous property, viscosity of nitrogen dioxide, with pressure. The experimental points indicated in Figure 21 have a standard deviation of 0.00058 Btu./(hr.)(ft.)(°F.) from the smooth curves that were drawn. Taken from these smooth curves, the thermal conductivity for even values of pressure and temperature is presented in Table IV.

Discussion of Results

The thermal conductivity of nitrogen dioxide in the liquid phase has been determined for pressures from bubble point to 5000 pounds per square inch at temperatures from 40° to 160°F. The errors involved in the experimental measurements fall into three classes: those caused by transfer of heat by other mechanisms than conduction through the nitrogen dioxide; those due to lack of accuracy in the determination of the physical quantities measured; and those due to operational difficulties or departures from the ideal behavior of the apparatus.

The errors due to transfer by other mechanisms were small. Conduction up the shaft was less than 0.0001 of the total energy flux, and radiation was negligible. There appeared to be no significant amount of convection between the shells E and F during any of the runs. The transport through the supporting pins was between 0.0043 and 0.0060 of the total and corrections were made for it. Errors from these factors should be under 0.1 per cent even if relatively large errors were made in evaluating any of the terms.

The thermocouple voltages could be determined to within 0.1 microvolt, which corresponds to an uncertainty of 0.008°F. The parasitic electromotive forces in the thermocouple circuits should not increase this to more than 0.02°F. in a total temperature difference that generally varied from one

to three degrees. The possibility that the temperature of the thermocouple junction was not the same as that of the metal-fluid interface must be considered. The method of constructing and mounting the thermocouples makes the thermal conduction through the leads very small, and the displacement of the junction from the surface is small and does not lead to appreciable errors. Errors in measuring the energy input were small, but the flux decreased slightly with time owing to changes in voltage of the power batteries used. This change in power was less than 0.1 per cent and constituted the greatest error in the determination of the gross thermal flux. The uncertainty in the determination of the mean values of the dimensions was less than 0.01 per cent. Irregularities in the spacing were small and not significant. It is believed that the measuring shells were concentric, but even if they were not perfectly placed, the error introduced as a result would be small. Based on an equation derived by Vargaftik (58) and studies reported by Ingersoll, Zobel, and Ingersoll (59), it was found that if the distance between the centers of the spheres was five per cent of the distance between the spheres, the error introduced by the assumption that the spheres were concentric would be only 0.1 per cent. The total error introduced by the measuring instruments and their calibration should be less than 1.5 per cent.

While the overall behavior of the cell conformed to

the ideal case used as a model, there were some deviations. These were manifested by the differences of the apparent thermal conductivity as determined from the measurements of the upper and lower thermocouples. While these differences were of significant size they did not appreciably affect the calculated values of the thermal conductivity. Some other factors that might lead to errors in the behavior of the system were the irregularities in the spheres due to the thermocouples, supports, and closures. Their effects were minimized by placing them appropriately and by making them as small as possible. The added uncertainties introduced by departures from ideal behavior should not more than double the other uncertainties. So it would seem that the probable error in the values of the thermal conductivity should be less than three per cent. It would have been desirable to check the accuracy of the reported results by measurements upon a fluid of known thermal conductivity, but the change in characteristics of the cell as a result of the attack by the high temperature nitrogen dioxide made this impossible.

The general operating characteristics of the thermal conductivity cell have been proved to be satisfactory, but some modifications would be desirable. Before any further work can be done the thermocouples must be recalibrated or replaced. Recalibration would have to be done with the thermocouples in place. If the cell were modified it would

be desirable to remove the thermocouples from contact with the sample, and the use of a resistance element in place of the thermocouples might offer advantages. It would also be desirable to refinish the surfaces where minor effects of the chemical attack can be seen. This could best be done by plating, which would be good also for reducing the radiant transport by lowering the emissivity. It might be possible to decrease the amount of circulation in the region around the shaft by altering the geometry. These repairs and alterations must be carefully planned before they are attempted because the time to assemble the apparatus is large. Nine months effort by two workers was required to assemble and test the cell initially.

The experimental plans of the project include measurement of the thermal conductivities of the other oxides of nitrogen and their mixtures. It would appear best to continue with the experimental program by recalibration of the thermocouples until a more complete understanding of the behavior of the cell is obtained.

References

1. Keyes, F. G., Trans. A.S.M.E., 73, 589 (1951).
2. Hilsenrath, J. and Touloukian, Y.S., Trans. A.S.M.E., 76, 967 (1954).
3. Hilsenrath, J. et al., "Tables of Thermal Properties of Gases," National Bureau of Standards Circular 564, U.S. Dept. of Comm., Washington, D.C. (1955).
4. Sakiadis, B. C. and Coates, J., Louisiana State Univ. Eng. Exptl. Sta. Bull. No. 34 (1952).
5. Sakiadis, B. C. and Coates, J., A.I.Ch.E. Journal, 1, 275 (1955).
6. Mason, H. L., Trans. A.S.M.E., 76, 817 (1954).
7. Comings, E. W. and Nathan, M. F., Ind. Eng. Chem., 39, 964 (1947).
8. Lenoir, J. M. and Comings, E. W., Chem. Eng. Prog., 47, 223 (1951).
9. Lenoir, J. M., Junk, W. A., and Comings, E. W., Chem. Eng. Prog., 49, 539 (1953).
10. Stolyarov, E. A., Zh. fiz. Khim. (U.S.S.R.), 24(3), 279 (1950).
11. Keyes, F. G., Trans. A.S.M.E., 76, 809 (1954).
12. Magnanini, G. and Zunino, V., Gazz. Chim. Ital., 30, 405 (1900).
13. Nernst, W., Ann. Physik, Boltzmann Festschr., 904 (1904).
14. Todd, G. W., Proc. Roy. Soc. (London), A83, 19 (1909).

15. Yost, D. M. and Russell, H. Jr., "Systematic Inorganic Chemistry," Chap. I, Prentice-Hall, Inc., New York (1944).

16. Gray, P. and Yoffe, A. D., Chem. Rev., 55, 1069 (1955).

17. Schlinger, W. G. and Sage, B. H., Ind. Eng. Chem., 42, 2158 (1950).

18. Reamer, H. H. and Sage, B. H., Ind. Eng. Chem., 44, 185 (1952).

19. Richter, G. N., Reamer, H. H., and Sage, B. H., Ind. Eng. Chem., 45, 2117 (1953).

20. Chapman, S., Phil. Trans. Roy. Soc., 211A, 433 (1912).

21. Ibid., 216A, 279 (1915).

22. Eucken, A., Phys. Zeit., 14, 324 (1913).

23. Jeans, J., "An Introduction to the Kinetic Theory of Gases," Chap. VII, Cambridge Univ. Press (1948).

24. Kennard, E. H., "Kinetic Theory of Gases," Chap. IV, McGraw Hill Book Co., Inc., New York (1938).

25. Hirschfelder, J. O., Curtiss, C. F., and Bird, R. B., "Molecular Theory of Gases and Liquids," Chap. I, VII, and VIII, John Wiley and Sons, Inc., New York (1954).

26. Bridgman, P. W., "The Physics of High Pressure," Reprinted Edition, page 316, G. Bell and Sons, Ltd., London (1949).

27. Kardos, A., Forsch. Geb. Ing., 5, 14 (1934).

28. Sakiadis, B. C. and Coates, J., A.I.Ch.E. Journal, 1, 281 (1955).

29. Uhlir, A. Jr., J. Chem. Phys., 20, 463 (1952).

30. Smith, J. F. D., Ind. Eng. Chem., 22, 1246 (1930).

31. Waelbroeck, F., Lafleur, S., and Prigogine, I., Physica, 21, 667 (1955).

32. Hirschfelder, J. O., J. Chem. Phys., 25, 000 (1957) (to be published).

33. McAdams, W. H., "Heat Transmission," 3rd Edit., Chap. III, McGraw Hill Book Co., Inc., New York (1954).

34. Kraussold, H., Forsch. Gebiete. Ing., 5B, 186 (1934).

35. Jeans, J., "An Introduction to the Kinetic Theory of Gases," page 190, Cambridge University Press (1948).

36. Kennard, E. H., "Kinetic Theory of Gases," Chap. VIII, McGraw Hill Book Co., Inc., New York (1938).

37. Dickens, B. G., Proc. Roy. Soc. (London), A143, 517 (1934).

38. Bates, O. K., Ind. Eng. Chem., 25, 431 (1931).

39. Martin, L. H. and Lang, K. C., Proc. Phys. Soc. London, 45, 523 (1933).

40. Schleirmacher, A., Ann. d. Physik, 36, 346 (1889).

41. Weber, S., Ann. d. Physik, 54, 325 (1917).

42. Taylor, W. J. and Johnston, H. L., J. Chem. Phys., 14, 219 (1946).

43. Goldschmidt, R., Phys. Zeit., 12, 418 (1911).

44. Weber, S., Ann. d. Physik, 82, 479 (1927).

45. Kannuluik, W. G. and Martin, L. H. Proc. Roy. Soc. (London), A141, 144 (1933).

46. Ibid., A144, 496 (1934).

47. Keyes, F. G. and Sandell, D. J. Jr., Trans. A.S.M.E., 72, 767 (1950).

48. Keyes, F. G., Trans. A.S.M.E., 76, 809 (1954).

49. Kannuluik, W. G. and Carman, E. H., Proc. Roy. Soc. (London), 65B, 701 (1952).

50. Riedel, L., Chem.-Ing.-Tech., 23, 321 (1951).

51. Ibid., 23, 465 (1951).

52. Curie, M. and Lepape, A., J. de Phys. et le Rad., 2, 392 (1931).

53. Carslaw, H. S. and Jaeger, J. C., "Conduction of Heat in Solids," Chap. I and IX, Oxford Univ. Press (1950).

54. Fourier, J., "The Analytical Theory of Heat," translated with notes by A. Freeman, Dover Publications, Inc., New York (1955).

55. Sage, B. H. and Lacey, W. N., Trans. A.I.M.M.E., 136, 136 (1940).

56. Reamer, H. H. and Sage, B. H., Rev. Sci. Instr., 24, 362 (1953).

57. Clusius, K. and Vecchi, M., Helv. Chim. Acta., 36, 930 (1930).

58. Vargaftik, N., Tech. Phys., U.S.S.R., 4, 341 (1937).

59. Ingersoll, L. R., Zobel, O. J., and Ingersoll, A. C., "Heat Conduction," page 207 , McGraw Hill Book Co., Inc., New York (1948).

Nomenclature

a, b, c constants

A component A

B component B

C_p heat capacity at constant pressure

C_v heat capacity at constant volume

C constant in Sutherland equation

$\mathcal{E}$ thermocouple voltage

$\mathcal{E}_c$ voltage drop across current resistor

$\mathcal{E}_d$ voltage drop across voltage divider segment

F constant in equation for thermal conductivity

k thermal conductivity

k_{st} thermal conductivity of steel

ℓ separation of plates in a thermal conductivity cell

L available intermolecular distance

M molecular weight

n coordinate normal to surface

$\mathcal{P}$ thermoelectric power = $\frac{d\mathcal{E}}{dT}$

$\mathring{q}$ heat flux at a point

$\mathring{Q}_c$ rate of heat transfer by conduction

$\mathring{Q}_m$ measured rate of energy addition

$\mathring{Q}_p$ rate of heat transfer through pins

$\mathring{Q}_r$ rate of heat transfer by radiation

$\mathring{Q}_s$ rate of heat transfer through shaft

r radius or radial coordinate

r_i inner radius

r_o outer radius

r_p radius of pins

R_c resistance of current resistor

R_d resistance of voltage divider segment

R_t resistance of voltage divider system

R gas constant

T temperature

T_i temperature at inner radius

T_o temperature at outer radius

T_∞ temperature at reference state

U_s velocity of sound

γ ratio of heat capacities = $\frac{C_p}{C_v}$

η viscosity

η_∞ viscosity at reference state

ρ density

τ temperature in (^oF-32)

ϕ_A ratio of area of complete sphere to that of sphere minus area intercepted by shaft

β coefficient of expansion

List of Figures

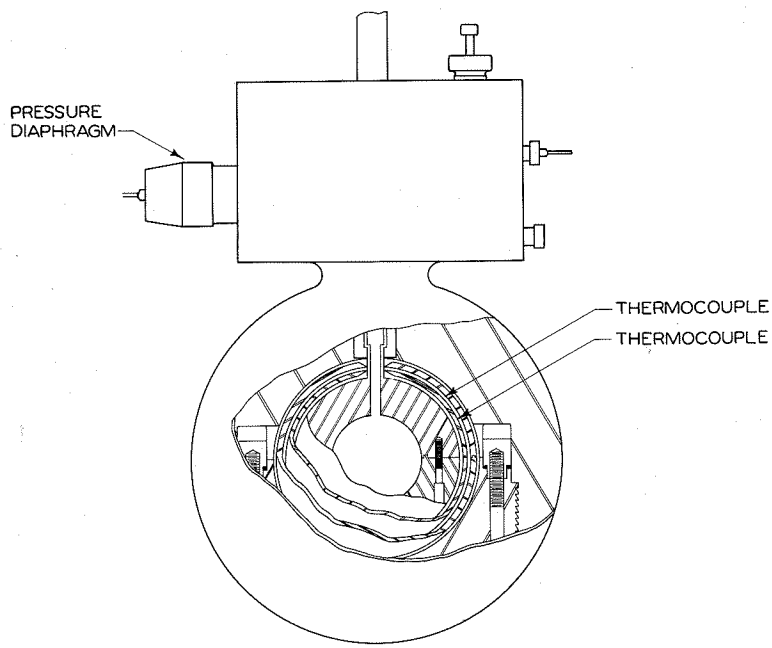

Figure 1. Schematic View of Thermal Conductivity Cell

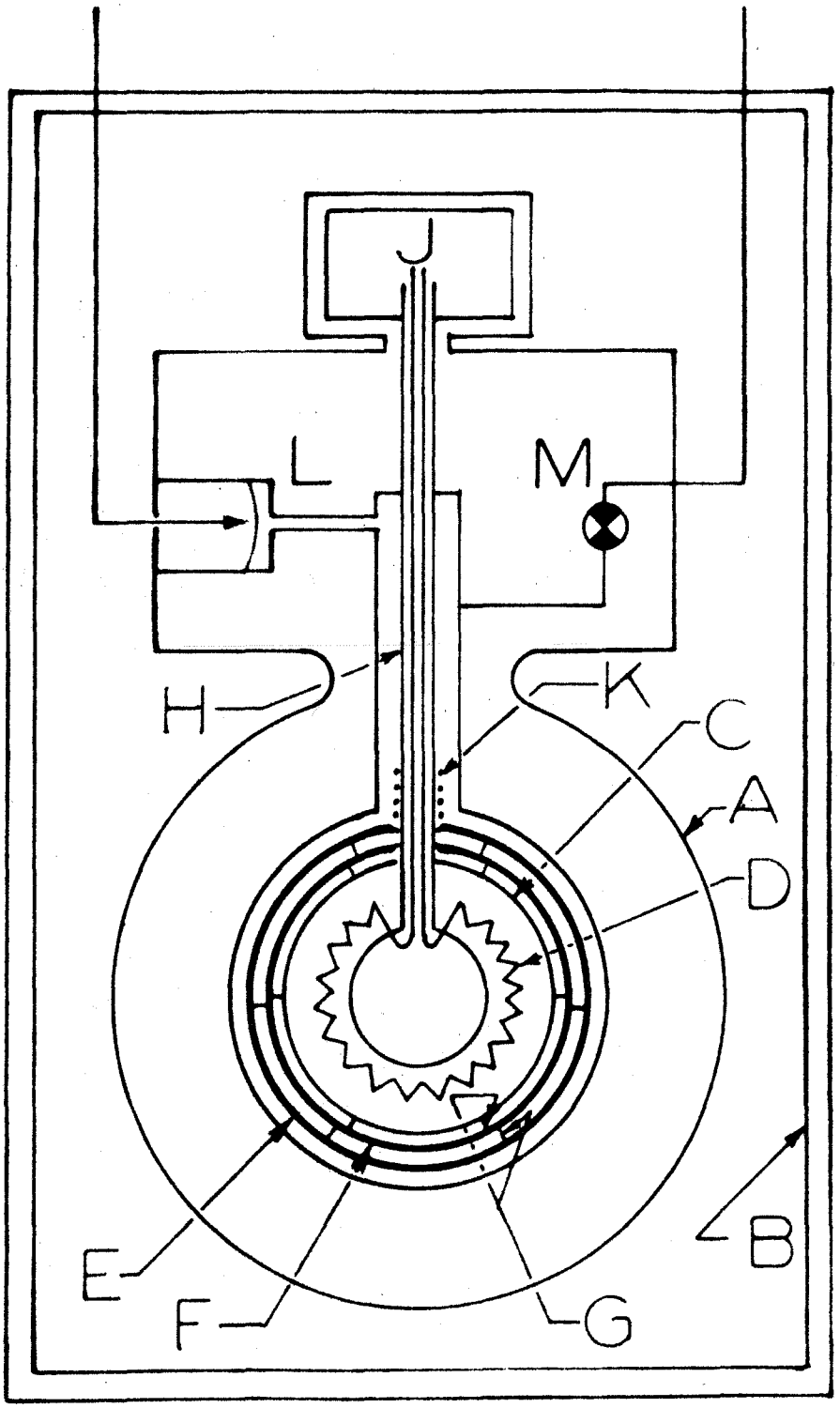

Figure 2. Arrangement of Thermal Conductivity Cell

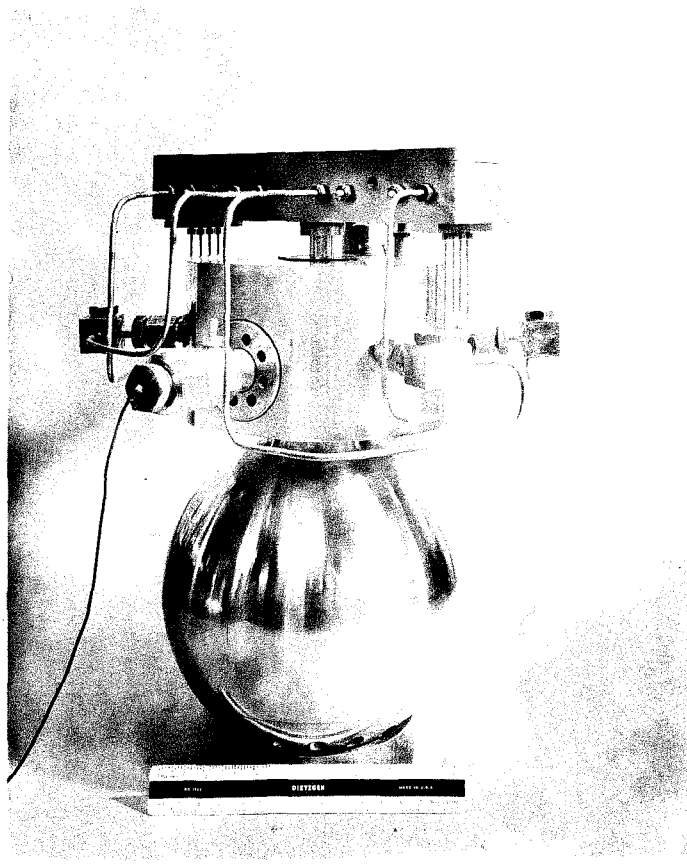

Figure 3. Assembled Thermal Conductivity Cell

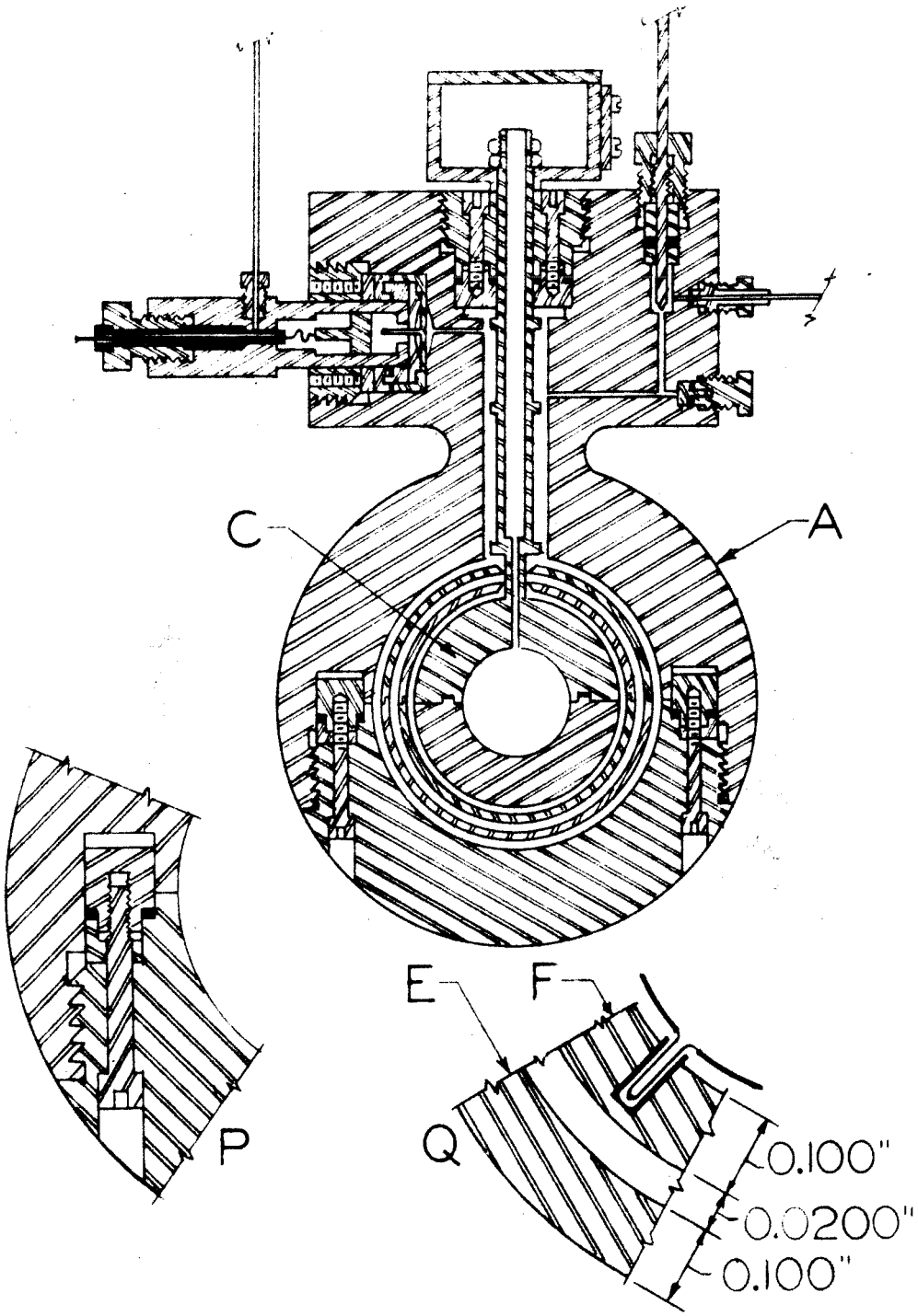

Figure 4. Sectional View of Thermal Conductivity Cell

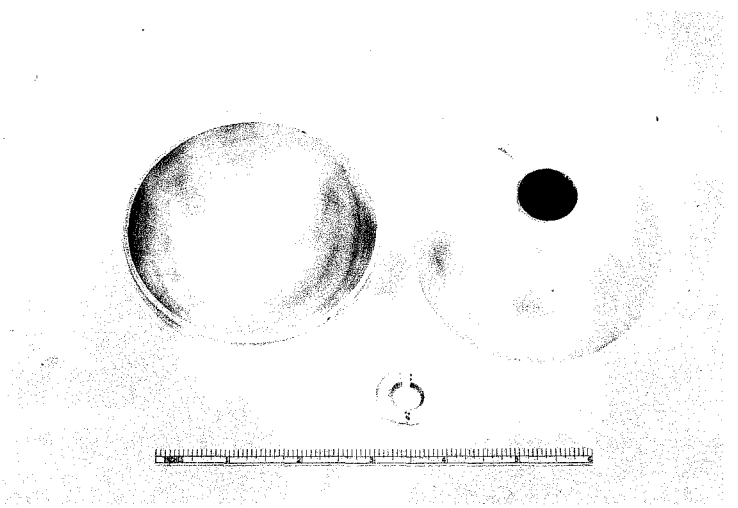

Figure 5. Appearance of Outer Shell

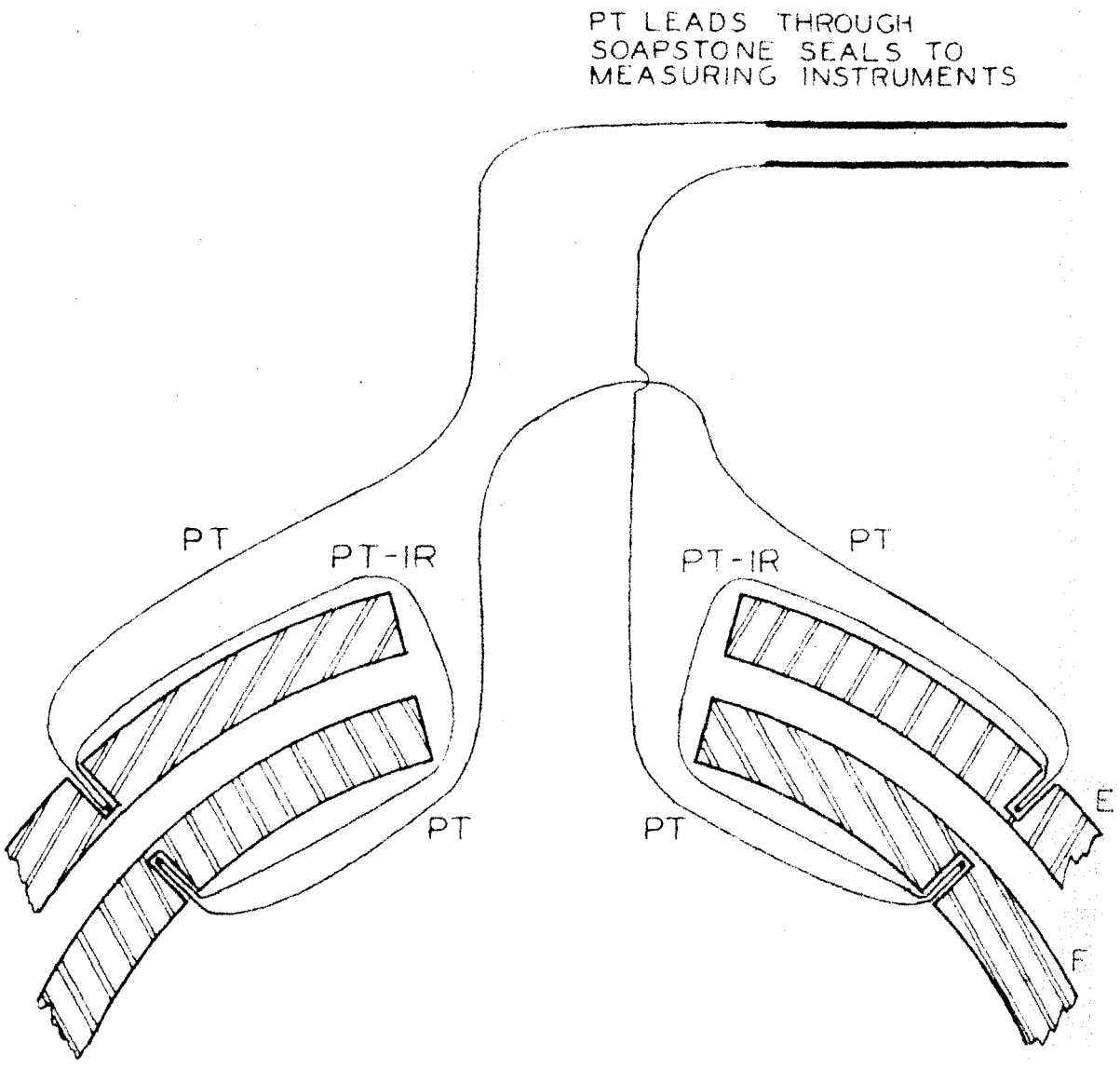

Figure 6. Schematic Arrangement of Thermocouples between Shells E and F

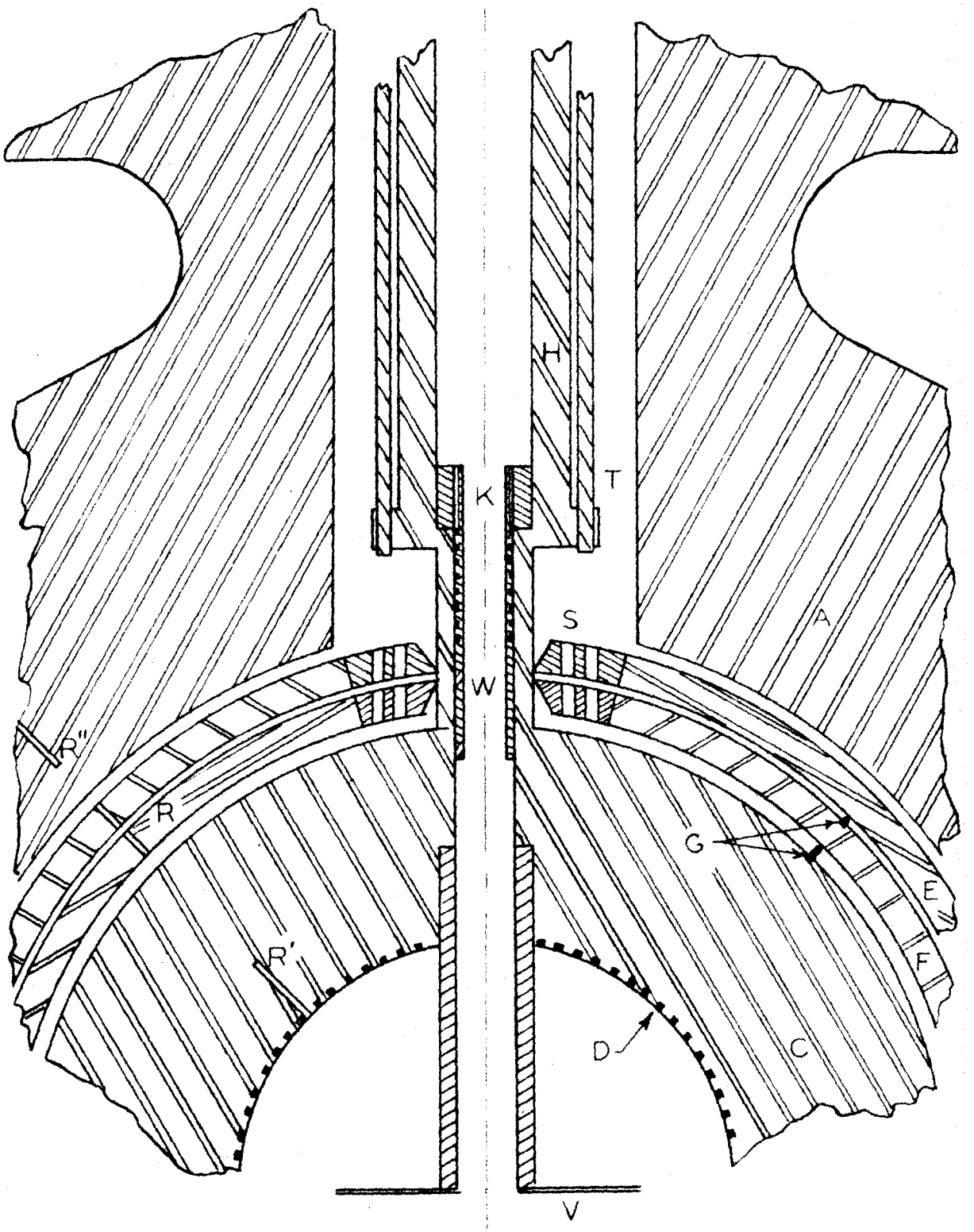

Figure 7. Details of Cell

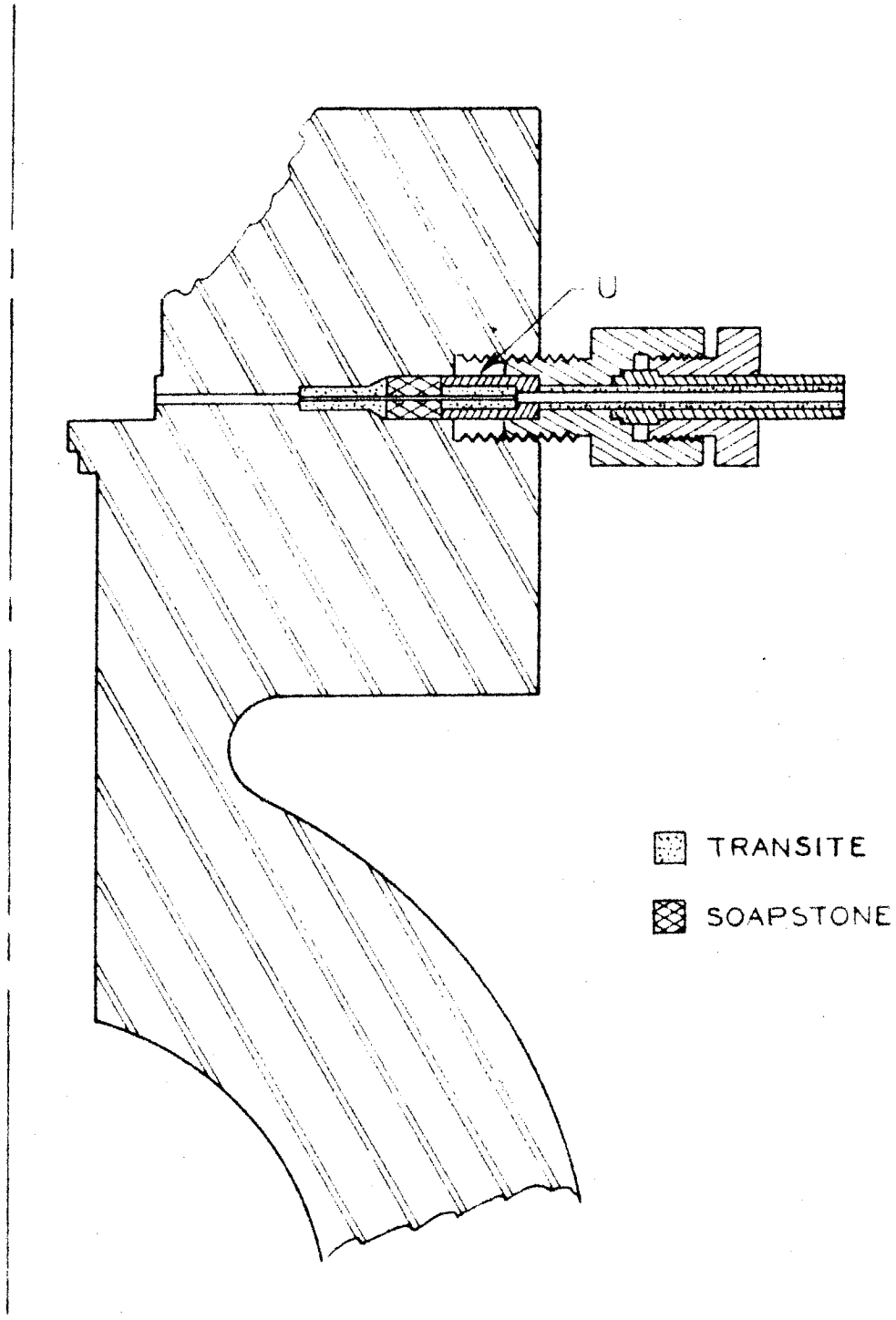

Figure 8. Details of Soapstone Pressure Seal for Thermocouple Leads

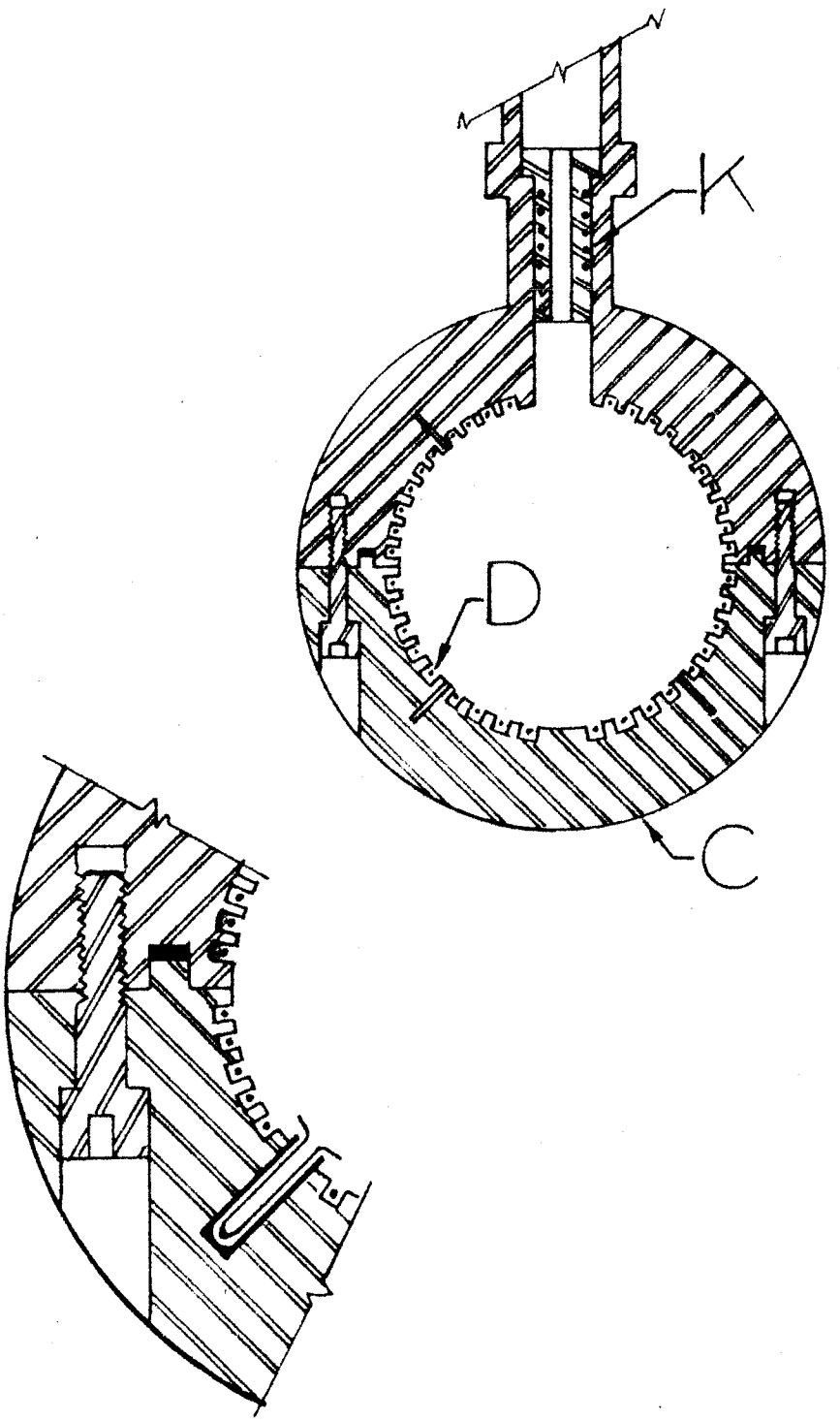

Figure 9. Details of Construction of Center Sphere

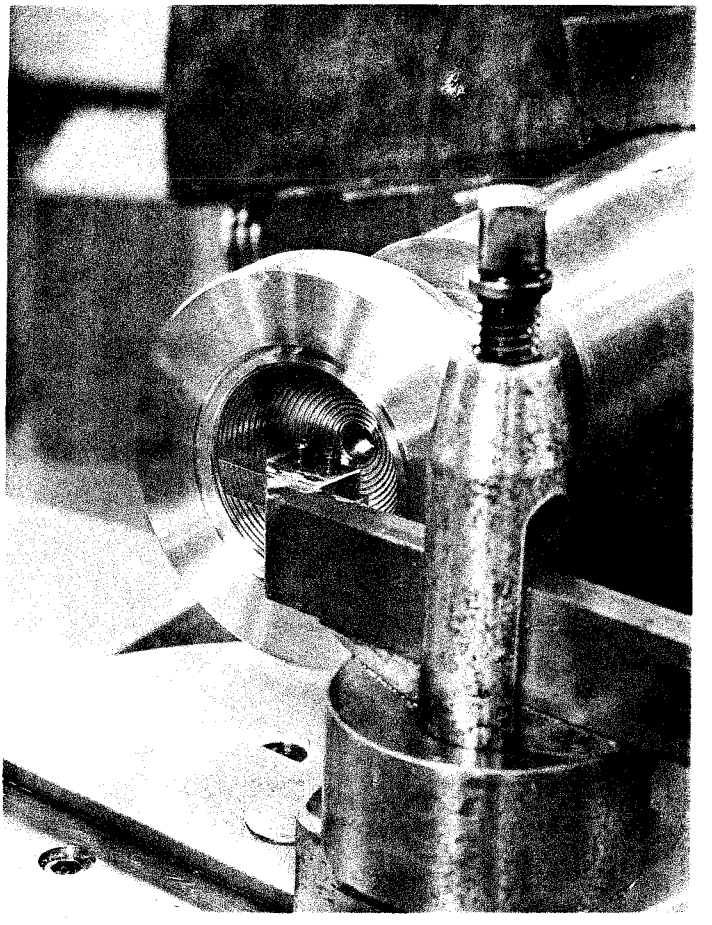

Figure 10. Center Sphere during Machining

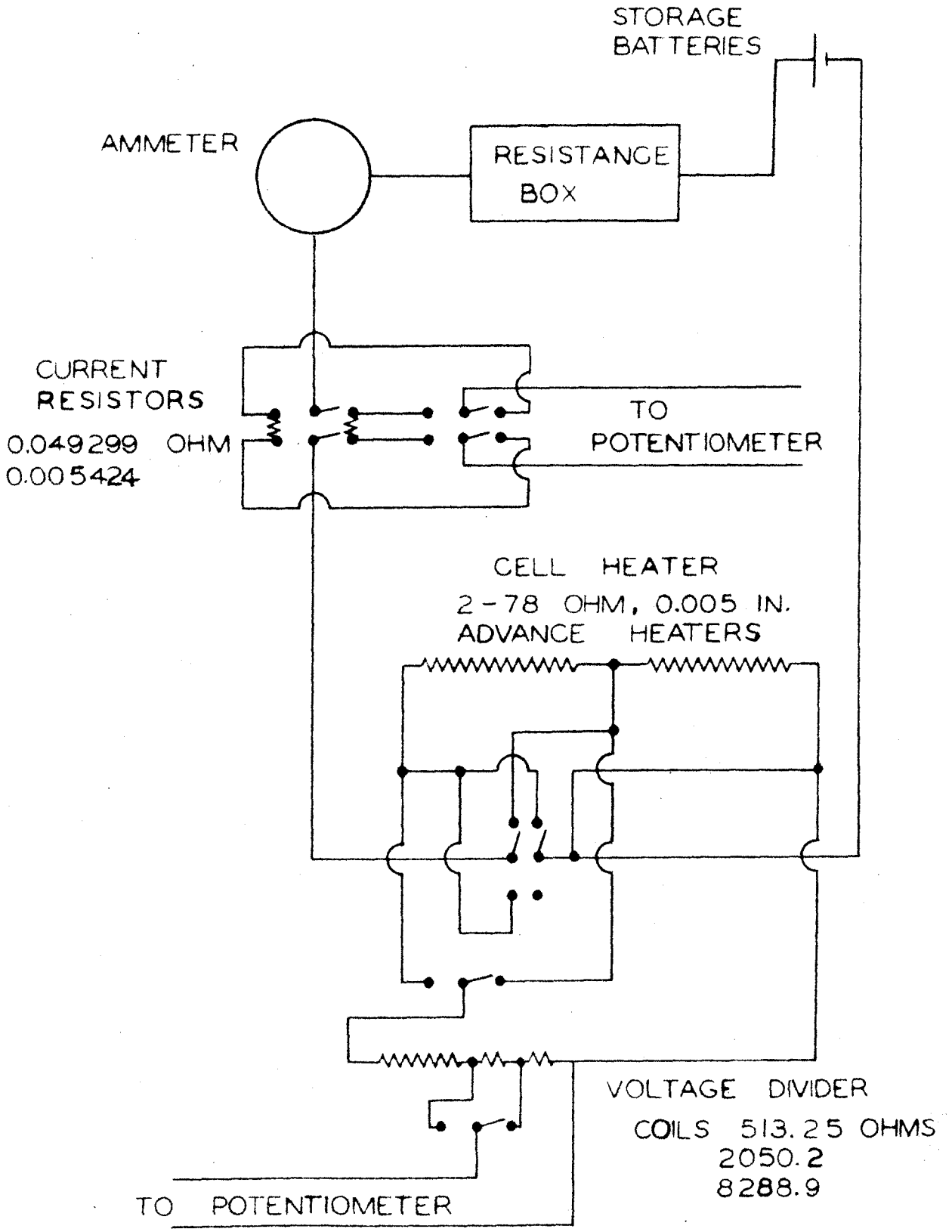

Figure 11. Energy Addition and Measurement Circuit

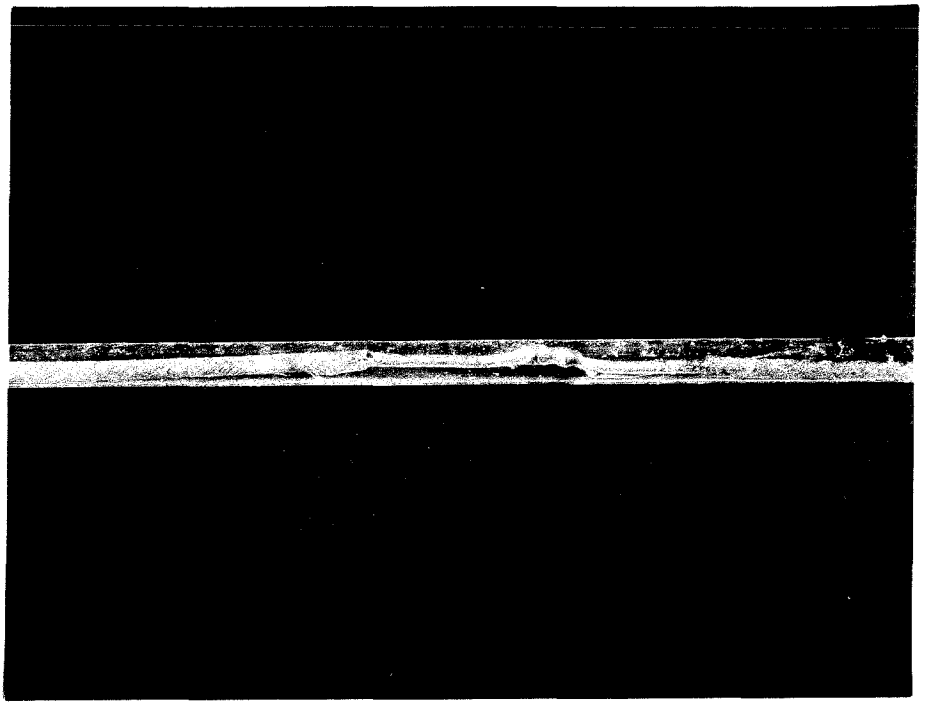

Figure 12. Details of Electrical Leads to Heater

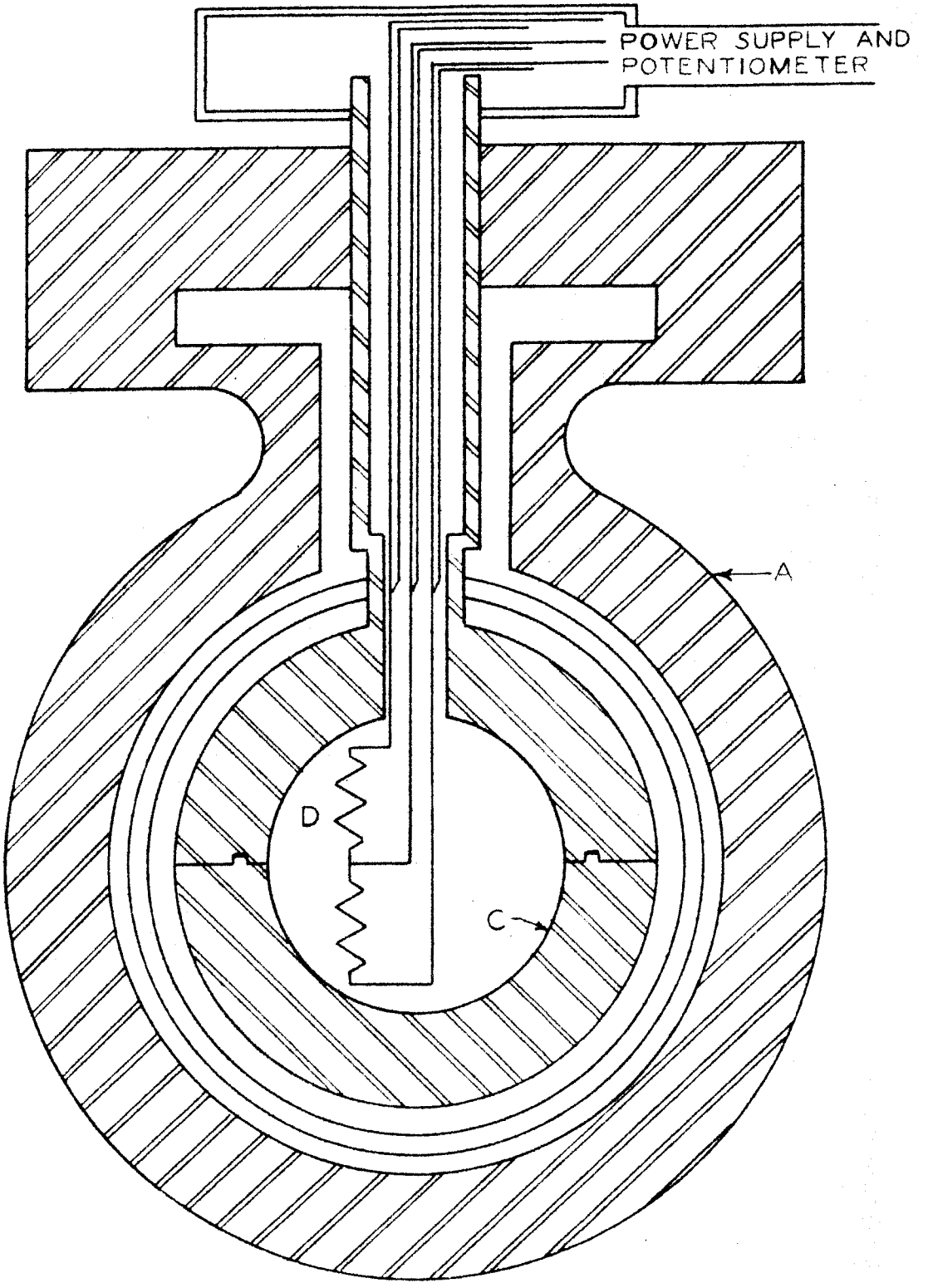

Figure 13. Schematic Arrangement of Heater and Potential Leads

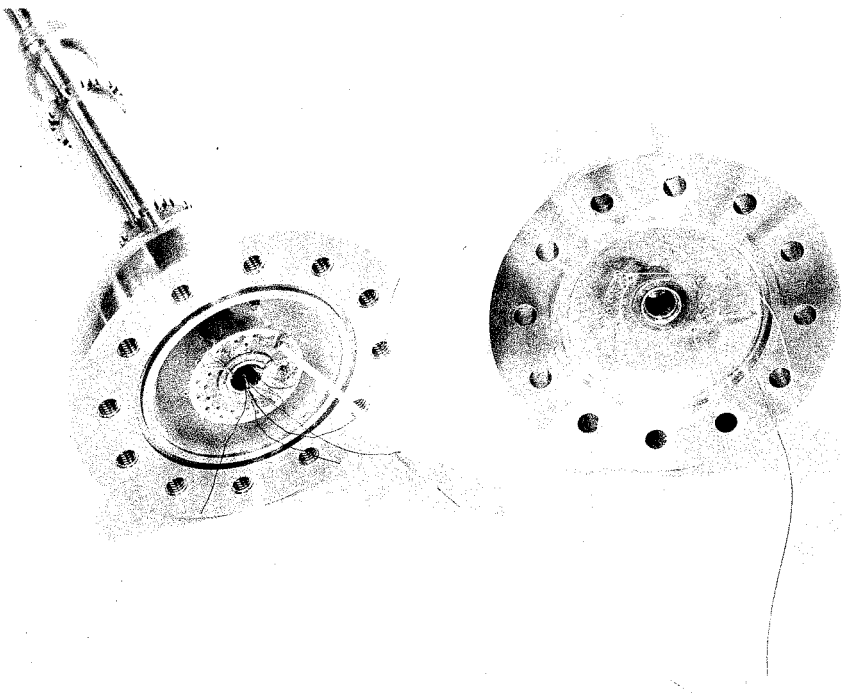

Figure 14. Interior of Center Sphere

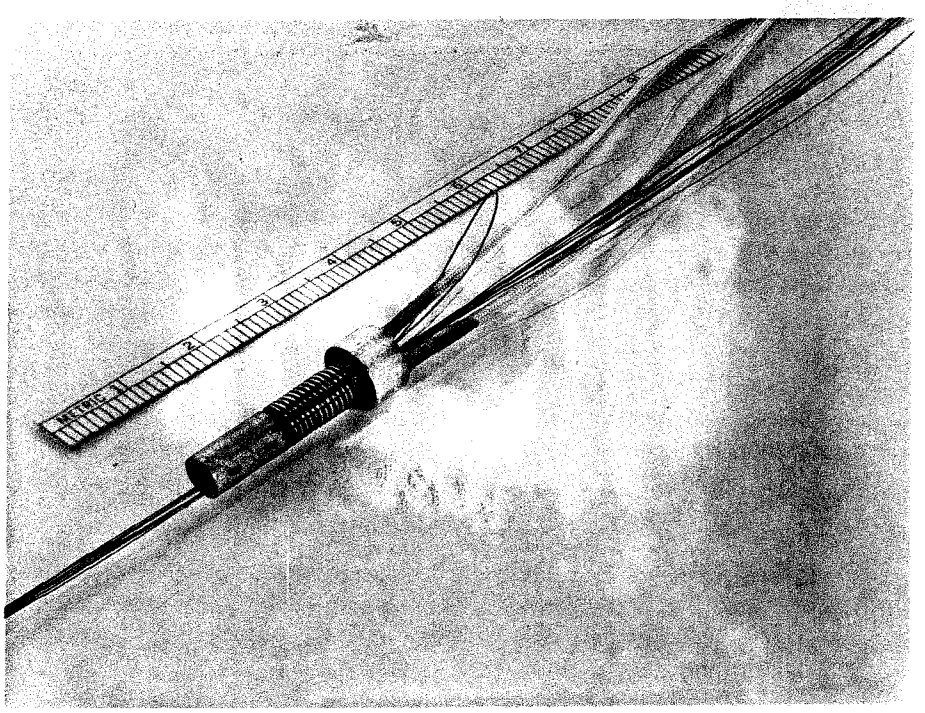

Figure 15. Guard Heater before Installation

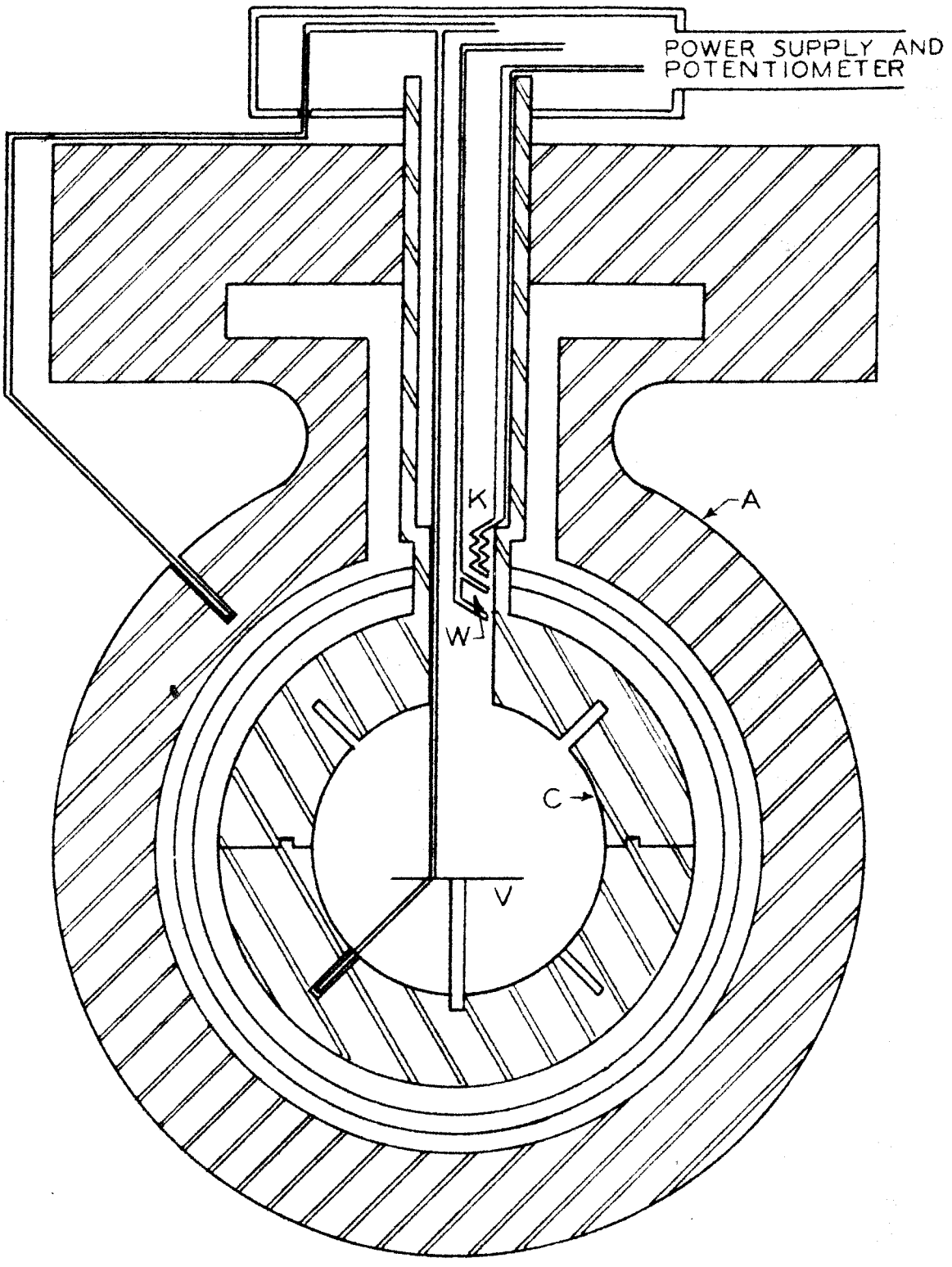

Figure 16. Schematic Arrangement of Guard Heater and Thermocouple and Typical Sphere A - Sphere C Thermocouple

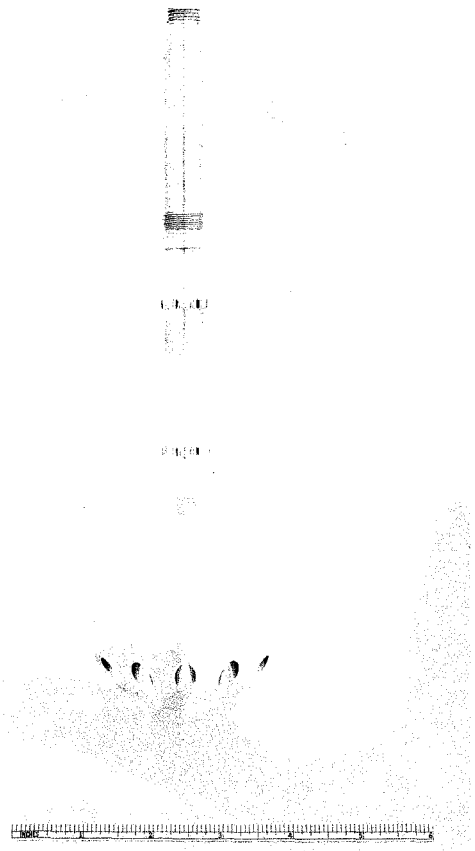

Figure 17. Exterior of Center Sphere

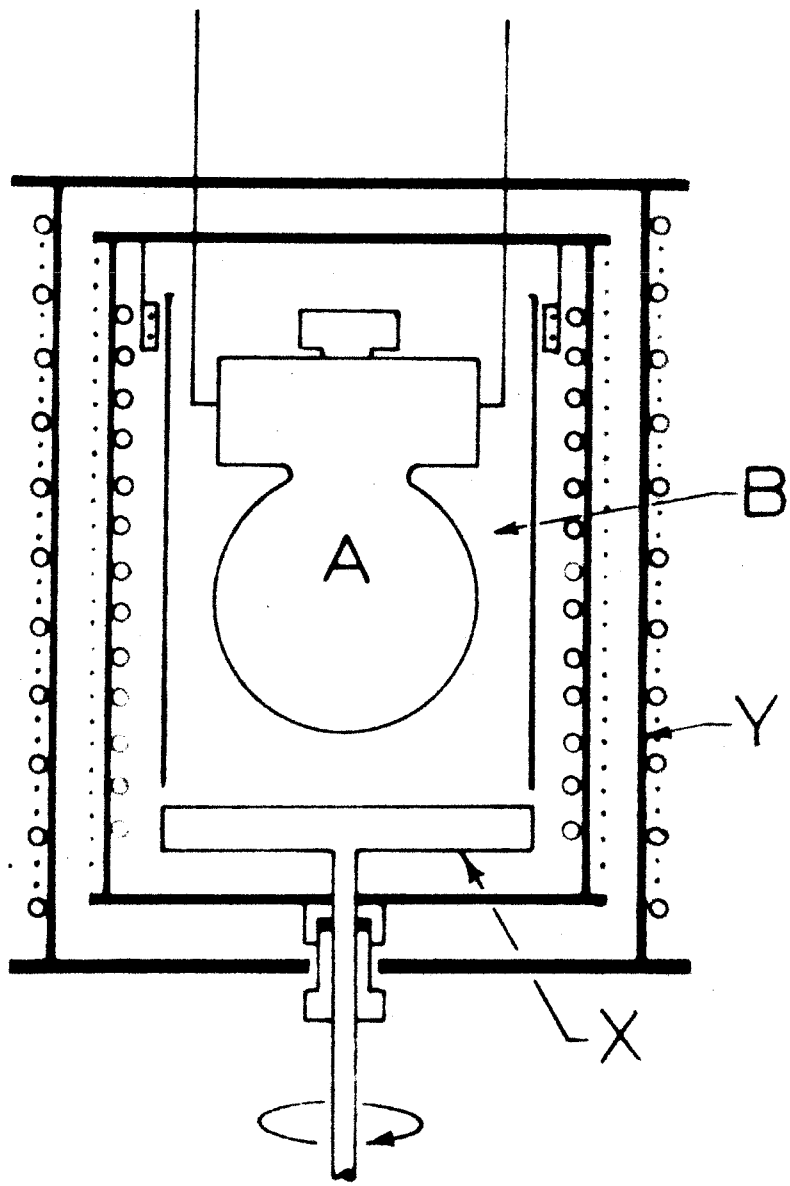

Figure 18. General Arrangement of Equipment

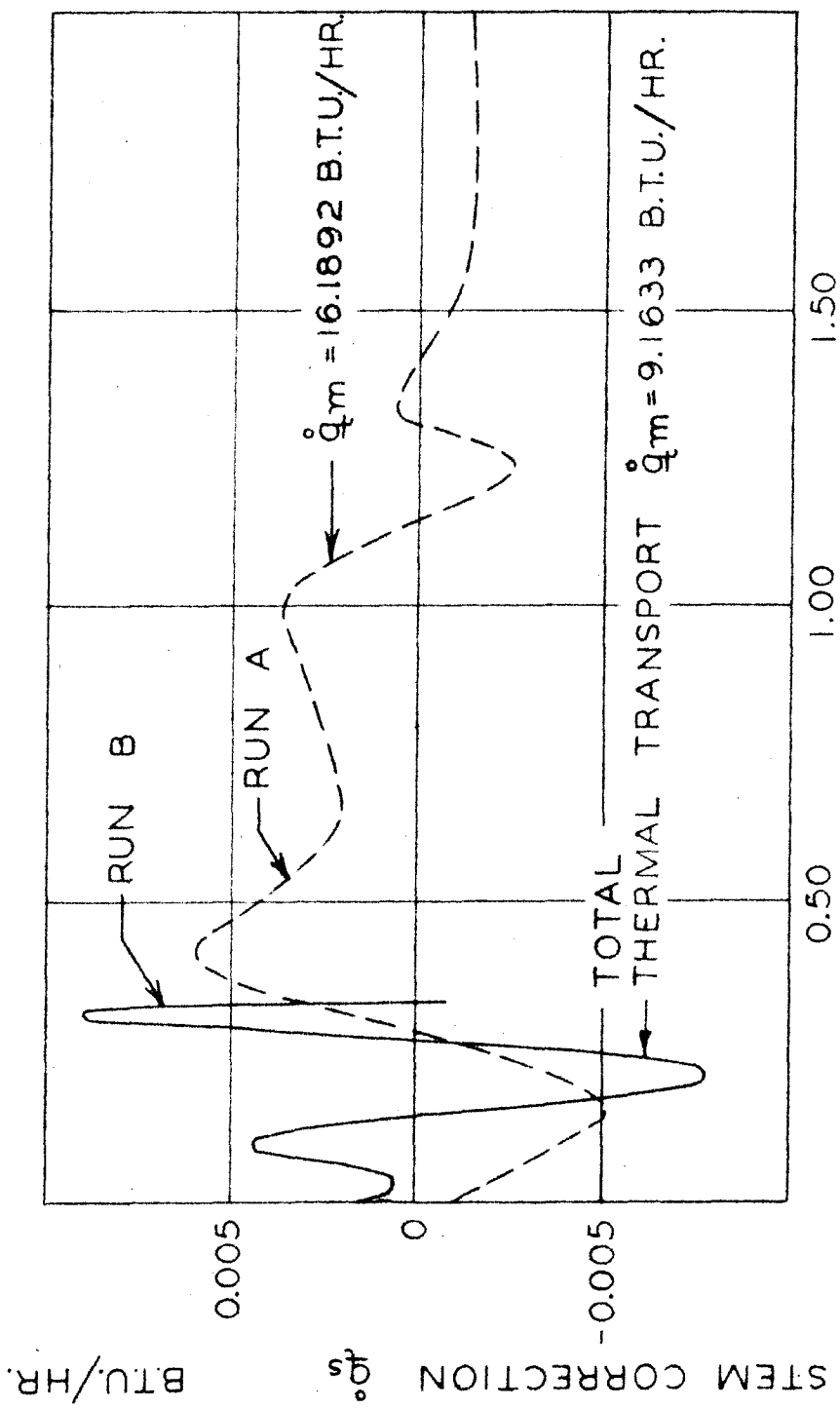

Figure 19. Heat Losses through Shaft as a Function of Time

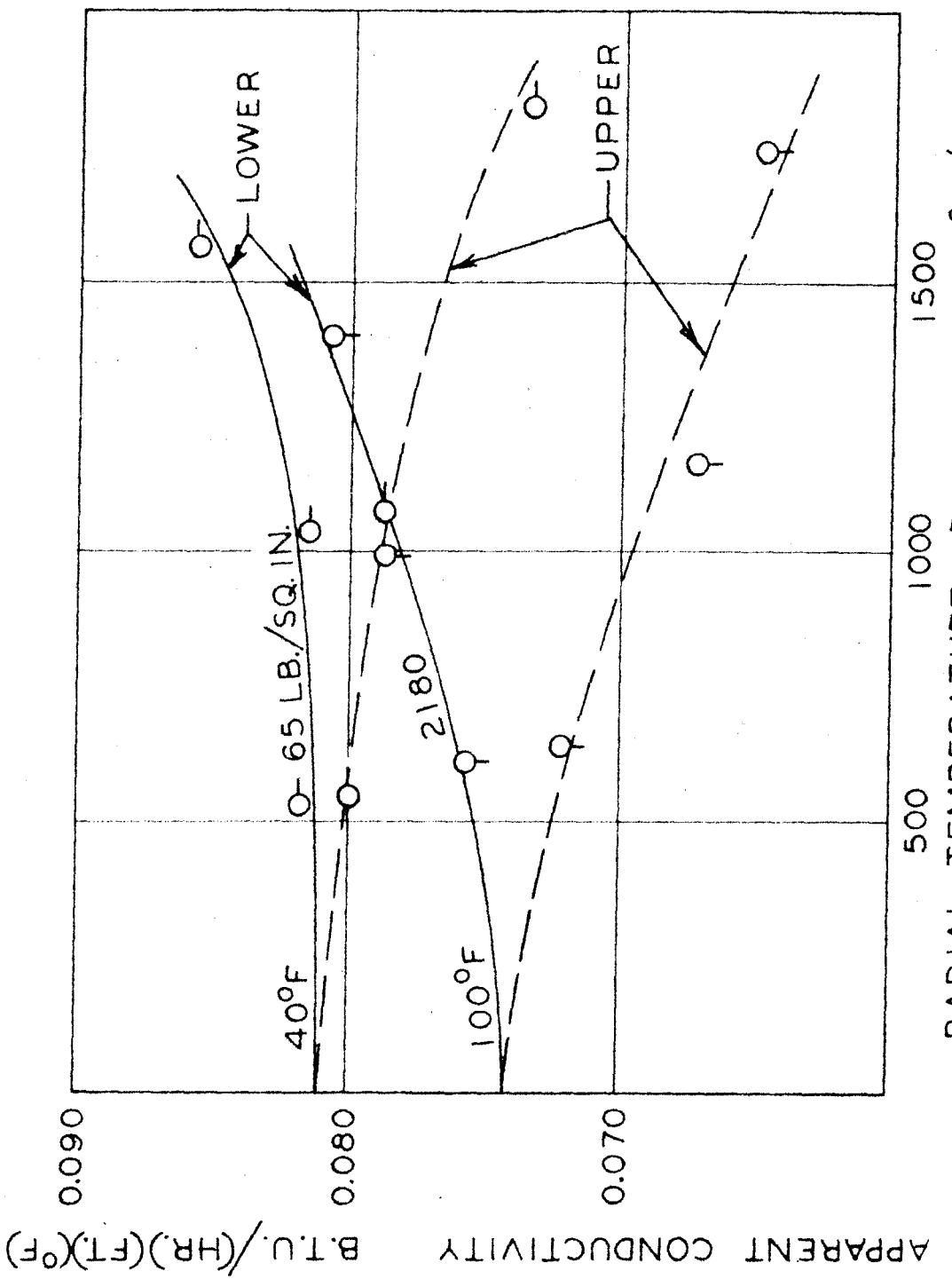

Figure 20. Influence of Temperature Gradient upon Apparent Thermal Conductivity

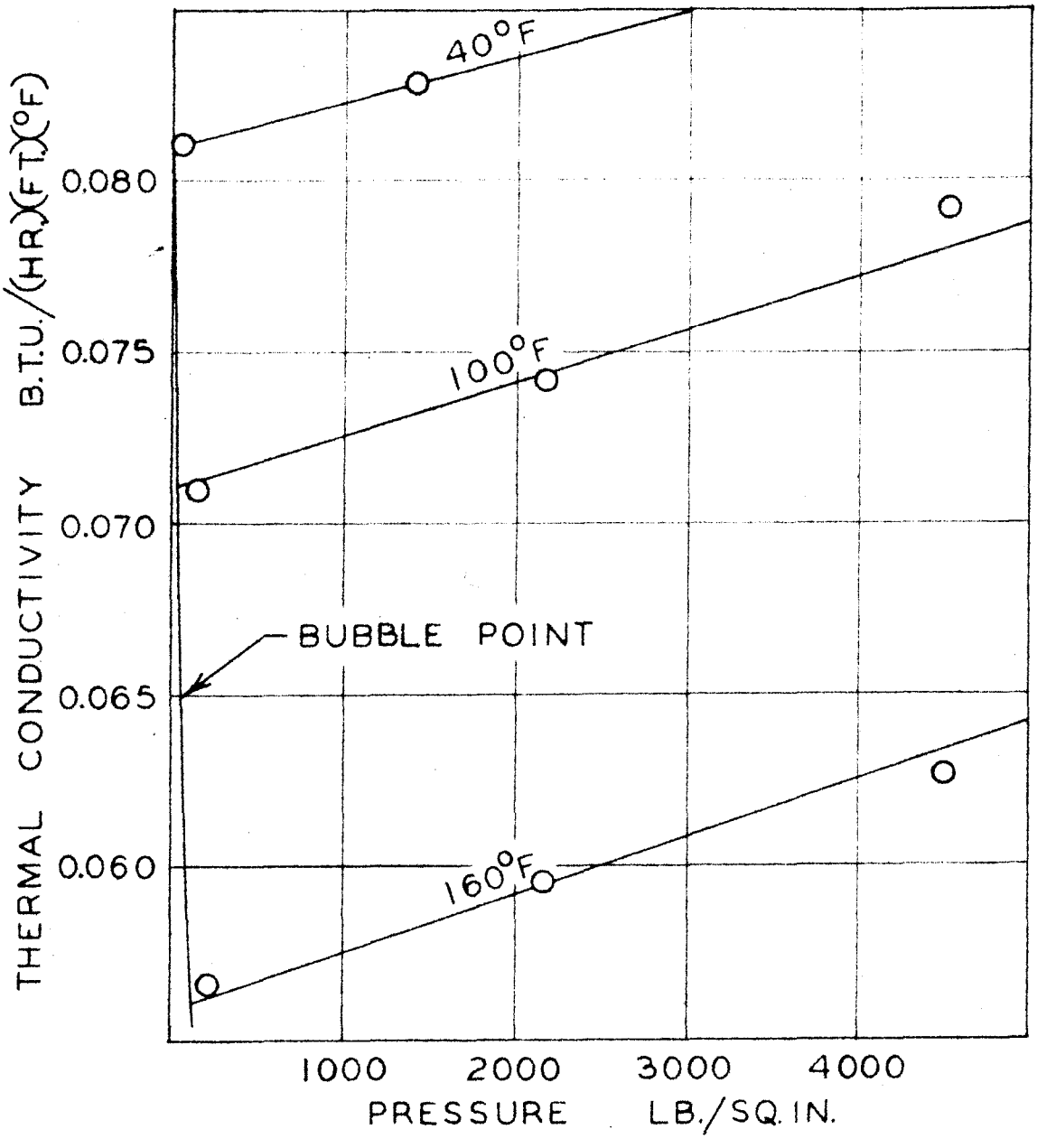

Figure 21. Thermal Conductivity of Nitrogen Dioxide in the Liquid Phase

LIST OF TABLES

TABLE I. DIMENSIONS OF EQUIPMENT

Temperature	$10^3(r_o-r_i)$	$\frac{10^3(r_o-r_i)}{4\pi r_i r_o}$
°F.	ft.	ft.$^{-1}$
40	1.6639	6.7958
100	1.6647	6.7926
160	1.6655	6.7893
220	1.6663	6.7861
280	1.6671	6.7828
340	1.6679	6.7796
400	1.6687	6.7763

TABLE II SAMPLE EXPERIMENTAL THERMAL CONDUCTIVITY MEASUREMENTS

Quantity	Units	Conditions		
Bath Temperature	°F.	40	40	40
Pressure at Zero Flux	lb./sq.in.abs.	65.0	65.0	65.0
Measured Energy Input Rate	Btu./hr.	10.6667	20.7281	32.7949
Pressure	lb./sq.in.abs.	315.6	529.5	766.7
Upper Half Sphere				
Temperature Difference	°F.	0.905	1.786	3.034
Rate of Loss through Pins	Btu./hr.	0.0415	0.0819	0.1392
Transfer by Conduction	Btu./hr.	10.6471	20.6898	32.7256
Apparent Thermal Conductivity	Btu./hr.ft.°F.	0.0780	0.0787	0.0733
Lower Half Sphere				
Temperature Difference	°F.	0.884	1.726	2.597
Rate of Loss through Pins	Btu./hr.	0.0405	0.0792	0.1191
Transfer by Conduction	Btu./hr.	10.6496	20.6941	32.7472
Apparent Thermal Conductivity	Btu./hr.ft.°F.	0.0818	0.0815	0.0857
Thermal Conductivity[a]	Btu./hr.ft.°F.	0.0811	0.0811	0.0811

a Extrapolated to zero flux

TABLE II SAMPLE EXPERIMENTAL THERMAL CONDUCTIVITY MEASUREMENTS (cont.)

Quantity	Units	Conditions		
Bath Temperature	°F.	40	40	40
Pressure at Zero Flux	lb./sq.in.abs.	1418	1418	1418
Measured Energy Input Rate	Btu./hr.	10.7228	23.9776	34.8977
Pressure	lb./sq.in.abs.	1652.0	2026.9	2235.5
Upper Half Sphere				
Temperature Difference	°F.	0.844	2.025	3.131
Rate of Loss through Pins	Btu./hr.	0.0387	0.0929	0.1436
Transfer by Conduction	Btu./hr.	10.7061	23.9354	34.8285
Apparent Thermal Conductivity	Btu./hr.ft.°F.	0.0863	0.0803	0.0756
Lower Half Sphere				
Temperature Difference	°F.	0.940	1.944	2.712
Rate of Loss through Pins	Btu./hr.	0.0431	0.0892	0.1244
Transfer by Conduction	Btu./hr.	10.7032	23.9407	34.8493
Apparent Thermal Conductivity	Btu./hr.ft.°F.	0.0774	0.0837	0.0873
Thermal Conductivity[a]	Btu./hr.ft.°F.	0.0827	0.0827	0.0827

[a] Extrapolated to zero flux

TABLE II SAMPLE EXPERIMENTAL THERMAL CONDUCTIVITY MEASUREMENTS (cont.)

Quantity	Units	Conditions		
Bath Temperature	°F.	100	100	100
Pressure at Zero Flux	lb./sq.in.abs.	2179.8	2179.8	2179.8
Measured Energy Input Rate	Btu./hr.	11.3104	19.2069	27.6692
Pressure	lb./sq.in.abs.	2414.2	2559.0	2705.1
Upper Half Sphere				
Temperature Difference	°F.	1.062	1.937	2.898
Rate of Loss through Pins	Btu./hr.	0.0507	0.0925	0.1384
Transfer by Conduction	Btu./hr.	11.2833	19.1551	27.5899
Apparent Thermal Conductivity	Btu./hr.ft.°F.	0.0722	0.0672	0.0647
Lower Half Sphere				
Temperature Difference	°F.	1.014	1.656	2.324
Rate of Loss through Pins	Btu./hr.	0.0484	0.0791	0.1110
Transfer by Conduction	Btu./hr.	11.2860	19.1690	27.6177
Apparent Thermal Conductivity	Btu./hr.ft.°F.	0.0756	0.0786	0.0807
Thermal Conductivity[a]	Btu./hr.ft.°F.	0.0742	0.0742	0.0742

[a] Extrapolated to zero flux

TABLE II SAMPLE EXPERIMENTAL THERMAL CONDUCTIVITY MEASUREMENTS (cont.)

Quantity	Units	Conditions				
Bath Temperature	°F.	100	100	100	100	100
Pressure at Zero Flux	lb./sq.in.abs.	157.9	157.9	157.9	157.9	157.9
Measured Energy Input Rate	Btu./hr.	10.2638	17.4355	25.5827	30.6436	37.4915
Pressure	lb./sq.in.abs.	292.1	478.4	615.3	694.5	818.1
Upper Half Sphere						
Temperature Difference	°F.	1.010	1.852	2.812	3.420	4.198
Rate of Loss through Pins	Btu./hr.	0.0482	0.0884	0.1343	0.1633	0.2005
Transfer by Conduction	Btu./hr.	10.2370	17.3839	25.5029	30.5458	37.3714
Apparent Thermal Conductivity	Btu./hr.ft.°F.	0.0689	0.0638	0.0616	0.0607	0.0605
Lower Half Sphere						
Temperature Difference	°F.	0.958	1.568	2.253	2.656	3.207
Rate of Loss through Pins	Btu./hr.	0.0457	0.0749	0.1076	0.1268	0.1531
Transfer by Conduction	Btu./hr.	10.2398	17.3979	25.5300	30.5827	37.4191
Apparent Thermal Conductivity	Btu./hr.ft.°F.	0.0726	0.0754	0.0770	0.0782	0.0793
Thermal Conductivity[a]	Btu./hr.ft.°F.	0.0710	0.0710	0.0710	0.0710	0.0710

[a] Extrapolated to zero flux

TABLE II SAMPLE EXPERIMENTAL THERMAL CONDUCTIVITY MEASUREMENTS (cont.)

Quantity	Units	Conditions		
Bath Temperature	°F.	100	100	100
Pressure at Zero Flux	lb./sq.in.abs.	4522.0	4522.0	4522.0
Measured Energy Input Rate	Btu./hr.	10.5775	20.5534	29.7556
Pressure	lb./sq.in.abs.	4746.9	4933.7	5094.1
Upper Half Sphere				
Temperature Difference	°F.	0.920	1.929	2.941
Rate of Loss through Pins	Btu./hr.	0.0439	0.0921	0.1404
Transfer by Conduction	Btu./hr.	10.5556	20.5049	29.6788
Apparent Thermal Conductivity	Btu./hr.ft.°F.	0.0779	0.0722	0.0686
Lower Half Sphere				
Temperature Difference	°F.	0.880	1.708	2.423
Rate of Loss through Pins	Btu./hr.	0.0420	0.0816	0.1157
Transfer by Conduction	Btu./hr.	10.5579	20.5158	29.7039
Apparent Thermal Conductivity	Btu./hr.ft.°F.	0.0815	0.0816	0.0833
Thermal Conductivity [a]	Btu./hr.ft.°F.	0.0791	0.0791	0.0791

[a] Extrapolated to zero flux

TABLE II SAMPLE EXPERIMENTAL THERMAL CONDUCTIVITY MEASUREMENTS (cont.)

Quantity	Units	Conditions	
Bath Temperature	°F.	160	160
Pressure at Zero Flux	lb./sq.in.abs.	219.3	219.3
Measured Energy Input Rate	Btu./hr.	9.1779	15.8070
Pressure	lb./sq.in.abs.	367.9	458.8
Upper Half Sphere			
Temperature Difference	°F.	1.138	2.028
Rate of Loss through Pins	Btu./hr.	0.0558	0.0994
Transfer by Conduction	Btu./hr.	9.1420	15.7418
Apparent Thermal Conductivity	Btu./hr.ft.°F.	0.0545	0.0527
Lower Half Sphere			
Temperature Difference	°F.	1.028	1.676
Rate of Loss through Pins	Btu./hr.	0.0504	0.0821
Transfer by Conduction	Btu./hr.	9.1473	15.7591
Apparent Thermal Conductivity	Btu./hr.ft.°F.	0.0604	0.0638
Thermal Conductivity[a]	Btu./hr.ft.°F.	0.0566	0.0566

[a] Extrapolated to zero flux

TABLE II SAMPLE EXPERIMENTAL THERMAL CONDUCTIVITY MEASUREMENTS (cont.)

Quantity	Units	Conditions		
Bath Temperature	°F.	160	160	160
Pressure at Zero Flux	lb./sq.in.abs.	2167.7	2167.7	2167.7
Measured Energy Input Rate	Btu./hr.	9.2171	15.8996	23.5635
Pressure	lb./sq.in.abs.	2333.5	2434.3	2545.0
Upper Half Sphere				
Temperature Difference	°F.	1.070	1.905	2.865
Rate of Loss through Pins	Btu./hr.	0.0524	0.0934	0.1404
Transfer by Conduction	Btu./hr.	9.1810	15.8407	23.4741
Apparent Thermal Conductivity	Btu./hr.ft.°F.	0.0582	0.0565	0.0556
Lower Half Sphere				
Temperature Difference	°F.	0.994	1.625	2.324
Rate of Loss through Pins	Btu./hr.	0.0487	0.0796	0.1139
Transfer by Conduction	Btu./hr.	9.1884	15.8544	23.5007
Apparent Thermal Conductivity	Btu./hr.ft.°F.	0.0627	0.0662	0.0687
Thermal Conductivity[a]	Btu./hr.ft.°F.	0.0596	0.0596	0.0596

[a] Extrapolated to zero flux

TABLE II SAMPLE EXPERIMENTAL THERMAL CONDUCTIVITY MEASUREMENTS (cont).

Quantity	Units	Conditions		
Bath Temperature	°F.	160	160	160
Pressure at Zero Flux	lb./sq.in.abs.	4517.5	4517.5	4517.5
Measured Energy Input Rate	Btu./hr.	9.2820	15.9398	21.4068
Pressure	lb./sq/in.abs.	4694.1	4797.9	4879.2
Upper Half Sphere				
Temperature Difference	°F.	1.037	1.788	2.424
Rate of Loss through Pins	Btu./hr.	0.0508	0.0876	0.1188
Transfer by Conduction	Btu./hr.	9.2513	15.8868	21.3344
Apparent Thermal Conductivity	Btu./hr.ft.°F.	0.0606	0.0603	0.0597
Lower Half Sphere				
Temperature Difference	°F.	0.952	1.554	2.045
Rate of Loss through Pins	Btu./hr.	0.0467	0.0762	0.1002
Transfer by Conduction	Btu./hr.	9.2555	15.8982	21.3530
Apparent Thermal Conductivity	Btu./hr.ft.°F.	0.0660	0.0695	0.0709
Thermal Conductivity [a]	Btu./hr.ft.°F.	0.0626	0.0626	0.0626

[a] Extrapolated to zero flux

TABLE III. EXPERIMENTAL VALUES OF THERMAL CONDUCTIVITY OF NITROGEN DIOXIDE IN THE LIQUID PHASE

Temperature °F.	Pressure Lb./Sq. Inch Absolute	Thermal Conductivity B.t.u./(Hr.)(Ft.)(°F.)
40	65.0	0.0811
	1418.-	0.0827
100	157.9	0.0710
	2179.8	0.0742
	4522.0	0.0791
160	219.3	0.0566
	2167.7	0.0596
	4517.5	0.0626

TABLE IV. THERMAL CONDUCTIVITY OF NITROGEN DIOXIDE IN THE LIQUID PHASE

Pressure Lb./Sq. Inch Absolute	40° F.	100° F.	160° F.
	(6.6)[ab]	(30.7)	(111.2)
Bubble Point	0.0809	0.0715	0.0560
200	0.0812[c]	0.0717	0.0562
400	0.0815	0.0720	0.0565
600	0.0817	0.0723	0.0568
800	0.0820	0.0726	0.0572
1000	0.0823	0.0729	0.0575
1250	0.0826	0.0733	0.0579
1500	0.0829	0.0736	0.0584
1750	0.0833	0.0740	0.0588
2000	0.0836	0.0744	0.0592
2250	0.0839	0.0747	0.0596
2500	0.0843	0.0751	0.0600
2750	0.0846	0.0754	0.0604
3000	0.0849	0.0758	0.0609
3500	-	0.0765	0.0617
4000	-	0.0772	0.0625
4500	-	0.0780	0.0634
5000	-	0.0787	0.0642

[a] Values in parentheses represent bubble-point pressures expressed in pounds per square inch absolute

[b] Bubble-point pressure at 40° F. extrapolated

[c] Thermal conductivity expressed in B.t.u./(hr.)(ft.)(°F.)

PART II

THERMAL CONDUCTIVITY OF NITRIC OXIDE

Introduction

There is only a limited amount of experimental data available concerning the thermal conductivity of nitric oxide and no investigations have been made to determine the change of this transport property with pressure. It was the object of this work to extend the studies of the thermal conductivity of nitric oxide to higher temperatures and pressures making use of the equipment described in the first part of this thesis.

Johnston and Grilly (1) determined the value of the thermal conductivity of nitric oxide at atmospheric pressure from 130° to 375°K., and Eucken (2) gives results at 200° and 273°K. Both made use of hot wire cells of the potential lead type. Todd (3) reports values for both nitrogen dioxide and nitric oxide determined in equipment of parallel plate design. His design and techniques combined, with the reported experimental difficulties in the case of nitric oxide, indicate his results are probably of little comparative value. Winkelmann (4) was the first to determine the value of this property, but his work is mainly of historical interest.

A knowledge of other properties of a compound is needed when its thermal conductivity is being studied. The physical and chemical properties of nitric oxide are summarized by Yost and Russell (5). Investigators at the Chemical Engi-

neering Laboratory of the California Institute of Technology have studied its pressure-volume-temperature relations (6) and calculated its thermodynamic properties (7). The available data on the thermal properties and viscosity of nitric oxide are summarized by Hilsenrath and Touloukian (8) and in two publications of the National Bureau of Standards (9,10).

Equipment Used

The basic principle of the apparatus used is that from measurements of the steady state thermal flux and resulting temperature difference between two concentric, isothermal spheres of known dimensions, the thermal conductivity of the fluid between the spheres can be computed. The measuring section of the cell consists of four concentric spheres. The center and outer ones are heavy walled vessels to confine the sample at high pressures. The measurements are based on the two middle spherical shells. Their dimensions are accurately known, and they are not affected by high pressure because they are surrounded by the sample. There is a heater in the center sphere which supplies a constant, known thermal flux through the spheres. The temperature difference between the spheres is measured by two thermocouples, one is in the upper hemisphere and one in the lower. The only departures from spherical geometry are a shaft to the center sphere, which contains the electrical leads to the heater, and small pins which hold the sphere in position. The complete apparatus is suspended in a constant temperature oil bath. Details of the equipment and its calibration are given in the first part of this thesis.

Experimental Methods

The methods of operation used in making the measurements needed to compute the thermal conductivity of gaseous nitric oxide were basically the same as those used in the case of nitrogen dioxide. In addition to the usual measurements it was necessary to determine the amount of energy transport by radiation, since nitric oxide does not absorb radiation, and to recalibrate the thermocouples used to measure the temperature difference between the spheres, since they had been damaged by the high temperature nitrogen dioxide.

Recalibration of Thermocouples

At the conclusion of the work with nitrogen dioxide it was found that the characteristics of the thermocouples used to measure the difference in temperature between the spheres had been changed. The thermocouples in the upper and lower half spheres showed significantly different behavior, and the thermoelectric power of both appeared to be higher. They were recalibrated by making measurements with helium in the cell, and using the known value of the thermal conductivity of helium to determine the relation between the voltage produced and the temperature difference.

The thermal conductivity of helium as a function of temperature at atmospheric pressure has been well established

by many investigators. The experimental results have been critically reviewed by Keyes (11) and Hilsenrath and Touloukian (8) who present the same equation to represent the data,*

$$\frac{k}{k_o} = \frac{1}{33.83 \times 10^{-5}} \left[\frac{2.347 \times 10^{-5} \sqrt{T}}{1 + \frac{43.54 \times 10^{-10/T}}{T}} \right] \qquad (1)$$

where T is the temperature in degrees Kelvin and the value of the thermal conductivity of helium at the reference state of one atmosphere and 32°F. is 8180 x 10^{-5} Btu./(hr.)(ft.)(°F.) or 33.83 x 10^{-5} cal./(sec.)(cm.)(°C.).

Helium at atmospheric pressure was studied in the apparatus at temperatures of 40°, 100°, 220°, 340°, and 400° F. At each bath temperature three levels of thermal flux were used.

The equation used for calculations was that derived in the first part of this thesis,

$$k = \frac{(\dot{Q}_m - \dot{Q}_p - \dot{Q}_r - \dot{Q}_s)(r_o - r_i)\phi_A}{4\pi r_o r_i (T_i - T_o)} \qquad (2)$$

This was rearranged to give an effective value of the thermoelectric power of the thermocouple at the particular rate

---

*Symbols appearing in the text are defined in the nomenclature on page 115 .

of energy addition,

$$\mathcal{P} = \frac{4\pi r_o r_i k \mathcal{E}}{(\mathring{Q}_m - \mathring{Q}_p - \mathring{Q}_r - \mathring{Q}_s)(r_o - r_i)\phi_A} \qquad (3)$$

The only parts of the measuring section of the cell that were affected by the nitrogen dioxide were the thermocouples and the surfaces, whose emissivities were changed. So the previous calibrations were still valid for the other quantitites needed to calculate the effective thermoelectric power. By extrapolating these effective values to a zero rate of energy addition the thermoelectric power at the bath temperature was found.

To determine the thermal transfer through the pins and by radiation, the temperature difference had to be known, and these fluxes were needed to establish the calibration needed to calculate the temperature difference. This dilemma was overcome by a trial solution, assuming a transfer rate for the pins and radiation, then computing a temperature difference. Using this difference the assumed rates were corrected. One such correction was adequate to make the error in the temperature difference due to uncertainties in these transfer rates negligible.

Radiation Calibration

When the pressure within the cell is reduced sufficiently so that the mean free path of the molecules is of the same magnitude as the distance between the spheres, the amount of heat transferred by conduction becomes small compared to that transferred by radiation and through the supporting pins. By use of a mercury diffusion pump and a mechanical vacuum pump operating in series, the pressure was maintained under 10^{-6} inches of mercury, at which point conduction through the fluid was negligible. Then operating at this pressure, the temperature difference for a known energy flux was determined at 40° and 220°F. The amount of the energy transferred through the pins was calculated from the temperature difference by the equation presented in the first part of this thesis,

$$\dot{Q}_p = \frac{24\pi k_{st} r_p^2 (T_i - T_o)}{5(r_o - r_i)} \qquad (4)$$

From the radiant energy transport, the dimensions of the spheres, and their temperatures, the emissivity of the surfaces of the spheres was calculated, making the assumption of gray body radiation. The calculations were not straightforward, as was explained, since the thermocouple calibration and the radiation calculations were mutually dependent. Since the radiation transport was only about one per cent of the

total transport when helium was used to calibrate the thermocouples, an approximate value of the radiation transport was sufficient to compute an accurate thermoelectric power. This final value of the thermocouple calibration was then used to calculate the emissivity. The calculations were based on the laws of radiation and made use of the equations and methods of McAdams (12), who discusses radiation in some detail.

The time to reach steady state with such low pressure in the apparatus was very long. To decrease the time required, the thermocouple readings were obtained at several different rates of change of voltage with time. By graphical means the reading at the point where the change with time was zero, which is the steady state, was obtained. The graphical procedure was based on an assumption that the temperatures approach their final values exponentially, which should be true.

The emissivity was found to be 0.50, which is in agreement with values found by other investigators for the same type of steel. It is believed that the value of the emissivity is known to within 10 per cent. For lack of more accurate means of determination, it was assumed that the emissivity was independent of temperature, which should not be greatly in error.

Study of Nitric Oxide

The method of taking the measurements needed to compute the thermal conductivity of gaseous nitric oxide was the same as that used in the study of liquid nitrogen dioxide. The time required to attain steady state was significantly longer, about eight hours, owing to the much lower thermal conductivity of nitric oxide. Because of the longer time required, greater precautions were needed to insure that the observed readings were constant. In general the values were measured over a period of at least one hour after they appeared to have reached their steady value. Measurements were made with nitric oxide at atmospheric pressure from 40° to 400°F. at 60°F. intervals. At 40°, 220°, and 340°F. measurements were attempted as a function of pressure, but at pressures over 1000 pounds per square inch decomposition of the nitric oxide into nitrogen and oxygen could be detected, and at pressures in excess of 1500 pounds per square inch the rate of decomposition became too rapid to permit measurements to be made. This apparently catalytic decomposition, which has not been observed by other investigators, limited the maximum pressure considered at the temperatures in the present work to the region of 1000 to 1400 pounds per square inch.

Methods of Calculation

The methods of calculation previously used were slightly modified to give a simpler method of correcting for thermal transport by mechanisms other than conduction through the fluid of interest. In the previous calculation scheme, equation 2 was used to compute the effective thermal conductivity at each level of energy addition studied. At each state, which is defined by a bath temperature and an amount of sample, three such levels were used. The effective conductivity was extrapolated to zero energy addition, thus giving the thermal conductivity of the fluid at the bath temperature and the pressure corresponding to that at zero energy addition. The procedure was simplified by expanding equation 2 to the following form

$$k = \frac{\dot{Q}_m (r_o - r_i)\phi_A}{4\pi r_i r_o (T_i - T_o)} - (\dot{Q}_p + \dot{Q}_r + \dot{Q}_s)\left(\frac{(r_o - r_i)\phi_A}{4\pi r_i r_o (T_i - T_o)}\right) \quad (5)$$

Each term can be extrapolated to zero energy separately, and each can be thought of as a coefficient of thermal transport by a particular mechanism,

$$k = k_m - (k_p + k_r + k_s) \quad (6)$$

Each coefficient is defined as is illustrated for k_m

$$k_m = \frac{\dot{Q}_m (r_o - r_i)\, \phi_A}{4\pi r_o r_i (T_i - T_o)} \qquad (7)$$

The final three terms on the right side of equation 6 are functions only of the bath temperature for a transparent fluid. If the sample absorbs radiation partially or completely, k_r will be reduced or become zero.

Each term approaches a finite, positive value at zero energy addition, since in each the numerator contains the thermal transport rate, which is proportional to the temperature difference, and the denominator contains the temperature difference. The other quantities are not functions of the energy rate. This may be shown as follows. By definition, the thermal conductivity k is independent of the temperature difference. It is directly proportional to a thermal transport rate that depends on the temperature difference, and inversely proportional to the temperature difference. Substituting the value of the energy transport through the pins into the relation for k_p gives

$$k_p = \frac{\left[\frac{24\pi k_{st} r_p^2 (T_i - T_o)}{(r_i - r_o)}\right] (r_i - r_o)\, \phi_A}{4\pi r_i r_o (T_i - T_o)} \qquad (8)$$

For small differences in temperature the transport by radiation can be approximated as

$$\dot{Q}_r = f(r_i, r_o) f(\epsilon)(T_i^4 - T_o^4) = f(r_i, r_o) f(\epsilon)\left(\frac{T_i^3 + T_o^3}{2}\right)(T_i - T_o) \tag{9}$$

So that k_r becomes

$$k_r = \frac{f(r_i, r_o) f(\epsilon)\left(\frac{T_i^3 + T_o^3}{2}\right)(T_i - T_o)}{(T_i - T_o)} \tag{10}$$

By proper regulation of the guard heater, the thermal transport through the shaft can be kept to a negligible level so that

$$k_s = 0 \tag{11}$$

Since all the terms constituting $\dot{Q}_m$ are proportional to the temperature difference, it follows that $\dot{Q}_m$ is also, so

$$k_m = \frac{f(r_i, r_o)(T_i - T_o)}{(T_i - T_o)} \tag{12}$$

Thus each term approaches a finite value as the energy rate, or temperature difference, approaches zero.

Since the coefficients of transport by conduction through the pins and by radiation do not depend upon the pressure or the fluid studied, unless it is not transparent to radiation, they can be calculated solely as a function of temperature for use with all fluids. Thus only k_m, which is calculated from the measured energy addition, must be computed from the experimental data. For each state studied, the apparent values of k_m are calculated and extrapolated to zero temperature difference, and the thermal conductivity then computed from equation 6. Values of the coefficients of transport by radiation k_r and by conduction through the pins k_p are given in Table I.

Preparation of Materials

The nitric oxide was obtained from the Matheson Company, Inc. The gas was stated to be 0.98 weight fraction nitric oxide. The primary impurities were nitrogen and the other oxides of nitrogen with a trace of water present. The nitric oxide was purified in accordance with the procedure of Johnston and Giauque (13). The impure gas at atmospheric pressure was bubbled through ninety-five per cent sulfuric acid and a fifty per cent solution of potassium hydroxide in water, then dried by passing through a trap at dry ice temperature and by passing over calcium sulfate and sodium hydroxide. Then the gas was collected at low pressure at liquid nitrogen temperature. The condensed gas was vaporized and distilled through phosphorus pentoxide with the initial and final portions of the vapor discarded. The purified material was stored in a stainless steel cylinder until it was used. In previous work it was found that this purification system was found to give a product containing less than 0.002 weight fraction impurities as determined by gas density measurements.

Results

Thermal Conductivity of Nitric Oxide

Details of the measurements made with nitric oxide are given in Table II. The apparent values of the coefficient of measured thermal transport k_m at each rate of energy addition were calculated from equation 7. There is a small, but uniform, difference in the results based on the thermocouples in the upper and lower hemispheres. The coefficient k_m based on the lower hemisphere thermocouple is on the average 2.5 per cent higher than the one based on the upper hemisphere thermocouple. The mean value of the results from the two thermocouples was used to calculate the thermal conductivity from equation 6. The experimental values of the thermal conductivity of nitric oxide are given in Table III. Nitric oxide absorbs radiation in only a few discrete bands in the region of the spectrum that is of importance in the transfer of energy at the temperatures of the experiments (5). The uncertainties in the value of the coefficient k_m at zero energy flux due to the discrepancies between the two hemispheres were small.

The experimental results are compared to the previous values reported by Johnston and Grilly (1) and Eucken (2) in Figure 1, which shows the effect of temperature on the thermal conductivity of nitric oxide at atmospheric pres-

sure. The measurements were made at about 0.5 pounds per square inch above atmospheric pressure, but the results can be considered to be the same as the values at one atmosphere since the variation in conductivity due to such a small pressure change is negligible. The present work is approximately 12 per cent lower than the values reported in the literature, which is a greater discrepancy than would be expected from the probable errors stated for the various results. A definite judgment on the nitric oxide data cannot be made until more work is done with fluids of known thermal conductivity to verify the accuracy of the present work. However the most likely errors to be made in measuring thermal conductivity are in not accounting for all of the end effects of the cell or thermal transport by means other than conduction through the fluid. Such errors tend to make the results too high, so it might appear that the present work could be more reliable than the previous studies.

An equation of the form

$$k = a + bT + cT^2 \qquad (13)$$

was fitted to the atmospheric pressure values of the thermal conductivity by least squares techniques. Over the limited temperature range considered, an equation of this form is adequate to represent the data. The derived equation is

$$k = 0.01128 + 2.014 \times 10^{-5} T - 1.198 \times 10^{-9} T^2 \qquad (14)$$

where k is in Btu./(hr.)(ft.)($^{\circ}$F.) and T is in degrees Fahrenheit. The standard deviation of the experimental points from the values predicted from the equation is 1.82×10^{-4} Btu./(hr.)(ft.)($^{\circ}$F.).

Figure 2 shows the effect of pressure on the thermal conductivity of nitric oxide. The values at atmospheric pressure for 40°, 220°, and 340°F. were taken from equation 14. The increase in thermal conductivity due to pressure was found to be larger than was predicted by the method of Comings and Nathan (14). They present a correlation for the increase of thermal conductivity with pressure based on the theorem of corresponding states. The deviation of the predicted and experimental increases varied from 27 to 57 per cent.

The values of the thermal conductivity of nitric oxide at even values of pressure for the temperatures considered are given in Table IV. These values were taken from equation 14 at atmospheric pressure and from the smooth curves at higher pressures.

Decomposition of Nitric Oxide

Investigations of the kinetics of the homogeneous de-

composition of nitric oxide by other workers have indicated that no reaction should be found in the temperature range of this work (5,15). The pressure-volume-temperature relations of nitric oxide were studied in the Chemical Engineering Laboratory of the California Institute of Technology over much of the same pressure and temperature ranges and no reaction occurred (6). Hence it was concluded that the reaction must have been catalytic in nature.

The decomposition was assumed to follow the overall equation

$$4\,NO = N_2 + 2\,NO_2 \qquad (15)$$

since the undecomposed nitric oxide would react with the oxygen produced. From a consideration of the free energy change of this reaction, it is seen that the equilibrium would lie almost completely to the right (5). When the sample was removed from the apparatus, large amounts of nitrogen dioxide were found, and the residual gases were found to contain nitrogen when tested. Thus the assumed reaction seems to be verified.

The regions in the temperature-pressure plane in which the reaction was found to occur are indicated in Figure 3. The apparent rates of decomposition of nitric oxide, as determined from the observed rate of change of pressure at constant temperature, are given in Table V for several

states where the reaction was found. No conclusions regarding the mechanism of the reaction or the nature of the catalyst can be reached with the data available. It is likely that the platinum thermocouples or, possibly, the chromium plating on part of the cell was the catalyst. It is of interest to note that the change of reaction rate with pressure at any temperature is greater than would be expected from the usual equation for the rate of decomposition of nitric oxide

$$\frac{d p_{NO}}{d \theta} = -k_d p_{NO}^2 \qquad (16)$$

Discussion of Results

The thermal conductivity of nitric oxide was determined at atmospheric pressure from 40° to 400°F. The variation of the thermal conductivity with pressure was studied at 40°, 220°, and 340°F. at pressures up to 1400 pounds per square inch. At higher pressures the nitric oxide decomposed at a rate too high to make measurements possible. The probable error of measurements made with this equipment was discussed in detail in the first part of this thesis.

Errors due to transfer by other means than conduction through the nitric oxide are small. The transport through the pins and by radiation was between 0.066 and 0.132 of the total energy transport. Errors from uncertainties in these fluxes should be less than one per cent. The error due to these causes is higher in this case because the gas is transparent and has a lower thermal conductivity. Both of these factors increase the size of the leakage fluxes in relation to the total transport.

In addition to the errors in the measuring methods mentioned in connection with the nitrogen dioxide studies, the calibrations of the thermocouples are not as well known since they were determined by an indirect method. The total error from uncertainties in determining the temperature differences, geometric constants, and energy rate should be less than 2.5 per cent.

Errors due to non ideal behavior of the cell would appear to be less than for nitrogen dioxide. The large deviations between the results based on the two thermocouples were not found for nitric oxide. The deviation was smaller and nearly constant, and could be attributed primarily to the increased uncertainty in the thermocouple calibration. It would appear that the total uncertainty in the final results should be less than 5 per cent. Testing of the cell with a gas, such as nitrogen, whose thermal conductivity has been well established, will give a better idea of the limits of accuracy of the measurements. It would seem that the results at least indicate that the previous values in the literature are too high.

The errors in the determination of the variation of the thermal conductivity with pressure might be slightly higher, due to the presence of small amounts of nitrogen dioxide which has a higher thermal conductivity than nitric oxide. The disagreement with the correlation of Comings and Nathan is significant, but the overall validity of their method has not been established. The general pattern of the pressure effect agrees with the theories of the thermal conductivity of gases at high density.

References

1. Johnston, H. L. and Grilly, E. R., J. Chem. Phys., 14, 233 (1946).
2. Eucken, A., Phys. Zeit., 14, 324 (1913).
3. Todd, G. W., Proc. Roy. Soc. (London), A83, 19 (1909)
4. Winkelmann, Ann. d. Phys., 156, 497 (1875).
5. Yost, D. M. and Russell, H. Jr., "Systematic Inorganic Chemistry," Chap. I, Prentice-Hall, Inc., New York (1944).
6. Golding, B. H. and Sage, B. H., Ind. Eng. Chem., 43, 160 (1951).
7. Opfell, J. B., Schlinger, W. G., and Sage, B. H., Ind. Eng. Chem., 46, 189 (1954).
8. Hilsenrath, J. and Touloukian, Y. S., Trans. A.S.M.E., 76, 967 (1954).
9. Wooley, H. W., "Thermodynamic Properties of Gaseous Nitric Oxide," National Bureau of Standards Report 2602, U.S. Dept. of Comm., Washington, D.C. (1955).
10. Hilsenrath, J. et al., "Tables of Thermal Properties of Gases," National Bureau of Standards Circular 564, U.S. Dept. of Comm., Washington, D.C. (1955).
11. Keyes, F. G., Trans. A.S.M.E., 73, 589 (1951).
12. McAdams, W. H., "Heat Transmission," 3rd Edit., Chap. III, McGraw Hill Book Co., Inc., New York (1954).

13. Johnston, H. L. and Giauque, W. F., J. Am. Chem. Soc., 51, 3194 (1929).

14. Comings, E. W. and Nathan, M. F., Ind. Eng. Chem., 39, 964 (1947).

15. Daniels, F., Chem. and Eng. News, 33, 2370 (1955).

Nomenclature

a, b, c	constants
$\mathcal{E}$	thermocouple voltage
ϵ	emissivity
$f(X)$	a function of **X**
k	thermal conductivity
k_d	reaction rate constant for decomposition of NO
k_m	coefficient of measured thermal transport
k_p	coefficient of thermal transport through pins
k_r	coefficient of thermal transport by radiation
k_s	coefficient of thermal transport through shaft
k_{st}	thermal conductivity of steel
k_o	thermal conductivity at reference state
$\mathcal{P}$	thermoelectric power
$\mathcal{P}_{NO}$	partial pressure of nitric oxide
$\dot{Q}_m$	measured rate of energy addition
$\dot{Q}_p$	rate of heat transfer through pins
$\dot{Q}_r$	rate of heat transfer by radiation
$\dot{Q}_s$	rate of heat transfer through shaft
r_i	inner radius
r_o	outer radius
r_p	radius of pins
T_i	temperature at inner radius
T_o	temperature at outer radius

ϕ_A ratio of area of complete sphere to that of sphere minus area intercepted by shaft

θ time

List of Figures

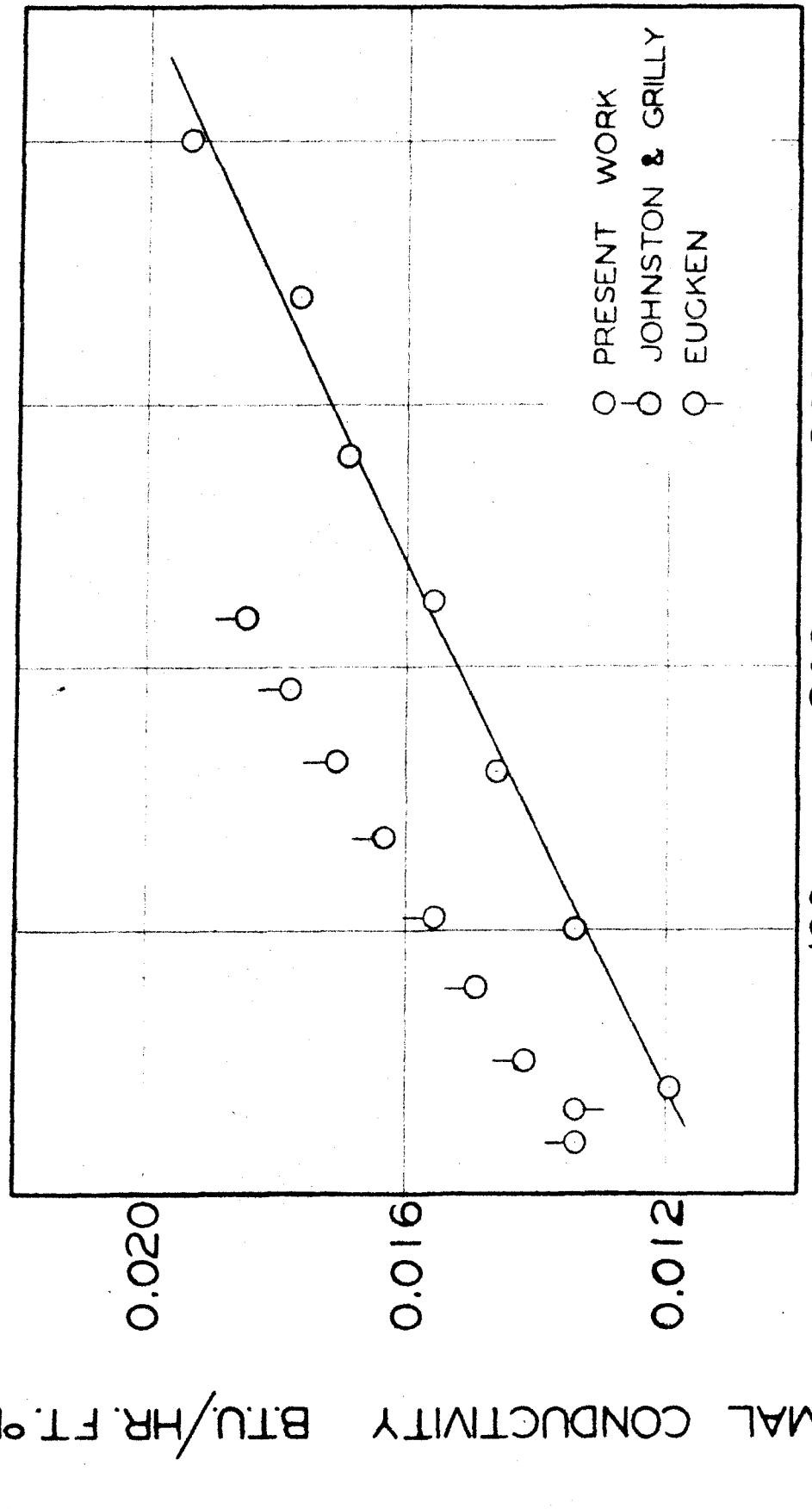

Figure 1. Thermal Conductivity of Nitric Oxide at Atmospheric Pressure

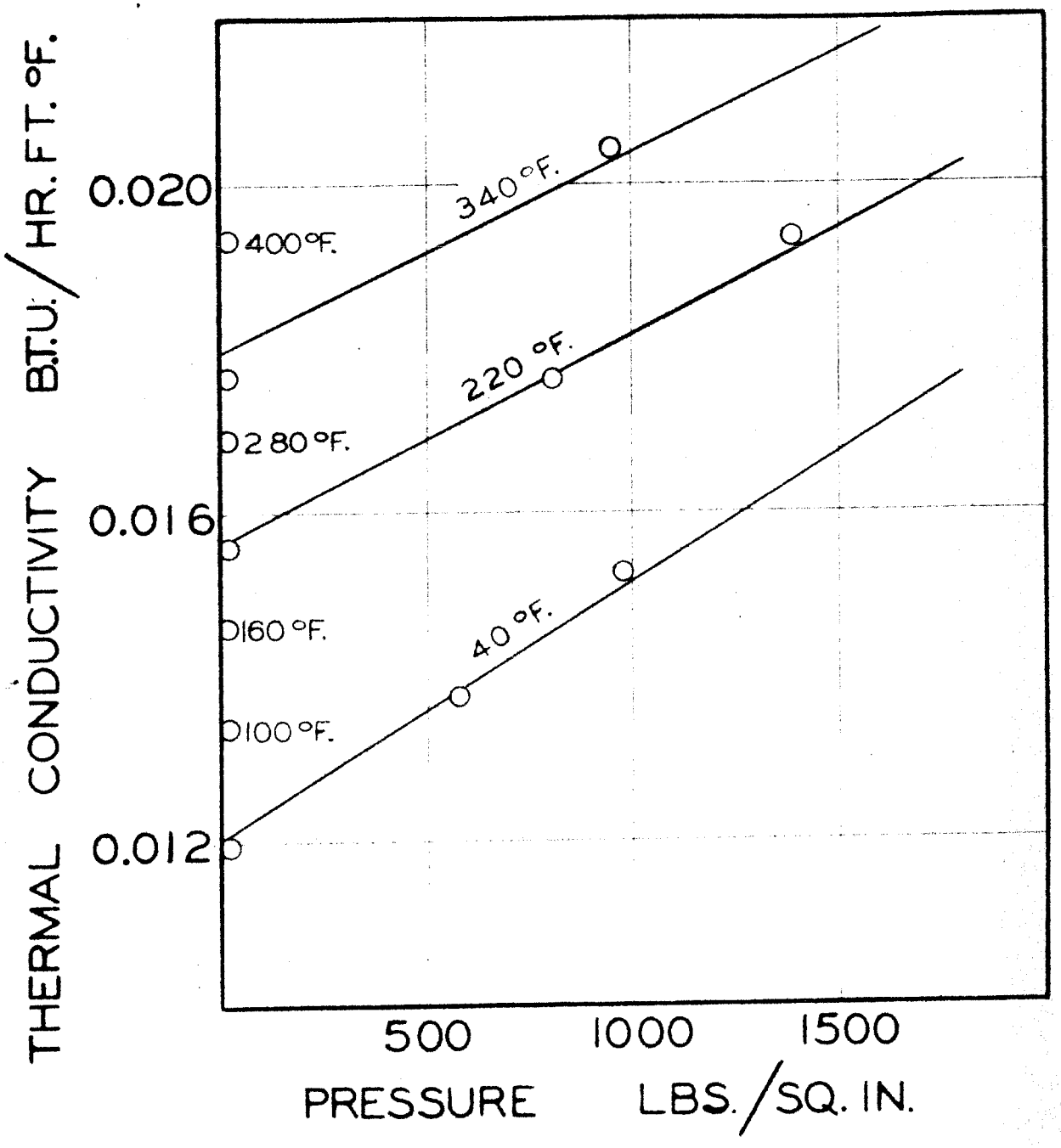

Figure 2. Effect of Pressure on the Thermal Conductivity of Nitric Oxide

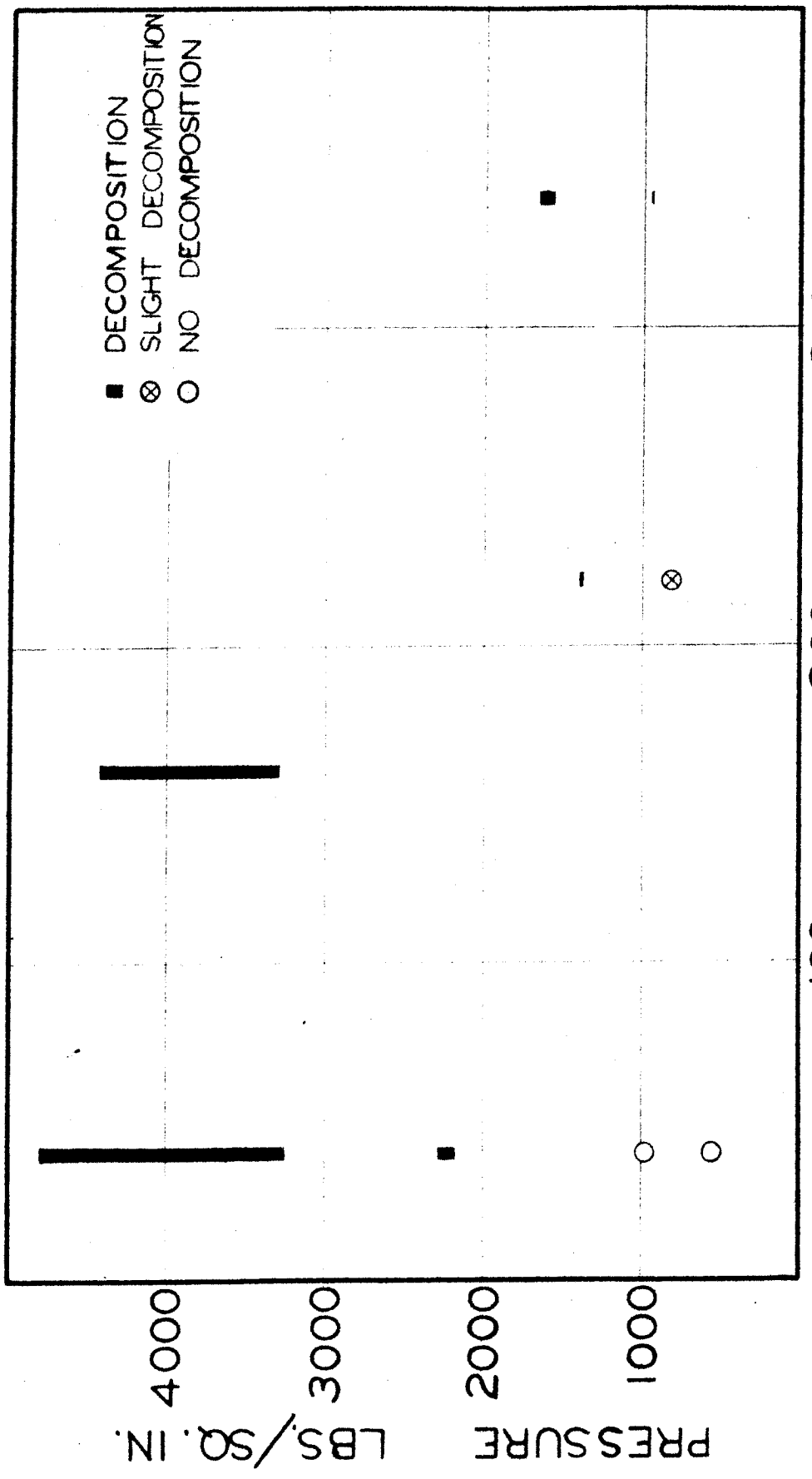

Figure 3. Regions of Observed Nitric Oxide Decomposition

List of Tables

TABLE I. COEFFICIENTS OF THERMAL TRANSPORT BY CONDUCTION THROUGH THE PINS AND BY RADIATION

T °F.	$k_p \times 10^4$ Btu./hr.ft.°F.	$k_r \times 10^4$ Btu./hr.ft.°F.
40	3.14	4.74
100	3.24	6.66
160	3.33	9.04
220	3.43	11.92
280	3.53	15.35
340	3.63	19.39
400	3.73	24.08

TABLE II DETAILS OF EXPERIMENTAL MEASUREMENTS

Quantity	Units	Conditions		
Bath Temperature	°F.	40	40	40
Pressure at Zero Flux	lb./sq.in.abs.	15.1	15.1	15.1
Measured Energy Input Rate	Btu./hr.	2.0717	4.5192	9.1506
Pressure	lb./sq.in.abs.	15.1	15.2	15.2
Upper Half Sphere				
Temperature Difference	°F.	1.110	2.420	4.874
Apparent k_m	Btu./hr.ft.°F.	0.01271	0.01272	0.01279
Lower Half Sphere				
Temperature Difference	°F.	1.097	2.375	4.785
Apparent k_m	Btu./hr.ft.°F.	0.01286	0.01296	0.01302
k_m[a]	Btu./hr.ft.°F.	0.01276	0.01276	0.01276
Thermal Conductivity[a]	Btu./hr.ft.°F.	0.01197	0.01197	0.01197

[a] Extrapolated to zero flux

TABLE II DETAILS OF EXPERIMENTAL MEASUREMENTS (cont.)

Quantity	Units	Conditions		
Bath Temperature	°F.	100	100	100
Pressure at Zero Flux	lb./sq.in.abs.	15.4	15.4	15.4
Measured Energy Input Rate	Btu./hr.	1.2673	2.6399	4.6699
Pressure	lb./sq.in.abs.	15.4	15.4	15.3
Upper Half Sphere				
Temperature Difference	°F.	0.605	1.271	2.233
Apparent k_m	Btu./hr.ft.°F.	0.01426	0.01414	0.01424
Lower Half Sphere				
Temperature Difference	°F.	0.590	1.233	2.167
Apparent k_m	Btu./hr.ft.°F	0.01461	0.01460	0.01467
k_m [a]	Btu./hr.ft.°F.	0.01439	0.01439	0.01439
Thermal Conductivity [a]	Btu./hr.ft.°F.	0.01340	0.01340	0.01340

[a] Extrapolated to zero flux

TABLE II DETAILS OF EXPERIMENTAL MEASUREMENTS (cont.)

Quantity	Units	Conditions		
Bath Temperature	°F.	160	160	160
Pressure at Zero Flux	lb./sq.ins.abs.	15.2	15.2	15.2
Measured Energy Input Rate	Btu./hr.	1.6382	3.1619	5.1125
Pressure	lb./sq.in.abs.	15.3	15.2	15.2
Upper Half Sphere				
Temperature Difference	°F.	0.717	1.365	2.243
Apparent k_m	Btu./hr.ft.°F.	0.01554	0.01576	0.01551
Lower Half Sphere				
Temperature Difference	°F.	0.694	1.327	2.170
Apparent k_m	Btu./hr.ft.°F.	0.01607	0.01622	0.01603
k_m^a	Btu./hr.ft.°F.	0.01585	0.01585	0.01585
Thermal Conductivity	Btu./hr.ft.°F.	0.01461	0.01461	0.01461

[a] Extrapolated to zero flux

TABLE II DETAILS OF EXPERIMENTAL MEASUREMENTS (cont.)

Quantity	Units	Conditions		
Bath Temperature	°F.	220	220	220
Pressure at Zero Flux	lb./sq.in.abs.	15.3	15.3	15.3
Measured Energy Input Rate	Btu./hr.	1.6268	3.1906	5.0177
Pressure	lb./sq.in.abs.	15.3	15.3	15.3
Upper Half Sphere				
Temperature Difference	°F.	0.653	1.287	2.000
Apparent k_m	Btu./hr.ft.°F.	0.01696	0.01686	0.01706
Lower Half Sphere				
Temperature Difference	°F.	0.632	1.258	1.943
Apparent k_m	Btu./hr.ft.°F.	0.01750	0.01724	0.01757
k_m^a	Btu./hr.ft.°F.	0.01712	0.01712	0.01712
Thermal Conductivity[a]	Btu./hr.ft.°F.	0.01558	0.01558	0.01558

[a] Extrapolated to zero flux

TABLE II DETAILS OF EXPERIMENTAL MEASUREMENTS (cont.)

Quantity	Units	Conditions		
Bath Temperature	°F.	280	280	280
Pressure at Zero Flux	lb./sq.in.abs	15.2	15.2	15.2
Measured Energy Input Rate	Btu./hr.	1.9018	3.1313	5.5763
Pressure	lb./sq.in.abs.	15.2	15.2	15.2
Upper Half Sphere				
Temperature Difference	°F.	0.700	1.151	2.034
Apparent k_m	Btu./hr.ft.°F.	0.01847	0.01850	0.01864
Lower Half Sphere				
Temperature Difference	°F.	0.671	1.111	1.964
Apparent k_m	Btu./hr.ft.°F.	0.01927	0.01915	0.01930
k_m [a]	Btu./hr.ft.°F.	0.01879	0.01879	0.01879
Thermal Conductivity [a]	Btu./hr.ft.°F.	0.01690	0.01690	0.01690

[a] Extrapolated to zero flux

TABLE II DETAILS OF EXPERIMENTAL MEASUREMENTS (cont.)

Quantity	Units	Conditions		
Bath Temperature	°F.	340	340	340
Pressure at Zero Flux	lb./sq.in.abs.	15.4	15.4	15.4
Measured Energy Input Rate	Btu./hr.	2.0199	3.4874	5.4943
Pressure	lb./sq.in.abs.	15.4	15.5	15.3
Upper Half Sphere				
Temperature Difference	°F.	0.697	1.179	1.865
Apparent k_m	Btu./hr.ft.°F.	0.01969	0.02009	0.02002
Lower Half Sphere				
Temperature Difference	°F.	0.669	1.141	1.792
Apparent k_m	Btu./hr.ft.°F.	0.02051	0.02076	0.02083
k_m [a]	Btu./hr.ft.°F.	0.01997	0.01997	0.01997
Thermal Conductivity [a]	Btu./hr.ft.°F.	0.01767	0.01767	0.01767

[a] Extrapolated to zero flux

TABLE II DETAILS OF EXPERIMENTAL MEASUREMENTS (cont.)

Quantity	Units	Conditions		
Bath Temperature	°F.	400	400	400
Pressure at Zero Flux	lb./sq.in.abs.	15.2	15.2	15.2
Measured Energy Input Rate	Btu./hr.	2.1165	3.4704	5.4220
Pressure	lb./sq.in.abs.	15.2	15.5	15.4
Upper Half Sphere				
Temperature Difference	°F.	0.654	1.083	1.685
Apparent k_m	Btu./hr.ft.°F.	0.02197	0.02177	0.02185
Lower Half Sphere				
Temperature Difference	°F.	0.634	1.048	1.635
Apparent k_m	Btu./hr.ft.°F.	0.02268	0.02248	0.02252
k_m^a	Btu./hr.ft.°F.	0.02212	0.02212	0.02212
Thermal Conductivity[a]	Btu./hr.ft.°F.	0.01934	0.01934	0.01934

[a] Extrapolated to zero flux

TABLE II DETAILS OF EXPERIMENTAL MEASUREMENTS (cont.)

Quantity	Units	Conditions		
Bath Temperature	°F.	40	40	40
Pressure at Zero Flux	lb./sq.in.abs.	972	972	972
Measured Energy Input Rate	Btu./hr.	2.2724	3.7075	5.2422
Pressure	lb./sq.in.abs.	977	980	980
Upper Half Sphere				
Temperature Difference	°F.	1.015	1.686	
Apparent k_m	Btu./hr.ft.°F.	0.01525	0.01498	
Lower Half Sphere				
Temperature Difference	°F.	0.874	1.364	1.908
Apparent k_m	Btu./hr.ft.°F.	0.01771	0.01852	0.01871
k_m [a]	Btu./hr.ft.°F.	0.01607	0.01607	0.01607
Thermal Conductivity [a]	Btu./hr.ft.°F.	0.01528	0.01528	0.01528

[a] Extrapolated to zero flux

TABLE II DETAILS OF EXPERIMENTAL MEASUREMENTS (cont.)

Quantity	Units	Conditions		
Bath Temperature	°F.	40	40	40
Pressure at Zero Flux	lb./sq.in.abs.	577.4	577.4	577.4
Measured Energy Input Rate	Btu./hr.	2.0044	3.4834	5.2031
Pressure	lb./sq.in.abs.	579.7	581.3	582.9
Upper Half Sphere				
Temperature Difference	°F.	0.945	1.651	2.446
Apparent k_m	Btu./hr.ft.°F.	0.01444	0.01437	0.01449
Lower Half Sphere				
Temperature Difference	°F.	0.932	1.593	2.391
Apparent k_m	Btu./hr.ft.°F.	0.01465	0.01489	0.01482
k_m[a]	Btu./hr.ft.°F.	0.01456	0.01456	0.01456
Thermal Conductivity[a]	Btu./hr.ft.°F.	0.01377	0.01377	0.01377

[a] Extrapolated to zero flux

TABLE II DETAILS OF EXPERIMENTAL MEASUREMENTS (cont.)

Quantity	Units	Conditions		
Bath Temperature	°F.	220	220	220
Pressure at Zero Flux	lb./sq.in.abs.	1391	1391	1391
Measured Energy Input Rate	Btu./hr.	2.2584	3.8122	5.5776
Pressure		1397	1397	1396
Upper Half Sphere				
Temperature Difference	°F.	0.745	1.258	1.806
Apparent k_m	Btu./hr.ft.°F.	0.02062	0.02062	0.02100
Lower Half Sphere				
Temperature Difference	°F.	0.731	1.218	1.740
Apparent k_m	Btu./hr.ft.°F.	0.02102	0.02129	0.02180
k_m[a]	Btu./hr.ft.°F.	0.02089	0.02089	0.02089
Thermal Conductivity[a]	Btu./hr.ft.°F.	0.01935	0.01935	0.01935

[a] Extrapolated to zero flux

TABLE II DETAILS OF EXPERIMENTAL MEASUREMENTS (cont.)

Quantity	Units	Conditions		
Bath Temperature	°F.	220	220	220
Pressure at Zero Flux	lb./sq.in.abs.	809	809	809
Measured Energy Input Rate	Btu./hr.	1.8556	3.3527	4.8720
Pressure	lb./sq.in.abs.	812	812	813
Upper Half Sphere				
Temperature Difference	°F.	0.658	1.181	1.700
Apparent k_m	Btu./hr.ft.°F.	0.01918	0.01931	0.01949
Lower Half Sphere				
Temperature Difference	°F.	0.646	1.163	1.677
Apparent k_m	Btu./hr.ft.°F.	0.01954	0.01961	0.01976
k_m [a]	Btu./hr.ft.°F.	0.01918	0.01918	0.01918
Thermal Conductivity [a]	Btu./hr.ft.°F.	0.01765	0.01765	0.01765

[a] Extrapolated to zero flux

TABLE II DETAILS OF EXPERIMENTAL MEASUREMENTS (cont.)

Quantity	Units	Conditions		
Bath Temperature	°F.	340	340	340
Pressure at Zero Flux	lb./sq.in.abs.	950	950	950
Measured Energy Input Rate	Btu./hr.	1.9173	3.2337	5.7499
Pressure	lb./sq.in.abs.	956	952	950
Upper Half Sphere				
Temperature Difference	°F.	0.572	0.961	1.679
Apparent k_m	Btu./hr.ft.°F.	0.02278	0.02286	0.02325
Lower Half Sphere				
Temperature Difference	°F.	0.567	0.949	1.680
Apparent k_m	Btu./hr.ft.°F.	0.02295	0.02314	0.02324
k_m[a]	Btu./hr.ft.°F.	0.02274	0.02274	0.02274
Thermal Conductivity[a]	Btu./hr.ft.°F.	0.020444	0.020444	0.020444

[a] Extrapolated to zero flux

TABLE III. EXPERIMENTAL VALUES OF THERMAL CONDUCTIVITY OF NITRIC OXIDE

Temperature °F.	Pressure Lb./Sq.In. absolute	Thermal Conductivity Btu./hr.ft.°F.
40	15.2	0.01197
	577.4	0.01377
	972.	0.01528
100	15.4	0.01340
160	15.2	0.01461
220	15.3	0.01559
	809.	0.01765
	1391.	0.01935
280	15.2	0.01690
340	15.4	0.01767
	950.	0.02044
400	15.4	0.01934

TABLE IV. THERMAL CONDUCTIVITY OF NITRIC OXIDE

Pressure Lb./Sq. Inch Absolute	40° F.	220° F.	340° F.
14.696	0.01209[a]	0.01566	0.01799
50	0.01220	0.01575	0.01808
100	0.01236	0.01588	0.01821
150	0.01251	0.01601	0.01834
200	0.01267	0.01614	0.01847
400	0.01329	0.01665	0.01898
600	0.01391	0.01717	0.01949
800	0.01454	0.01769	0.02001
1000	0.01516	0.01820	0.02052
1250	(0.01594)[b]	0.01884	(0.02116)
1500	(0.01671)	0.01949	(0.02180)

[a] Thermal conductivity expressed in B.t.u./(hr.)(ft.)(°F.)

[b] Values in parentheses are extrapolated

TABLE V. OBSERVED RATES OF DECOMPOSITION OF NITRIC OXIDE

Temperature °F.	Pressure lb./sq.in.abs.	Rate of Decomposition (lb./sq.in.)/(hr.)
40	4800	130.
	972	not measurable
220	1391	0.94
	809	0.10
340	1655	6.0
	950	0.55

PART III

VISCOSITY OF NITROGEN DIOXIDE AND NITROGEN DIOXIDE-NITRIC OXIDE MIXTURES

16 in *n*-hexadecyl mercaptan. Each of these five mercaptans was dissolved in the same ratio of benzene-heptane solvent mixture, 30 volume % of benzene and 70 volume % of *n*-heptane, and desulfurization was carried out on each using the same treating conditions. The 30–70 volume ratio of solvents was selected because of the noticeable drop in per cent desulfurization of *n*-dodecyl disulfide with 30% toluene in the solvent. The data for these tests are recorded in Table IX, which shows a slight reduction in desulfurization for the lower mercaptans with benzene present and a very sharp decrease after the C_{11} mercaptan.

HYDROCARBON SOLVENTS

Table X includes the results of a few tests with other solvents, methylcyclohexane, a naphthenic-type solvent, and mixtures of amylene in *n*-heptane.

As would be expected, the raffinate yields with amylene in the solvent were somewhat lower than those with straight heptane or methylcyclohexane because of the inclusion of some of the olefin in the acid extract layer. This reduced the effectiveness of the desulfurizing agent to some extent, as indicated by results with the use of only 5 volume % of amylene in the paraffinic solvent. A considerably greater reduction in desulfurization was observed with 10 volume % of amylene present.

SUMMARY

Nitrogen dioxide dissolved in 95.5% sulfuric acid was found to be an effective desulfurizing agent for aliphatic sulfides, disulfides, and mercaptans dissolved in *n*-heptane. Other sulfur compounds, including thiophene and a few aromatic types, were also removed from heptane solutions by the nitrogen dioxide–sulfuric acid mixture. Treating mixtures containing 2.3% nitrogen dioxide and also 5.33% nitrogen dioxide in 95.5% sulfuric acid were found to be satisfactory. The former was effective in removing low molecular weight sulfur compounds from heptane solutions; the 5.33% nitrogen dioxide treating agent was slightly more effective for the removal of mercaptans. The presence of aromatic hydrocarbons in the heptane solvent reduced the effectiveness of the nitrogen dioxide–sulfuric acid treating agent for the removal of high molecular weight aliphatic sulfur compounds.

LITERATURE CITED

(1) *Am. Soc. Testing Materials, Standards*, Pt. III, *Designation* D 90-347, 626-9 (1939).
(2) Borgstrom, P., IND. ENG. CHEM., **22**, 249 (1930).
(3) Borgstrom, P., Bost., R. W., and McIntire, J. C., *Ibid.*, **22**, 87 (1930).
(4) Bost, R. W., and Conn, M. W., *Ibid.*, **23**, 93 (1931).
(5) Meadow, J. R., U. S. Patent 2,366,453 (Jan. 2, 1945).
(6) Meadow, J. R., and White, T. A., IND. ENG. CHEM., **42**, 925 (1950).
(7) Noller, C., and Gordon, J., *J. Am. Chem. Soc.*, **55**, 1090 (1933).
(8) Yost, D. M., and Russell, H., Jr., "Systematic Inorganic Chemistry," p. 48, New York, Prentice-Hall, 1944.

RECEIVED for review March 23, 1953. ACCEPTED June 11, 1953.

Viscosity of Nitrogen Dioxide in the Liquid Phase

G. N. RICHTER, H. H. REAMER, AND B. H. SAGE

Chemical Engineering Laboratory, California Institute of Technology, Pasadena, Calif.

VISCOSITY data were not available for nitrogen dioxide in the liquid phase at pressures in excess of bubble point. Limited information concerning the viscosity of this compound in the liquid phase at vapor pressure was obtained by Thorpe and Rodger (*16*) at temperatures between 32° and 60° F. Scheuer (*14*) investigated the viscosity of the bubble point liquid at temperatures as low as 7° F. His results differ markedly from those of Thorpe and Rodger. Titani (*17*) also made a limited number of measurements in capillary tubes at temperatures above the normal boiling point. Primary interest was focused upon the development of an analytical expression to describe the effect of temperature upon the viscosity of liquids. As a result of the absence of data directly useful for the prediction of the characteristics of flow or thermal transfer, the viscosity of the liquid phase of nitrogen dioxide was measured at pressures up to 5000 pounds per square inch in the temperature interval between 40° and 280° F.

Experimental information concerning the volumetric behavior of nitrogen dioxide is available. The vapor pressure was studied by Scheffer and Treub (*13*) and the volumetric behavior of the gas at low pressures was investigated by Verhoek and Daniels (*18*) and by Bennewitz and Windisch (*1*). The effect of pressure and temperature upon the specific volume of nitrogen dioxide in the liquid and gas phases was investigated recently in some detail (*7*, *15*) at pressures up to 6000 pounds per square inch in the temperature interval between 70° and 310° F. This work reviewed the experimental volumetric and phase equilibrium data available, and the new measurements were in good agreement with earlier experimental information. These investigations (*7*, *15*) furnished necessary volumetric data for use in connection with the measurements of viscosity.

METHODS AND APPARATUS

A rolling ball viscometer of the type first proposed by Flowers (*3*) and developed by Hersey (*4*, *5*) was employed. The instrument was used earlier for studies of the viscosity of liquid and gaseous hydrocarbons (*9–12*) and was revised to permit measurements of the viscosity of ammonia (*2*).

In principle, the equipment (*2*) involved a stainless steel tube inclined at an angle of approximately 15°, down which a closely fitting, stainless steel ball was permitted to roll under the influence of gravity. Arrangements were provided (*2*) for determining the time of traverse of the ball between two sets of three coils located near the ends of the roll tube. A centrifugal circulating pump assisted in bringing the fluid to equilibrium and provided a means of returning the ball to the upper end of the roll tube. The circulating system was closed off during the time the ball was in motion down the tube.

The roll times were determined with an uncertainty of not more than 0.3% and the temperature of the roll tube was known within 0.1° F. with respect to the international platinum scale. The pressure was determined by means of a balance (*11*) which was calibrated against the vapor pressure of carbon dioxide at the ice point. The pressure within the viscometer was known within 2 pounds per square inch or 0.2%, whichever was the larger measure of uncertainty.

The characteristics of the rolling ball viscometer were investigated by Watson (*19*), Hersey and Shore (*5*), and Hubbard and

Brown (*6*). These matters were considered earlier for the viscometer used in these studies (*2*) and are not treated here. The apparatus was calibrated against the viscosity of *n*-pentane in the liquid phase. The data of Thorpe and Rodger (*16*) together with the recent critically chosen values of Rossini (*8*) for the viscosity of *n*-pentane liquid at atmospheric pressure were employed to determine the coefficients of the following equation (*2*):

$$\eta = A\theta(\sigma_B - \sigma_f) - \frac{B\sigma_f}{\theta} \qquad (1)$$

Equation 1 was used to establish the viscosity from the measured roll time. The dimensional coefficients, A and B, assumed the values of 0.4262 and 1489.76, respectively, when the viscosity was expressed in micropoises, the roll time in seconds, and the specific weight in pounds per cubic foot. The specific weight of the ball was 481.94 pounds per cubic foot. The behavior of the combination of ball and tube used in this investigation with fluids of low viscosity was established experimentally (*2*). Recalibration of the instrument with *n*-pentane after completion of the measurements upon nitrogen dioxide indicated less than 1% change in the behavior of the instrument in the course of the measurements recorded here. All the present measurements were carried out at sufficiently large roll times so that the correction for the acceleration of the fluid around the ball was less than 5% of the total roll time. The viscosity has been expressed in micropoises because of the widespread acceptance of this unit, even though it is not dimensionally consistent with the independent variables present in the figures and tables.

The pressure was produced by filling the instrument at 40° F. with liquid nitrogen dioxide at a pressure equal to the vapor pressure of this compound at a temperature of approximately 160° F. This viscometer was then closed and the instrument brought to the desired temperature, resulting in a marked increase in pressure. The measurements were made at a series of decreasing pressures for a predetermined temperature by withdrawing small portions of the nitrogen dioxide from the apparatus.

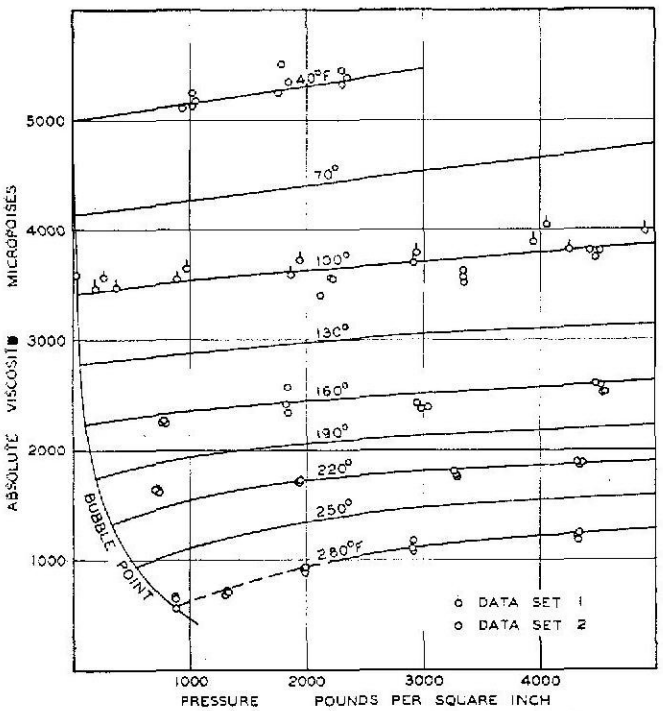

Figure 1. Effect of Pressure upon Viscosity of Nitrogen Dioxide

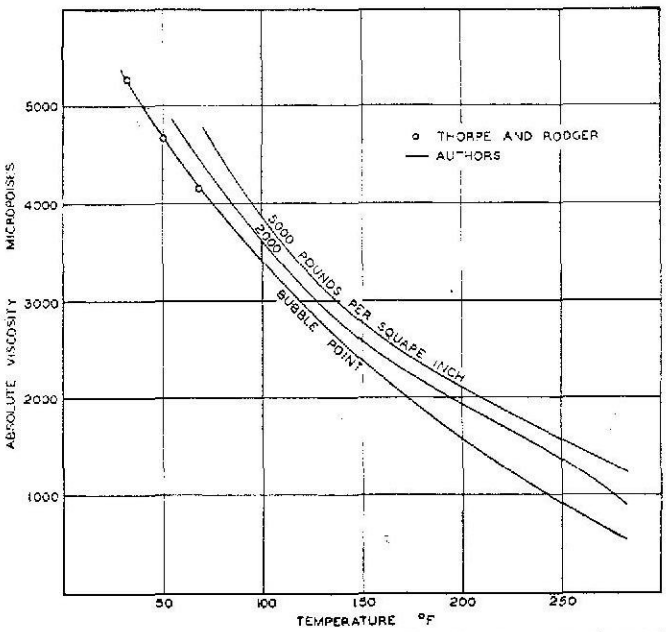

Figure 2. Viscosity of Nitrogen Dioxide in the Liquid Phase

RESULTS

The experimental results obtained in the course of these measurements are presented in Figure 1. The experimental data

TABLE EXPERIMENTAL MEASUREMENTS OF VISCOSITY OF NITROGEN DIOXIDE

Pressure, Lb./Sq. Inch Abs.	Abs. Viscosity, Micropoises	Pressure, Lb./Sq. Inch Abs.	Abs. Viscosity, Micropoises
40° F.		160° F.	
951	5118	780	2274
1026	5243	781	2254
1035	5134	782	2262
1055	5179	1828	2413
1761	5247	1841	2572
1798	5506	1848	2336
1853	5350	2960	2434
2321	5321	2986	2372
2323	5461	3047	2387
2361	5387	4497	2614
100° F.		4524	2589
		4555	2522
71[a]	3590	4563	2532
198	3481	220° F.	
258	3578		
372	3484		
879	3547	706	1654
		723	1647
976	3647	726	1625
1873	3594	1920	1712
1944	3722	1937	1713
2938	3697		
2942	3798	1941	1727
		3266	1813
3950	3887	3273	1794
4262	3815	3279	1774
4916	3987	4333	1895
5076	4046		
5451	3912	4349	1878
		4352	1874
6142	3954	280° F.	
		877	559
2126[b]	3407	878	663
2208	3576	879	652
2239	3552	1313	682
3341	3623	1316	724
3356	3519	1325	709
3358	3568	1962	910
4427	3810	1980	931
4493	3743	1981	881
4528	3803	2905	1108
		2914	1084
		2927	1178
		4320	1226
		4337	1258
		4339	1180

[a] Series 1.
[b] Series 2.

TABLE II. VISCOSITY OF NITROGEN DIOXIDE IN THE LIQUID PHASE

Pressure, Lb./Sq. Inch Abs.	Temperature, ° F. 40	70	100	130	160	190	220	250	280
	Bubble Point Pressure, Pounds per Square Inch Absolute								
Bubble Point		14.8	30.7	60.0	111.2	196.4	332.8	543.9	864.1
	Viscosity, Micropoises								
	4990	4132	3420	2784	2235	1752	1325	924	570
200	5021	4155	3441	2800	2250	1753	...	..	..
400	5055	4180	3470	2820	2281	1804	1850	...	..
600	5090	4208	3495	2840	2310	1850	1420	948	..
800	5121	4232	3520	2861	2334	1896	1482	1028	..
1000	5150	4260	3544	2880	2355	1939	1539	1100	630
1250	5190	4297	3566	2906	2380	1975	1599	1179	713
1500	5230	4330	3587	2929	2400	2010	1646	1252	798
1750	5270	4366	3608	2949	2420	2040	1686	1319	881
2000	5310	4400	3628	2965	2440	2063	1720	1370	940
2250	5345	4433	3649	2990	2459	2080	1742	1400	990
2500	5382	4470	3670	3010	2480	2098	1764	1430	1045
2750	5422	4502	3691	3024	2496	2110	1785	1444	1090
3000	5465	4535	3713	3042	2510	2127	1800	1470	1120
3500	..	4593	3753	3070	2540	2151	1822	1510	1170
4000	..	4655	3792	3095	2568	2183	1850	1532	1210
4500	..	4714	3830	3118	2600	2200	1880	1555	1249
5000	..	4782	3869	3145	2625	2229	1900	1579	1280

showed a standard deviation of 90 micropoises and an average deviation of 4 micropoises, taking into account the sign of the difference. There is only a relatively small change in viscosity with pressure in comparison to the behavior of paraffin hydrocarbons (*9–12*). An initial set of data was obtained at 100° F. The instrument was then disassembled, a new, four-stage, centrifugal, circulating pump was installed, and the rest of the measurements were made. The results of these measurements are shown in Table I along with interpolated curves for intermediate temperatures.

Smoothed values of the viscosity as a function of pressure for each of the temperatures investigated are recorded in Table II. It is believed that the calibrations were made with sufficient care and the data presented in Figure 1 were of such reproducibility that the standard error of the smoothed values recorded in the table is estimated to be 90 micropoises.

The effect of temperature upon the viscosity of nitrogen dioxide is presented in Figure 2. The measurements of Thorpe and Rodger (*16*) were included. Satisfactory agreement between the two sets of measurements was realized.

ACKNOWLEDGMENT

The laboratory work was supported by the Office of Naval Research. G. N. Richter was a recipient of a fellowship from the Dow Chemical Co. L. T. Carmichael assisted with the operation of the apparatus. Olga Strandvold contributed to the assembly of the manuscript. The assistance of W. N. Lacey in its review is acknowledged.

NOMENCLATURE

A = dimensional coefficient of Equation 1
B = dimensional coefficient of Equation 1
η = absolute viscosity, micropoises
σ_B = specific weight of ball, pounds per cubic foot
σ_f = specific weight of fluid, pounds per cubic foot
θ = roll time of ball, seconds

LITERATURE CITED

(1) Bennewitz, K., and Windisch, J. J., *Z. physik. Chem.*, **A166**, 401 (1933).
(2) Carmichael, L. T., and Sage, B. H., IND. ENG. CHEM., **44**, 2728 (1952).
(3) Flowers, A. E., *Proc. Am. Soc. Testing Materials*, **14**, II, 565 (1914).
(4) Hersey, M. D., *J. Wash. Acad. Sci.*, **6**, 525, 628 (1916).
(5) Hersey, M. D., and Shore, H., *Mech. Eng.*, **50**, 221 (1928).
(6) Hubbard, R. M., and Brown, G. G., IND. ENG. CHEM., ANAL. ED., **15**, 212 (1943).
(7) Reamer, H. H., and Sage, B. H., IND. ENG. CHEM., **44**, 185 (1952).
(8) Rossini, F. D., "Selected Values of Properties of Hydrocarbons," Washington, D. C., National Bureau of Standards, 1947.
(9) Sage, B. H., and Lacey, W. N., IND. ENG. CHEM., **30**, 829 (1938).
(10) Sage, B. H., and Lacey, W. N., *Trans. Am. Inst. Mining Met. Engrs.*, **127**, 118 (1938).
(11) *Ibid.*, **174**, 102 (1948).
(12) Sage, B. H., Sherborne, J. E., and Lacey, W. N., IND. ENG. CHEM., **27**, 954 (1935).
(13) Scheffer, F. E. C., and Treub, J. P., *Z. physik. Chem.*, **81**, 308 (1913).
(14) Scheuer, O., *Anz. Wien. Akad.*, **48**, 307 (1911).
(15) Schlinger, W. G., and Sage, B. H., IND. ENG. CHEM., **42**, 2158 (1950).
(16) Thorpe, T. E., and Rodger, J. W., *Phil. Trans. Roy. Soc. (London)*, **A185**, 397 (1895).
(17) Titani, T., *Bull. Chem. Soc. Japan*, **2**, 95 (1927).
(18) Verhoek, F. H., and Daniels, F., *J. Am. Chem. Soc.*, **53**, 1250 (1931).
(19) Watson, K. M., IND. ENG. CHEM., **35**, 398 (1943).

RECEIVED for review March 28, 1953. ACCEPTED May 22, 1953.

Distribution of Formic Acid between Water and Methyl Isobutyl Ketone

HARVEY J. VOGT[1] AND CHRISTIE J. GEANKOPLIS

Department of Chemical Engineering, Ohio State University, Columbus, Ohio

PURIFICATION and separation of organic acids by physical means such as extraction rather than distillation or other methods has stimulated interest in solubility relations and distribution of organic compounds between water and immiscible organic solvents. However, in order to better predict the distribution behaviors of certain specific compounds, it is helpful to know how members of a homologous series react in a given water-organic solvent system. Then, generalized rules can be formulated to aid in predicting behaviors of other compounds in these same solvent systems.

The objective of this work was to study the distribution coefficient in dilute solutions of formic acid between the immiscible solvents water and methyl isobutyl ketone; the latter is a good solvent for many organic compounds and plastics. The distribution ratio of formic acid was then compared with that of acetic acid and propionic acid which are the next higher members of the saturated carboxylic acid series.

[1] Present address, Columbia-Southern Chemical Co., Corpus Christie, Tex.

should take place. However, for both the pure high frequency and the crossed discharge, the yields were independent of the frequency within the experimental error.

LITERATURE CITED

(1) Briner, E., *Helv. Chim. Acta*, 19, 287, 308, 320 (1936).
(2) Cotton, W. J., *Trans. Electrochem. Soc.*, Preprints (1946); U. S. Patents, 2,468,173-4-5-6-7, 2,485,476-7-8-9, and 2,485,480-1 (1946); *Chem. Eng.*, 54, 252 (September 1947).
(3) Willey, E. J. B., *Proc. Roy. Soc. (London)*, **A127**, 511 (1930).

RECEIVED for review May 19, 1953. ACCEPTED March 13, 1954. Presented before Section 14, Physical and Inorganic Chemistry, at the XIIth International Congress of Pure and Applied Chemistry, New York, N. Y., September 1951. Abstract from a dissertation submitted by W. S. Partridge in June 1951 to the Graduate School of the University of Utah in partial fulfillment of the requirements for the degree of doctor of philosophy. Work supported by a grant from the University of Utah Research Fund and the Atomic Energy Commission.

Viscosity of Nitric Oxide–Nitrogen Dioxide System in Liquid Phase

H. H. REAMER, G. N. RICHTER, AND B. H. SAGE
California Institute of Technology, Pasadena, Calif.

NO EXPERIMENTAL data for the viscosity of the nitric oxide–nitrogen dioxide system were found. Pure nitrogen dioxide in the liquid phase was investigated by Thorpe and Rodger (*20*). Scheuer (*17*) studied the viscosity of this pure compound, but his results differ markedly from the measurements of Thorpe and Rodger. Measurements of the viscosity of pure nitrogen dioxide in the liquid phase were made at pressures up to 5000 pounds per square inch in the temperature interval between 40° and 280° F. (*10*).

The volumetric and phase behavior of mixtures of nitric oxide and nitrogen dioxide has been described (*19*). These data extend to pressures in excess of 5000 pounds per square inch at temperatures from 40° to 340° F. and serve as the basis for the volumetric corrections required to determine the absolute viscosity of this binary system. They are in reasonable agreement with the measurements of Purcell and Cheesman (*7*) for temperatures at which the two investigations may be compared. Baume and Robert (*1*) also studied the phase behavior of the nitric oxide–nitrogen dioxide system at temperatures below 68° F., and Wittorf (*22*) determined the limits of solubility of nitric oxide in nitrogen dioxide. The effect of pressure and temperature upon the specific volume of nitrogen dioxide was investigated (*9, 18*), and a review of the available data for this compound was presented.

METHODS AND APPARATUS

The present measurements were made with a rolling ball viscometer of a type proposed by Flowers (*3*) and developed by Hersey (*4, 5*). The instrument employed was described in connection with measurements of the viscosity of ammonia (*2*). This equipment involved a stainless steel tube inclined at an angle of approximately 15° down which a closely fitting steel ball was permitted to roll. The time of traverse of the ball between two sets of three coils located near the ends of the tube was determined electronically. A centrifugal pump was employed to return the ball to the upper end of the tube and to bring the system to a uniform composition and temperature. The exit from the roll tube was closed during measurements of the time of traverse of the ball down the tube.

Roll times were measured with a probable error of 0.2% and the temperature of the roll tube was known, with respect to the international platinum scale, within 0.1° F. Pressures were determined by use of a balance (*14*) calibrated against the vapor pressure of carbon dioxide at the ice point. The pressure of the fluid within the instrument was established through a balanced aneroid-type diaphragm (*18*) and was known within 2 pounds per square inch or 0.2%, whichever was the larger measure of uncertainty.

Hydrodynamic characteristics of rolling ball viscometers were investigated by Watson (*21*), Hersey and Shore (*5*), and Hubbard and Brown (*6*) and have been considered in the application of this instrument (*2*).

The apparatus was calibrated with *n*-pentane in the liquid phase using the critically chosen values of Rossini (*11*) for the viscosity of this compound at atmospheric pressure. An equation of the following form (*2*) was used to establish the viscosity from the measured roll time:

$$\eta = A\theta(\sigma_B - \sigma_f) - \frac{B\sigma_f}{\theta} \qquad (1)$$

The coefficients A and B were determined from the measured roll times with *n*-pentane as a function of temperature and were

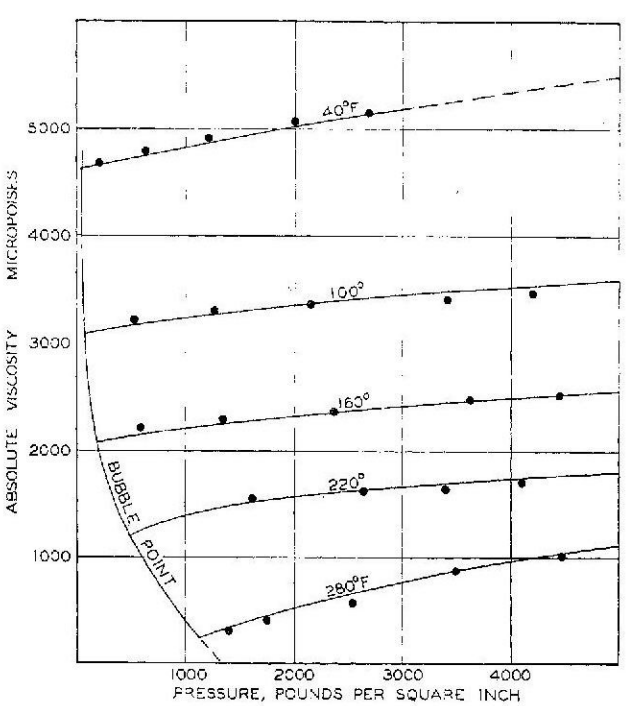

Figure 1. Viscosity of the Liquid Phase of a Mixture Containing 0.920 Weight Fraction Nitrogen Dioxide

checked with water. Recalibration of the instrument without cleaning the roll tube after completion of the investigation of two of the mixtures of nitric oxide and nitrogen dioxide indicated a change in calibration of less than 0.3%. All measurements reported were carried out at sufficiently low velocities so that the effect of the acceleration of the fluid around the ball was less than 5% of the measured roll time. It is believed that the first order correction for acceleration included in Equation 1 suffices for such hydrodynamic conditions. The viscosities were expressed in micropoises as a result of widespread usage, even though this unit is not dimensionally consistent with the independent variables.

Nitrogen dioxide was first introduced into the apparatus and the roll times were checked at a known temperature. The desired quantity of nitric oxide was then added from a weighing bomb while the apparatus was at a temperature of approximately 40° F. Bubble point pressures of the nitric oxide–nitrogen dioxide system (*19*) were sufficiently low at this temperature to permit the desired quantities of nitric oxide to be introduced without difficulty. The composition was determined from the weights of the nitric oxide and nitrogen dioxide introduced into the viscometer and was checked by the measured bubble point pressures. In addition, a sample of the liquid phase was withdrawn and its specific weight determined by pycnometer techniques at a known pressure and temperature. The information concerning the volumetric and phase behavior of the nitric oxide-nitrogen dioxide system (*19*) was employed in order to relate the measured bubble point pressures and specific weights of the liquid phase to composition. The maximum difference between the composition as measured by the different methods was 0.012 weight fraction nitric oxide.

RESULTS

The effect of pressure upon the viscosity of a mixture of nitric oxide and nitrogen dioxide containing 0.991 weight fraction nitrogen dioxide was determined at four temperatures between 40° and 280° F. as a preliminary part of this investigation. The measurements involved rather large standard deviations as com-

TABLE I. VISCOSITY[a] OF MIXTURES OF NITRIC OXIDE AND NITROGEN DIOXIDE

Pressure, Lb./Sq. In. Absolute	Wt. Frac. Nitrogen Dioxide				
	0.80	0.85	0.90	0.95	1.00
			40° F.		
Bubble Point	(80)[b] 4360	(29) 4720	(27) 4610	(22) 4680	(6.5) 4900
200	4980	4760	4660	4730	4940
400	5000	4800	4700	4760	4970
600	5030	4830	4740	4800	5020
800	5060	4860	4770	4830	5040
1000	5070	4880	4820	4870	5050
1250	5120	4940	4870	4920	5100
1500	5140	4960	4910	4970	5140
1750	5190	5020	4960	5020	5180
2000	5220	5060	5000	5060	5220
2250	5270	5120	5060	5100	5260
2500	5310	5140	5090	5140	5290
2750	5360	5190	5130	5180	5340
3000	5380	5220	5170	5220	5370
3500	[5470][c]	[5300]	[5260]	[5320]	[5450]
4000	[5550]	[5380]	[5330]	[5380]	[5530]
4500	[5620]	[5460]	[5420]	[5490]	[5625]
5000	[5580]	[5510]	[5480]	[5580]	[5740]
			100° F.		
Bubble Point	(86) 3260	(79) 3120	(71) 3070	(60) 3120	(31) 3320
200	3300	3200	3100	3200	3400
400	3300	3200	3100	3200	3400
600	3340	3200	3170	3240	3410
800	3360	3230	3200	3270	3430
1000	3380	3260	3220	3300	3450
1250	3410	3300	3260	3320	3480
1500	3440	3330	3280	3350	3510
1750	3470	3350	3310	3390	3540
2000	3500	3380	3350	3420	3560
2250	3520	3400	3370	3440	3580
2500	3550	3440	3400	3480	3620
2750	3560	3500	3420	3500	3640
3000	3580	3536	3446	3520	3660
3500	3630	3510	3480	3560	3700
4000	3690	3540	3500	3580	3740
4500	3760	3600	3550	3620	3780
5000	3840	3660	3580	3660	3820
			160° F.		
Bubble Point	(270) 2110	(239) 2070	(204) 2080	(162) 2090	(111) 2170
200	...	...	...	2100	2200
400	2200	2100	2100	2100	2200
600	2200	2100	2100	2180	2230
800	2200	2180	2180	2200	2260
1000	2220	2200	2210	2240	2280
1250	2250	2240	2240	2260	2310
1500	2270	2260	2270	2290	2340
1750	2300	2280	2290	2320	2360
2000	2320	2310	2320	2340	2380

Pressure, Lb./Sq. In. Absolute	Wt. Frac. Nitrogen Dioxide				
	0.80	0.85	0.90	0.95	1.00
			160° F. (*Contd.*)		
Bubble Point	(270) 2110	(239) 2070	(204) 2080	(162) 2090	(111) 2170
2250	2340	2320	2330	2360	2400
2500	2360	2350	2350	2380	2430
2750	2390	2370	2370	2400	2460
3000	2420	2400	2410	2440	2480
3500	2470	2460	2460	2470	2540
4000	2520	2490	2490	2500	2580
4500	2570	2540	2530	2540	2600
5000	2620	2580	2560	2570	2620
			220° F.		
Bubble Point	(701) 1220	(610) 1180	(516) 1190	(424) 1220	(333) 1320
200	...	...	...	...	...
400	...	...	...	...	1400
600	...	...	1240	1310	1420
800	1280	1280	1310	1370	1480
1000	1320	1340	1380	1440	1540
1250	1360	1380	1430	1510	1600
1500	1400	1422	1480	1550	1650
1750	1440	1460	1520	1600	1650
2000	1480	1500	1560	1630	1720
2250	1510	1530	1580	1660	1740
2500	1520	1550	1590	1660	1760
2750	1560	1600	1620	1690	1780
3000	1590	1620	1640	1700	1800
3500	1630	1640	1680	1740	1820
4000	1680	1690	1720	1780	1850
4500	1740	1740	1760	1820	1880
5000	1790	1780	1780	1830	1900
			280° F.		
Bubble Point	(1570) 160	(1388) 160	(1201) 200	(1026) 340	(864) 570
200	...	...	...	...	...
400	...	...	...	...	...
600	...	...	...	...	...
800	...	...	...	...	...
1000	...	...	...	...	630
1250	...	...	220	410	710
1500	...	180	290	490	800
1750	220	260	360	580	880
2000	270	320	450	650	940
2250	340	400	520	720	990
2500	390	450	570	770	1040
2750	450	520	640	830	1090
3000	500	560	690	880	1120
3500	620	690	810	980	1170
4000	750	800	910	1040	1210
4500	880	920	1000	1110	1250
5000	980	1010	1080	1160	1280

[a] Viscosity expressed in micropoises.
[b] Figures in parentheses represent bubble point pressures expressed in pounds per square inch absolute.
[c] Figures in brackets were obtained by extrapolation.

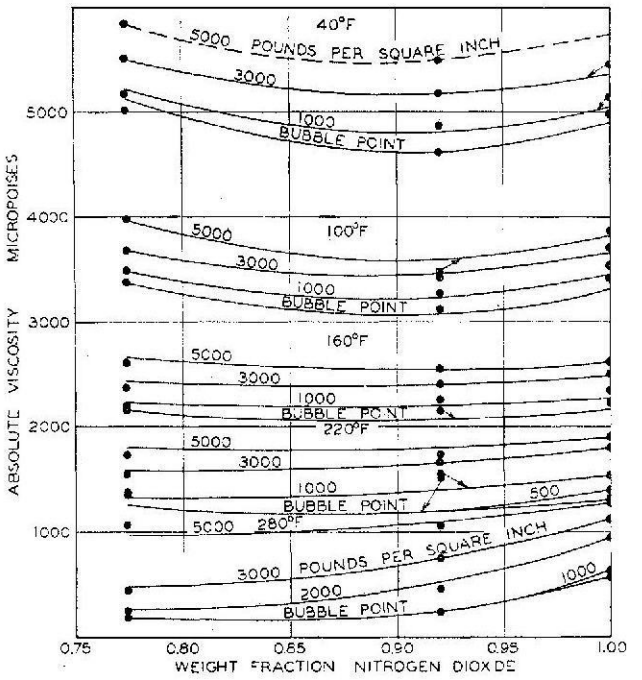

Figure 2. Viscosity-Composition Diagram

pared to later data reported here. The data for this sample have not been given more than 20% of the weight given to each of the other mixtures investigated. Two mixtures containing 0.920 and 0.774 weight fractions nitrogen dioxide were investigated at five temperatures between 40° and 280° F. The experimental results obtained for the mixture containing 0.920 weight fraction nitrogen dioxide are shown in Figure 1. The detailed experimental measurements for all of the mixtures are available (*8*). The full curves shown in Figure 1 represent data smoothed with respect to pressure, temperature, and composition. For the two mixtures and nitrogen dioxide (*10*), the standard deviation of the experimental data from the smoothed curves was 47 micropoises and the average deviation was 3.8 micropoises if regard was taken of sign. If the measurements for the mixture containing 0.991 nitrogen dioxide are included, the standard and average deviations are several times as large.

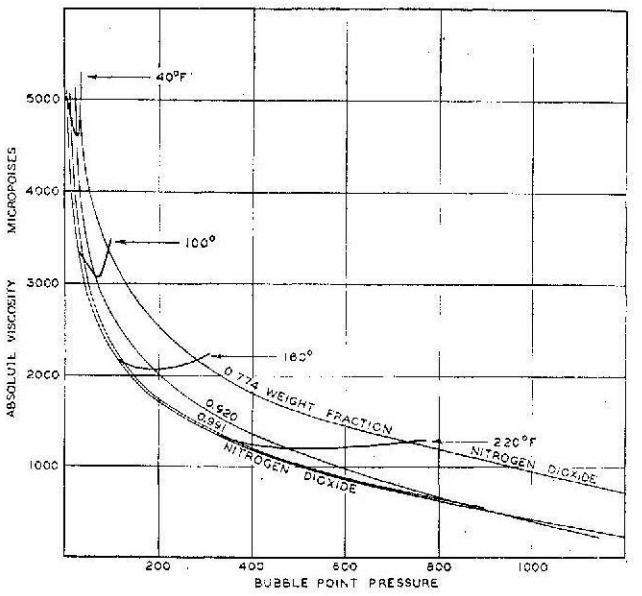

Figure 3. Viscosity of Nitric Oxide–Nitrogen Dioxide System at Bubble Point

Values of the viscosity of the liquid phase of this system are reported in Table I for even values of pressure, temperature, and composition. These data include earlier measurements upon the viscosity of nitrogen dioxide (*10*) which were modified slightly at the lower temperatures on the basis of the present measurements. The standard deviation of 47 micropoises was comparable to that found in the earlier studies of the viscosity of nitrogen dioxide (*10*).

The influence of composition upon the viscosity of the nitric oxide–nitrogen dioxide system is shown in Figure 2 for each of the temperatures investigated. The solid points represent the data obtained from smoothing the experimental measurements for the individual mixtures, whereas the full curves correspond to the values recorded in Table I. The reproducibility of the data for an individual composition at a particular time was much better than that found for the entire set of measurements. The viscosity of the liquid phase at bubble point is depicted in Figure 3. The small effect of changes in composition upon the viscosity of the liquid phase is evident. Data recorded in Table I indicate that, within the range of pressures and compositions investigated, the influence of these variables is small. Such behavior is in contradistinction to the marked variations in viscosity with changes in pressure or composition in the case of hydrocarbon systems (*12, 13, 15, 16*). Pressure and temperature influence the viscosity of mixtures of nitric oxide and nitrogen dioxide to much the same extent as that found for pure nitrogen dioxide (*10*).

ACKNOWLEDGMENT

This experimental program was supported by the Office of Naval Research. G. N. Richter was the recipient of a Union Carbide and Carbon Corp. graduate fellowship. Betty Kendall carried out the calculations and Elizabeth McLaughlin aided in the assembly of the manuscript. The assistance of W. N. Lacey in its review is acknowledged.

NOMENCLATURE

A = dimensional coefficient of Equation 1
B = dimensional coefficient of Equation 1
η = absolute viscosity, micropoises
σ_B = specific weight of ball, pounds/cubic foot
σ_f = specific weight of fluid, pounds/cubic foot
θ = roll time of ball, seconds

LITERATURE CITED

(1) Baume, G., and Robert, M., *Compt. rend.*, **169**, 967 (1919).
(2) Carmichael, L. T., and Sage, B. H., IND. ENG. CHEM., 44, 2728 (1952).
(3) Flowers, A. E., *Proc. Am. Soc. Testing Materials*, **14**, II, 565 (1914).
(4) Hersey, M. D., *J. Wash. Acad. Sci.*, **6**, 525, 628 (1916).
(5) Hersey, M. D., and Shore, H., *Mech. Eng.*, **50**, 221 (1928).
(6) Hubbard, R. M., and Brown, G. G., IND. ENG. CHEM., ANAL. ED., **15**, 212 (1943).
(7) Purcell, R. H., and Cheesman, G. H., *J. Chem. Soc. (London)*, **1932**, 826.
(8) Reamer, H. H., Richter, G. N., and Sage, B. H., Washington, D. C., Am. Doc. Inst., Doc. No. 4199 (1953).
(9) Reamer, H. H., and Sage, B. H., IND. ENG. CHEM., 44, 185 (1952).
(10) Richter, G. N., Reamer, H. H., and Sage, B. H., *Ibid.*, 45, 2117 (1953).
(11) Rossini, F. D., "Selected Values of Properties of Hydrocarbons," Washington, D. C., National Bureau of Standards, 1947.
(12) Sage, B. H., Inman, B. N., and Lacey, W. N., IND. ENG. CHEM., **29**, 888 (1937).
(13) Sage, B. H., and Lacey, W. N., *Ibid.*, **32**, 587 (1940).
(14) Sage, B. H., and Lacey, W. N., *Trans. Am. Inst. Mining Met. Engrs.*, **174**, 102 (1948).
(15) Sage, B. H., Sherborne, J. E., and Lacey, W. N., API *Prod. Bull.* **216**, 40 (1936); *Oil Weekly*, **80**, No. 12, 36 (1936).

(16) Sage, B. H., Yale, W. D., and Lacey, W. N., IND. ENG. CHEM., 31, 223 (1939).
(17) Scheuer, O., *Anz. Wien. Akad.*, 48, 307 (1911).
(18) Schlinger, W. G., and Sage, B. H., IND. ENG. CHEM., 42, 2158 (1950).
(19) Selleck, F. T., Reamer, H. H., and Sage, B. H., *Ibid.*, 45, 814 (1953).
(20) Thorpe, T. E., and Rodger, J. W., *Phil. Trans. Roy. Soc. (London)*, A185, 397 (1895).
(21) Watson, K. M., IND. ENG. CHEM., 35, 398 (1943).
(22) Wittorf, N. V., *Z. anorg. Chem.*, 41, 85 (1904).

RECEIVED for review November 9, 1953. ACCEPTED January 19, 1954. A more detailed form of this paper (or extended version, or material supplementary to this article) has been deposited as Document No. 4199 with the ADI Auxiliary Publications Project, Photoduplication Service, Library of Congress, Washington 25, D. C. A copy may be secured by citing the document number and by remitting $1.25 for photoprints or $1.25 for 35-mm. microfilm. Advance payment is required. Make checks or money orders payable to Chief, Photoduplication Service, Library of Congress.

Ternary Liquid-Liquid Equilibria

ETHYLBENZENE–DIACETONE ALCOHOL–WATER AND STYRENE–DIACETONE ALCOHOL–WATER

L. F. CROOKE, JR.[1], AND MATTHEW VAN WINKLE
University of Texas, Austin 12, Tex.

IN CERTAIN separation processes an extracting agent is used which has affinity for one of the materials being separated. Subsequently the extracting agent must be removed from the extracted material by distillation, liquid-liquid extraction, or other means. Systems composed of certain hydrocarbons, alcohols, and water are of interest in this connection.

The systems ethylbenzene–diacetone alcohol–water and styrene–diacetone alcohol–water were studied in this investigation, and the phase boundary compositions and equilibrium tie-line data at 25° C. were determined.

This is one of a series of investigations in which the selectivities of certain solvents for certain materials produced in commercial processes are being studied. Previous investigations (*5*, *8*) in the series involved the determination of the selectivity of heptadecanol and 3-heptanol for acetic acid and ethyl alcohol in water solutions and the evaluation of the liquid-liquid equilibrium data.

MATERIALS

The diacetone alcohol (4-hydroxy-4-methyl-2-pentanone) used in this investigation was obtained from the Eastern Chemical Co. The alcohol was purified by distillation in a 48-inch column, 1 inch in diameter, packed with glass helices. The column was operated at a 5 to 1 reflux ratio (L/D). Two successive "heart" or middle cuts of 80% were made to obtain material of satisfactory purity. The index of refraction of the final distillate product was determined as 1.4235 and compared with the literature value of 1.4232 (*6*).

The ethylbenzene specified as 99.1 to 99.4% purity was supplied by the Monsanto Chemical Co.

The styrene, also supplied by the Monsanto Chemical Co., was of 99.9% purity.

Distilled water was used throughout the investigation.

PROCEDURE

The procedure described by Othmer *et al.* (*4*) was used to find points on the solubility curve in this investigation. Because a portion of the final solution had to be removed and examined in a refractometer, the stepwise method of determination of the solubility curve was considered inadvisable. The modification used has been discussed (*5*, *8*).

A known quantity of the solvent (ethylbenzene or styrene) was placed in a clean, weighed flask. The flask was weighed again and a known quantity of the solute (diacetone alcohol) was added. The flask containing the mixture was weighed again and then placed in a bath controlled at a constant temperature of 25° C. After 20 to 30 minutes the flask was removed and distilled water was added from a buret to the mixture. After each addition the mixture was agitated vigorously. Water addition was continued until a cloudiness appeared which did not disappear with mixing. The flask containing the mixture was again placed in the constant temperature bath. If after a period of time the solution cleared, more water was added. If the mixture remained turbid for 20 minutes, the flask was reweighed. The weight of the water in the saturated mixture was determined by difference. From the weights of the components in the saturated mixture, the weight fraction of each was calculated.

A sample of the saturated phase was removed and the refractive index determined in a refractometer using a monochromatic sodium d light source. The prisms were maintained at 30° C. This small increase in temperature was enough to produce a single-phase solution.

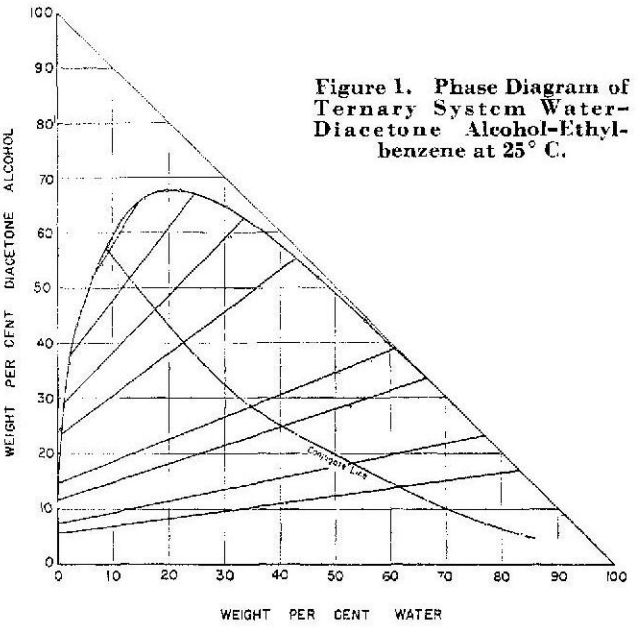

Figure 1. Phase Diagram of Ternary System Water–Diacetone Alcohol–Ethylbenzene at 25° C.

This procedure was repeated as the ratio of solvent (ethylbenzene) to solute (diacetone alcohol) was varied to determine the composition of the ethylbenzene- or solvent-rich layer.

A second series of mixtures was made up of water and diacetone alcohol. The solvent, ethyl benzene or styrene, was added dropwise with vigorous mixing until a "stable" turbidity was produced. This procedure made it possible to determine the composition of the water-rich phase portion of the solubility curve. Compositions of these mixtures were also determined by refractive index methods.

[1] Present address, Creole Petroleum Co., Caracas, Venezuela.

Propositions

1. Teflon and soapstone can be combined to form a material that may be useful in making high pressure electrical seals. It is resistant to many forms of chemical attack, can be used at temperatures up to 700° F., and, while sealing more easily than soapstone, does not extrude as easily as teflon.

2. The use of Green's functions in the numerical or graphical solution of differential equations can lead to easier methods of obtaining approximate answers to many problems of engineering interest.

3. The error in the thermal conductivity due to neglect of possible eccentricities of the cylinders in a cylindrical cell has been considered by Burton and Ziebland (1). An error in their results is corrected and a simpler equation is proposed.

4. The use of nitroxyl perchlorate (NO_2ClO_4), and similar compounds, as solid fuels in rocket motors should be investigated.

5. A resistance element would appear to have many advantages over thermocouples for measuring temperatures in research equipment. A method of using a resistance thermometer in the thermal conductivity cell used in the present work is proposed.

6. Vargaftik (2) determined the change of thermal conductivity with pressure to 90 atmospheres for several gases. In his equipment he used a resistance thermometer to measure the temperatures. The thermometer was exposed to the high pressure. The strains introduced in it as a result of the pressure would be expected to have a significant effect on his results. Thus the pressure dependence of the thermal conductivity that was observed by him, and by others with similar cells, would appear to be in error.

7. During the measurements of the thermal conductivity of nitric oxide, decomposition of the nitric oxide was found to occur. It was assumed that it was catalytic in nature, and the reaction appeared to be

$$4NO = N_2 + 2NO_2$$

The pressure dependence of the reaction rate did not agree with that expected from the usual kinetic equations for the decomposition. This unusual pressure effect should be further investigated.

8. A program of research in methods of making high pressure seals for electrical leads in research equipment is proposed. The problem of introducing small thermocouples into a high pressure vessel that is to be used over a wide temperature range is one encountered. At the present no completely satisfactory solution to this problem has been developed.

9. A rolling ball viscometer is not a satisfactory instrument for precise determinations of viscosity over wide ranges of fluid properties.

10. The thermal conductivity of reacting systems, and of systems near their critical states, is anomalously high. This increase may be of value in heat transfer operations.

References

1. Burton, J. T. A. and Ziebland H., Explosives Research and Development Establishment Report No. 2/R/56, Ministry of Supply (Great Britain).

2. Vargaftik, N., Tech. Phys., U.S.S.R., 4, 341 (1937).